

EVALUATING AND ENHANCING THE GEOARCHAEOLOGICAL RESOURCE OF THE LOWER SEVERN VALLEY (APPENDICES)

Robin Jackson, Andrew Mann and Tony Roberts

With contributions by Tony Brown, Keith Challis, Christopher Bronk Ramsey,
Gordon Cook, Andy Howard, John Meadows, Elizabeth Pearson and Phil Toms

Illustrations by Carolyn Hunt

4th February 2011

© Historic Environment and Archaeology Service,
Worcestershire County Council



INVESTOR IN PEOPLE

Historic Environment and Archaeology Service,
Worcestershire County Council,
Woodbury Building,
University of Worcester,
Henwick Grove,
Worcester WR2 6AJ

PNUM 5725MAIN
WHEAS P3179
Report 1819

Appendices

- 1 Methods used in the mapping of geomorphological features from LiDAR derived terrain models (Keith Challis, Robin Jackson, Andrew Mann and Tony Roberts)
- 2 Methods used in the mapping of cultural features from LiDAR derived terrain models (Keith Challis, Robin Jackson, Andrew Mann and Tony Roberts)
- 3 Pilot optical dating of terraces in the Lower Severn Valley (Phil Toms)
- 4 Methods used in mapping features with palaeoenvironmental potential from OS and other historic mapping (Elizabeth Pearson)
- 5 Model report forms and methods
- 6 Report forms: Clifton study area (Andrew Mann)
- 7 Report forms: Frampton-on-Severn area (Tony Roberts)

Appendix 1

Detailed methods statement:

Mapping geoarchaeological landforms from LiDAR derived data (Keith Challis, Andrew Mann, Robin Jackson and Tony Roberts)

Mapping was undertaken using LiDAR data that had been processed to generate first pulse and last pulse DSMs and DTMs.

These were processed to create hill-shade models that were lit from 8 different directions at the same elevation.

This was undertaken within the project GIS (ArcGIS 9, ARCMAP: Version 9.3) using the Spatial Analyst and 3-D Analyst extensions.

The specific approaches, standards and mapping conventions for geomorphological features described below were developed by the Birmingham University Team in consultation with other project partners.

These were developed within a similar methodological framework to that used for mapping of cultural features and also within the overall framework utilised for mapping landscape features (as employed within HLC projects).

The overall aim was to produce a simple and relatively rapid approach to this task which did not require a high level of geoarchaeological knowledge and could be achieved following a brief training session on the character and identification of geomorphological features; thereby making the approach both cost effective and as accessible as possible.

Mapping was completed by 1km² tile. Features identified on the LiDAR models were digitised on layers within the GIS thus allowing transfer at the end of the project to the respective HERs as shape files. The mapping symbology for geoarchaeological features was based on those identified in Jones *et al* 2007.

A single unique number was used to identify each digitised point, polygon or line regardless of the actual number of LiDAR features this represented. The location of each feature was also recorded within the corresponding GIS layers attributes including the relevant OS 1km grid square and its centroid coordinates. The centroid elevation of each unique identified feature was also recorded.

The transcriber was responsible for ensuring that the numerical series for each study area was maintained and where features were found in more than one square; *e.g.* where linear features or large areas were mapped as polygons the transcriber assigned the grid square in which the centre point of the feature was located.

As part of the process, each newly mapped feature was also cross-checked and compared with other sources of information within the GIS such as air-photographs, other remotely sensed data, HER data and landscape character mapping to improve the reliability and quality of the mapped data.

Information about each geoarchaeological landform unit was collated within the GIS through use of Attribute tables. The latter were maintained in a Microsoft Access (2003) database linked into the GIS and using terminology controlled through use of look-up tables. The attribute table and look-up tables employed are presented below.

Geoarchaeology attribute table

Heading	Instructions
OS Km sq ID*	e.g. SO6013
UID*	Unique numeric ID for the feature being digitised. Provides link field to GIS polygon
HER Reference	Unique HER reference number. GSMR or WSM
HER Cross-reference	If related to an existing HER monument – Use to cross-reference to HER reference number (Parent Record)
Parent/Child HER Reference	If not related to an existing HER Monument – Use to cross-reference any parent/child relationship established within project (only required if no external parent record)
HLC Type	Check GIS to establish cross-reference to HLC type
Central NGR*	Central NGR reference point (e.g. SO602135)
Centroid Easting*	Six figure easting (e.g. 443000)
Centroid Northing*	Six figure northing (e.g. 633889)
Centroid Elevation	Elevation in metres. Derive from LiDAR DSM (e.g. 56.25)
Polygon Area (ha)	Area enclosed by feature polygon (from GIS)
Morphological Form*	Select from lookup table. Use to record the physical form of the feature
Evidence Type*	Select from lookup table. Use to record how the feature is visible
Geoarchaeological Interpretation	Select from lookup table. Use to provide interpretation where possible
Feature interpretation confidence level	Select from lookup table. Use to record the level of confidence which can be applied to the interpretation of the feature. One of the three confidence levels (<i>HIGH</i> , <i>MEDIUM</i> and <i>LOW</i>) should be selected from the drop-down menu. If the feature has not been interpreted, <i>NOT APPLICABLE</i> should be selected.
Feature summary*	Use to provide a brief description of the features (e.g. Poorly defined palaeochannel west of Clifton Brook Farm)
Feature description	Optional free text field to extend above summary.
Period general*	Select from lookup table. If in any doubt select <i>UNKNOWN</i>
Period specific*	Select from lookup table. Use where features can be more specifically dated. If in any doubt select <i>UNKNOWN</i>

Heading	Instructions
Comments	Use to record any other information the transcriber feels is relevant but which is not covered by other fields. It is not anticipated that this field will be used often
Pixilated area – Level of pixilation	Used to grade the level of pixilation and is an attempt to determine the extent to which this will have obscured LiDAR features. One of two levels (<i>LIGHT</i> and <i>HEAVY</i>) should be selected from the lookup table.
Irregular surface	This is a YES/NO toggle to identify polygons which have been digitised around an area which appear on the hillshaded images as very irregular surfaces and which may represent undergrowth which obscures LiDAR features - the polygon should only encompass areas which appear on all four hillshaded images, and the smallest area should be digitised.
Primary source*	Select from lookup table. Use to record the primary source from which the feature has been identified. (e.g. <i>LIDAR DSM</i>)
Earliest source	Select from lookup table. Use to record the earliest source on which the feature can be identified
Latest source	Select from lookup table. Use to record the most recent source on which the feature can be identified
Last recorded condition	Select from lookup table. Use to record condition. Only use <i>DESTROYED</i> where it is known that no sub-surface elements survive (e.g. where quarried). Use <i>MODIFIED</i> where a feature has been altered such as where a watercourse has been canalised or embanked.
Source work reference*	Automatic entry to provide bibliography reference to project
Compiler*	Initials of transcriber/compiler
Date*	Date compiled

*Compulsory field

Lookup Tables

Morphological form

POSITIVE LINEAR
NEGATIVE LINEAR
POSITIVE DISCRETE
NEGATIVE DISCRETE
PIXELATED AREA
UNDULATING SURFACE

Evidence type - Geoarchaeology

CROP/SOIL/MOISTURE MARK
EXCAVATED PALAEOCHANNEL
FIELD BOUNDARY
PARISH BOUNDARY
PLANATED SURFACE
POSTULATED CONTINUATION OF CHANNEL
POSTULATED CONTINUATION OF SCARP
DATA PROCESSING ARTEFACT
RIDGE AND SWALE
SCARP (TERRACE EDGE)
STANDING WATER
TOPOGRAPHIC DEPRESSION
TOPOGRAPHIC RISE
VEGETATION CHANGE

Geoarchaeological interpretation

AEOLIAN DEPOSIT
ALLUVIAL DEPOSIT
ALLUVIAL FAN
COLLUVIAL DEPOSIT
INDETERMINATE
INTERTIDAL CREEK
MID-CHANNEL BAR
MODERN CHANNEL (ADAPTED)
MODERN CHANNEL (NATURAL)
NO DATA
PALAEOCHANNEL
PERIGLACIAL FEATURE
RIDGE AND SWALE
RODDEN
TERRACE
TERRACE EDGE
TIDAL SCOUR
VALLEY FLOOR EDGE

Confidence level

HIGH
MEDIUM
LOW
NOT APPLICABLE

Sources
AP - 1940S
AP - CROPMARK PLOT (MG)
AP - CROPMARK PLOT (NMP)
AP - CROPMARK PLOT (NMR OVERLAY)
AP - GOOGLE EARTH
AP - POST 1940S
GEOLOGY - DRIFT
GEOLOGY - SOILS
GEOLOGY - SOLID
HER RECORD
LIDAR DSM
LIDAR DTM
LIDAR INTENSITY
MAP - OS 1ST EDN
MAP - OS MODERN
MAP - OS OTHER EDN
MAP - OTHER MODERN
MAP - TITHE/ESTATE/OTHER HISTORIC
Last recorded condition
EXTANT
DEGRADED
DESTROYED
MODIFIED

Analysis: Cross reference order (Geoarchaeology)

1. Lidar / contemporary photographic imagery (Google Earth)
 2. Tithe/Estate maps
 3. 1st Edition OS mapping
 4. 1940s APs
 5. Later epochs of APs
 6. Modern mapping
 7. HER data (for excavated channels, etc)
-

Appendix 2

Detailed methods statement:

Mapping cultural landforms from LiDAR derived data (Keith Challis, Andrew Mann, Robin Jackson and Tony Roberts)

Mapping was undertaken using LiDAR data that had been processed to generate first pulse and last pulse DSMs and DTMs.

These were processed to create hill-shade models that were lit from 8 different directions at the same elevation.

This was undertaken within the project GIS (ArcGIS 9, ARCMAP: Version 9.3) using the Spatial Analyst and 3-D Analyst extensions.

The approaches for cultural mapping were based on methods and standards developed by GCC within their Forest of Dean Survey Project (PNUM 4798) for use in mapping cultural features from LiDAR derived DSMs. This methodology has been further developed by WCC within a forestry commission sponsored project covering the Wyre Forest.

No further methodological development was necessary and the approach taken is summarised below.

The LiDAR DSMs and DTMs were examined to identify cultural features such as watermeadow systems, flood defences, other water management features, ridge and furrow, field systems and former settlement areas.

Mapping was completed by 1km² tile. Features identified on the LiDAR models were digitised on layers within the GIS thus allowing transfer at the end of the project to the respective HERs as shape files.

A single unique number was used to identify each digitised point, polygon or line regardless of the actual number of LiDAR features this represented. The location of each feature was also recorded within the corresponding GIS layers attributes including the relevant OS 1km grid square and its centroid coordinates. The centroid elevation of each unique identified feature was also recorded.

The transcriber was responsible for ensuring that the numerical series for each study area was maintained and where features were found in more than one square; *e.g.* where linear features or large areas were mapped as polygons the transcriber assigned the grid square in which the centre point of the feature was located.

As part of the process, each newly mapped feature was also cross-checked and compared with other sources of information within the GIS such as air-photographs, other remotely sensed data, HER data and landscape character mapping to improve the reliability and quality of the mapped data.

Information about each cultural feature was collated within the GIS through use of Attribute tables. The latter were maintained in a Microsoft Access (2003) database linked into the GIS and using terminology controlled through use of look-up tables. The attribute table and look-up tables employed are presented below and employ GCC and WCC HER standards themselves based on national HER data standards (MIDAS).

Cultural archaeology attribute table

Heading	Instructions
OS Km sq ID*	e.g. SO6013
UID*	Unique numeric ID for the feature being digitised. Provides link field to GIS polygon
HER Reference*	Unique HER reference number. GSMR or WSM
HER Cross-reference	If related to an existing HER monument – Use to cross-reference to HER reference number (Parent Record)
Parent/Child HER Reference	If not related to an existing HER Monument – Use to cross-reference any parent/child relationship established within project (only required if no external parent record)
HLC Type	Check GIS to establish cross-reference to HLC type
Central NGR*	Central NGR reference point (e.g. SO602135)
Centroid Easting*	Six figure easting (e.g. 443000)
Centroid Northing*	Six figure northing (e.g. 633889)
Centroid Elevation	Elevation in metres. Derive from LiDAR DSM (e.g. 56.25)
Polygon Area (ha)	Area enclosed by feature polygon (from GIS)
Evidence Type*	Select from lookup table. Use to record the physical form of the feature
Cultural Interpretation*	Select from lookup table. Use to provide interpretation where possible. The lookup table provides a list of the more common feature/site type liable to be identified and uses MIDAS/HER Thesaurus terminology. Where a feature/site type is different from those listed in the lookup table – Select <i>OTHER</i> and use the next section for entering a type drawn from full HER terminology
Cultural Interpretation – OTHER	Where <i>OTHER</i> is entered for Cultural Interpretation above, use this free text field to enter the correct type drawn from MIDAS/HER terminology. If in doubt – consult HER staff
Feature interpretation confidence level*	Select from lookup table. Use to record the level of confidence which can be applied to the interpretation of a feature. One of the three confidence levels (<i>HIGH</i> , <i>MEDIUM</i> and <i>LOW</i>) should be selected from the drop-down menu. If the feature has not been interpreted, <i>NOT APPLICABLE</i> should be selected.
Feature summary*	Use to provide a brief description of the features (e.g. Poorly defined ridge and furrow west of Clifton Brook Farm)

Feature description	Optional free text field to extend above summary.
Period general*	Select from lookup table. If in any doubt select <i>UNKNOWN</i>
Period specific*	Select from lookup table. Use where features can be more specifically dated. If in any doubt select <i>UNKNOWN</i>
Comments	Use to record any other information the transcriber feels is relevant but which is not covered by other fields. It is not anticipated that this field will be used often
Pixilated area – Level of pixilation	Used to grade the level of pixilation and is an attempt to determine the extent to which this will have obscured Lidar features. One of two levels (<i>LIGHT</i> and <i>HEAVY</i>) should be selected from the lookup table.
Irregular surface	This is a YES/NO toggle to identify polygons which have been digitised around an area which appear on the hillshaded images as very irregular surfaces and which may represent undergrowth which obscures LiDAR features - the polygon should only encompass areas which appear on all four hillshaded images, and the smallest area should be digitised.
Primary source*	Select from lookup table. Use to record the primary source from which the feature has been identified. (e.g. <i>LIDAR DSM</i>)
Earliest source	Select from lookup table. Use to record the earliest source on which the feature can be identified
Latest source	Select from lookup table. Use to record the most recent source on which the feature can be identified
Last recorded condition*	Select from lookup table. Use to record condition. Only use <i>DESTROYED</i> where it is known that no sub-surface elements survive (e.g. where quarried). Use <i>MODIFIED</i> where a feature has been altered such as where a watercourse has been canalised or embanked.
Source work reference*	Automatic entry to provide bibliography reference to project
Compiler*	Initials of transcriber/compiler
Date*	Date compiled

*Compulsory field

Evidence Type (Cultural)

1. CROPMARK
2. EARTHWORK BANK
3. EARTHWORK DITCH
4. FIELD BOUNDARY
5. LARGE AREA FEATURE
6. LARGE CUT FEATURE
7. PARCHMARK
8. PROCESSING ARTEFACT
9. SOILMARK
10. STRUCTURE/BUILDING/STONE WALLS
11. VEGETATION CHANGE

Cultural Interpretation

1. BANK
 2. BOUNDARY
 3. BUILDING
 4. BUILDING PLATFORM
 5. CANAL
 6. CAUSEWAY
 7. DESERTED VILLAGE
 8. DRAIN
 9. EARTHWORK
 10. EMBANKMENT
 11. ENCLOSURE
 12. FEATURE
 13. FIELD SYSTEM
 14. FISH POND
 15. FISHWEIR
 16. FLOOD DEFENCES
 17. HOLLOWAY
 18. LEAT
 19. LINEAR FEATURE
 20. LYNCHET
 21. MILL
 22. MILL DAM
 23. MILL POND
 24. MILL RACE
 25. MOATED SITE
 26. OTHER
 27. POND
 28. DATA PROCESSING ARTEFACT
 29. QUARRY
 30. RIDGE AND FURROW
 31. ROAD
 32. SETTLEMENT
 33. STRUCTURE
 34. TRACKWAY
 35. WATER MEADOW
-

WCC Period general	GCC Period General (where different)
PALAEOLITHIC (-500000 to -100001)	
PREHISTORIC (10000BC to AD42)	
MESOLITHIC (-10000 to 4001)	
NEOLITHIC (-4000 to -2351)	
BRONZE AGE (-2350 to -801)	
IRON AGE (-800 to 42)	
ROMAN (AD43 to 410)	
POST ROMAN (411 to 1065)	EARLY MEDIEVAL
MEDIEVAL (1066 to 1539)	
POST MEDIEVAL (1540 to 1899)	
MODERN (1900 to PRESENT)	
UNKNOWN	

Period specific	GCC Period General (where different)		
LOWER PALAEOLITHIC	-500000	-150001	
MIDDLE PALAEOLITHIC	-150000	-40001	
UPPER PALAEOLITHIC	-40000	-10001	
EARLY MESOLITHIC	-10000	-7001	
LATE MESOLITHIC	-7000	-4001	
EARLY NEOLITHIC	-4000	-3501	
MIDDLE NEOLITHIC	-3500	-2701	
LATE NEOLITHIC	-2700	-2351	
EARLY BRONZE AGE	-2350	-1601	
MIDDLE BRONZE AGE	-1600	-1001	
LATE BRONZE AGE	-1000	-801	
EARLY IRON AGE	-800	-401	
MIDDLE IRON AGE	-400	-101	
LATE IRON AGE	-100	42	
1ST CENTURY AD	43	99	
2ND CENTURY AD	100	199	
3RD CENTURY AD	200	299	
4TH CENTURY AD	300	399	
ROMAN 5TH CENTURY AD	400	410	
POST ROMAN	411	849	EARLY MEDIEVAL
PRE CONQUEST	850	1065	EARLY MEDIEVAL
LATE 11TH CENTURY AD	1066	1099	
12TH CENTURY AD	1100	1199	
13TH CENTURY AD	1200	1299	
14TH CENTURY AD	1300	1399	
15TH CENTURY AD	1400	1499	
16TH CENTURY AD	1500	1599	
17TH CENTURY AD	1600	1699	
18TH CENTURY AD	1700	1799	
19TH CENTURY AD	1800	1899	
20TH CENTURY AD	1900	1999	
21ST CENTURY AD	2000	2050	
UNKNOWN	9000	9999	

Confidence level
HIGH
MEDIUM
LOW
NOT APPLICABLE

Sources
AP - 1940S
AP - CROPMARK PLOT (MG)
AP - CROPMARK PLOT (NMP)
AP - CROPMARK PLOT (NMR OVERLAY)
AP - GOOGLE EARTH
AP - POST 1940S
GEOLOGY - DRIFT
GEOLOGY - SOILS
GEOLOGY - SOLID
HER RECORD
LIDAR DSM
LIDAR DTM
LIDAR INTENSITY
MAP - OS 1ST EDN
MAP - OS MODERN
MAP - OS OTHER EDN
MAP - OTHER MODERN
MAP - TITHE/ESTATE/OTHER HISTORIC

Last recorded condition
EXTANT
DEGRADED
DESTROYED
MODIFIED

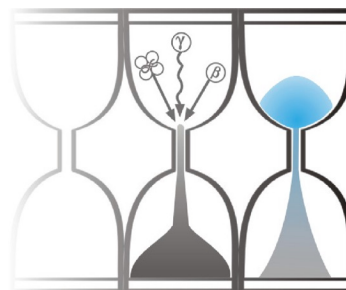
Analysis Cross reference order (Cultural)

1. Lidar / contemporary photographic imagery (Google Earth)
2. HER
3. NMP/Mike Glyde mapping
4. Aerial photography
5. Tithe/Estate maps
6. 1st Edition OS mapping
7. Modern mapping



University of Gloucestershire

Geochronology Laboratories



Piloting Optical dating of terraces in the Lower Severn Valley

**Contributing to 'Evaluating and Enhancing the
Geoarchaeological Resource of the Lower Severn Valley'**

(EH Project Ref: PNUM 5725 (PD))

Prepared by Dr P.S. Toms, 24 December 2010

Piloting Optical dating of terraces in the Lower Severn Valley

Dr P.S. Toms¹, Prof. A.G. Brown², R. Jackson³ and A. Mann³

Summary

This study contributes to Stage 2 of the English Heritage project 'Evaluating and Enhancing the Geoarchaeological Resource of the Lower Severn Valley'. It aims to assess the potential of Optical dating of terraces in the project area as part of a prospection toolkit that will increase the effectiveness of archaeological mitigation strategies within the particular environment of the Severn Valley. Twelve samples of sediments associated with terraces were collected from active quarry sites at Frampton, Clifton and Ball Mill. Each yielded sufficient datable mass and signal to generate Optical age estimates. The terrace deposits at Frampton and Clifton formed after the Last Glacial Maximum of Marine Isotope Stage (MIS) 2 and prior to mid MIS 1. Those at Ball Mill were created between MIS 5e and early MIS 4. Most of the age estimates are accompanied by analytical caveats though are on the whole consistent with their relative stratigraphic positions. The occurrence of samples at Frampton and Clifton exhibiting traits of partial bleaching suggests that future Optical dating of Terraces 1 and 2 should draw upon single grain approaches to acquire ages more consistent with the burial period. Intrinsic assessment of reliability would also be improved by obtaining at least two samples from each unit to be dated that have distinct dose rates, identified either by profiling before or prioritising after sampling.

Authors' addresses

¹Geochronology Laboratories, Department of Natural and Social Sciences, University of Gloucestershire, Swindon Road, Cheltenham. GL50 4AZ. Tel: 01242 544091. Email: ptoms@glos.ac.uk.

²School of Geography, University of Southampton, University Road, Southampton, SO17 1BJ.

³Worcestershire Historic Environment and Archaeology Service, Woodbury, University of Worcester, Henwick Grove, Worcester. WR2 6AJ.

1.0 Introduction

This study contributes to Stage 2 of the English Heritage project 'Evaluating and Enhancing the Geoarchaeological Resource of the Lower Severn Valley (Ref: PNUM 5725 PD)'. The Lower Severn Valley remains one of the few major UK valley floors that holds significant aggregate resources. In anticipation of increased aggregate extraction, the overarching aim of the project is to improve methodological approaches and baseline information underpinning strategic planning, individual application decisions and evaluation and mitigation strategies relating to mineral extraction in this area. Stage 2, in part, pilots Optical dating of terraces within the Lower Severn Valley focussing on three active quarries, Frampton, Clifton and Ball Mill (Map 1 and Images 1 to 3), and draws on recent research at the University of Gloucestershire (Earle, 2009). This report summarises the findings of the initial Optical dating programme.

2.0 Optical dating: mechanisms and principles

Upon exposure to ionising radiation, electrons within the crystal lattice of insulating minerals are displaced from their atomic orbits. Whilst this dislocation is momentary for most electrons, a portion of charge is redistributed to meta-stable sites (traps) within the crystal lattice. In the absence of significant optical and thermal stimuli, this charge can be stored for extensive periods. The quantity of charge relocation and storage relates to the magnitude and period of irradiation. When the lattice is optically or thermally stimulated, charge is evicted from traps and may return to a vacant orbit position (hole). Upon recombination with a hole, an electron's energy can be dissipated in the form of light generating crystal luminescence providing a measure of dose absorption.

Herein, quartz is segregated for dating. The utility of this minerogenic dosimeter lies in the stability of its datable signal over the mid to late Quaternary period, predicted through isothermal decay studies (e.g. Smith *et al.*, 1990; retention lifetime 630 Ma at 20°C) and evidenced by optical age estimates concordant with independent chronological controls (e.g. Murray and Olley, 2002). This stability is in contrast to the anomalous fading of comparable signals commonly observed for other ubiquitous sedimentary minerals such as feldspar and zircon (Wintle, 1973; Templer, 1985; Spooner, 1993)

Optical age estimates of sedimentation (Huntley *et al.*, 1985) are premised upon reduction of the minerogenic time dependent signal (Optically Stimulated Luminescence, OSL) to zero through exposure to sunlight and, once buried, signal reformulation by absorption of litho- and cosmogenic radiation. The signal accumulated post burial acts as a dosimeter recording total dose absorption, converting to a chronometer by estimating the rate of dose absorption quantified through the assay of radioactivity in the surrounding lithology and streaming from the cosmos.

$$\text{Age} = \frac{\text{Mean Equivalent Dose (D}_e\text{, Gy)}}{\text{Mean Dose Rate (D}_r\text{, Gy.ka}^{-1}\text{)}}$$

Aitken (1998) and Bøtter-Jensen *et al.* (2003) offer a detailed review of optical dating.

3.0 Sample Collection and Preparation

A total of twelve samples are reported herein; three collected by Earle (2009; GL08057, GL08058, GL08060) and nine as part of Stage 2 of this project (Table 1). All are conventional sediment samples, located within matrix-supported units composed predominantly of sand and silt collected in daylight from sections by means of opaque plastic tubing (150x45 mm) forced into each face. Each was taken from primary terrace material with the exception of GL08059/GL08060 (Clifton) and GL10024 (Ball Mill), where alluviated and aeolian sediments capping the terrace deposits were sampled, respectively. In order to attain an intrinsic metric of reliability and where possible, two samples were obtained from stratigraphically equivalent units targeting positions likely divergent in dosimetry on the basis of textural and colour differences (see section 8.0). Each sample was wrapped in cellophane and parcel tape in order to preserve moisture content and integrity until ready for laboratory preparation. For each sample, an additional c 100 g of sediment was collected for laboratory-based assessment of radioactive disequilibrium. The location of each optical dating sample are shown in Images 1 to 3.

To preclude optical erosion of the datable signal prior to measurement, all samples were prepared under controlled laboratory illumination provided by Encapsulite RB-10 (red) filters. To isolate that material potentially exposed to daylight during sampling, sediment located within 20 mm of each tube-end was removed.

The remaining sample was dried and then sieved. Quartz within the fine sand (125-180, 180-250 μm) or fine silt (5-15 μm) fraction was segregated, based on modal grain size (Table 1). Samples were then subjected to acid and alkaline digestion (10% HCl, 15% H_2O_2) to attain removal of carbonate and organic components respectively.

For fine sand fractions, a further acid digestion in HF (40%, 60 mins) was used to etch the outer 10-15 μm layer affected by α radiation and degrade each samples' feldspar content. During HF treatment, continuous magnetic stirring was used to effect isotropic etching of grains. 10% HCl was then added to remove acid soluble fluorides. Each sample was dried, resieved and quartz isolated from the remaining heavy mineral fraction using a sodium polytungstate density separation at $2.68\text{g}\cdot\text{cm}^{-3}$. 12 multi-grain aliquots (c. 3-6 mg) of quartz from each sample were then mounted on aluminium discs for determination of D_e values.

Fine silt sized quartz, along with other mineral grains of varying density and size, was extracted by sample sedimentation in acetone (<15 μm in 2 min 20 s, >5 μm in 21 mins at 20°C). Feldspars and amorphous silica were then removed from this fraction through acid digestion (35% H_2SiF_6 for 2 weeks, Jackson *et al.*, 1976; Berger *et al.*, 1980). Following addition of 10% HCl to remove acid soluble fluorides, grains degraded to <5 μm as a result of acid treatment were removed by acetone sedimentation. 6 aliquots (ca. 1.5 mg) were then mounted on aluminium discs for D_e evaluation.

All drying was conducted at 40°C to prevent thermal erosion of the signal. All acids and alkalis were Analar grade. All dilutions (removing toxic-corrosive and non-minerogenic luminescence-bearing substances) were conducted with distilled water to prevent signal contamination by extraneous particles.

4.0 Acquisition and accuracy of D_e value

All minerals naturally exhibit marked inter-sample variability in luminescence per unit dose (sensitivity). Therefore, the estimation of D_e acquired since burial requires calibration of the natural signal using known amounts of laboratory dose. D_e values were quantified using a single-aliquot regenerative-dose (SAR) protocol (Murray and Wintle 2000; 2003) facilitated by a Risø TL-DA-15 irradiation-stimulation-detection system (Markey *et al.*, 1997; Bøtter-Jensen *et al.*, 1999). Within this apparatus, optical signal stimulation is provided by an assembly of blue diodes (5 packs of 6 Nichia NSPB500S), filtered to 470 ± 80 nm conveying $15 \text{ mW}\cdot\text{cm}^{-2}$ using a 3 mm Schott GG420 positioned in front of each diode pack. Infrared (IR) stimulation, provided by 6 IR diodes (Telefunken TSHA 6203) stimulating at 875 ± 80 nm delivering $\sim 5 \text{ mW}\cdot\text{cm}^{-2}$, was used to indicate the presence of contaminant feldspars (Hütt *et al.*, 1988). Stimulated photon emissions from quartz aliquots are in the ultraviolet (UV) range and were filtered from stimulating photons by 7.5 mm HOYA U-340 glass and detected by an EMI 9235QA photomultiplier fitted with a blue-green sensitive alkali photocathode. Aliquot irradiation was conducted using a $1.48 \text{ GBq } ^{90}\text{Sr}/^{90}\text{Y}$ β source calibrated for multi-grain aliquots of each isolated quartz fraction against the 'Hotspot 800' ^{60}Co γ source located at the National Physical Laboratory (NPL), UK.

SAR by definition evaluates D_e through measuring the natural signal (Fig. 1) of a single aliquot and then regenerating that aliquot's signal by using known laboratory doses to enable calibration. For each aliquot, 5 different regenerative-doses were administered so as to image dose response. D_e values for each aliquot were then interpolated, and associated counting and fitting errors calculated, by way of exponential plus linear regression (Fig. 1). Weighted (geometric) mean D_e values were calculated from 12 aliquots using the central age model outlined by Galbraith *et al.* (1999) and are quoted at 1σ confidence. The accuracy with which D_e equates to total absorbed dose and that dose absorbed since burial was assessed. The former can be considered a function of laboratory factors, the latter, one of environmental issues. Diagnostics were deployed to estimate the influence of these factors and criteria instituted to optimise the accuracy of D_e values.

4.1 Laboratory Factors

4.1.1 Feldspar contamination

The propensity of feldspar signals to fade and underestimate age, coupled with their higher sensitivity relative to quartz makes it imperative to quantify feldspar contamination. At room temperature, feldspars generate a signal (IRSL) upon exposure to IR whereas quartz does not. The signal from feldspars contributing to OSL can be depleted by prior exposure to IR. For all aliquots the contribution of any remaining feldspars was estimated from the OSL IR depletion ratio (Duller, 2003). If the addition to OSL by feldspars is insignificant, then the repeat dose ratio of OSL to post-IR OSL should be statistically consistent with unity (Fig. 1 and Fig. 6). If any aliquots do not fulfil this criterion, then the sample age estimate should be accepted tentatively. The source of feldspar contamination is rarely rooted in sample preparation; it predominantly results from the occurrence of feldspars as inclusions within quartz.

4.1.2 Preheating

Preheating aliquots between irradiation and optical stimulation is necessary to ensure comparability between natural and laboratory-induced signals. However, the multiple irradiation and preheating steps

that are required to define single-aliquot regenerative-dose response leads to signal sensitisation, rendering calibration of the natural signal inaccurate. The SAR protocol (Murray and Wintle, 2000; 2003) enables this sensitisation to be monitored and corrected using a test dose, here set at 5 Gy preheated to 220°C for 10s, to track signal sensitivity between irradiation-preheat steps. However, the accuracy of sensitisation correction for both natural and laboratory signals can be preheat dependent. Two diagnostics were used to assess the optimal preheat temperature for accurate correction and calibration.

D_e preheat dependence (Fig. 2) quantifies the combined effects of thermal transfer and sensitisation on the natural signal. Insignificant adjustment in D_e values in response to differing preheats may reflect limited influence of these effects. Samples generating D_e values <10Gy and exhibiting a systematic, statistically significant adjustment in D_e value with increasing preheat temperature may indicate the presence of significant thermal transfer; in such instances low temperature (<220°C) preheats provide the apposite measure of D_e . For this diagnostic, 18 aliquots were divided into sets of 3; each set was assigned a 10 s preheat between 180°C and 280°C and the D_e value from each aliquot was then assessed.

Dose Recovery (Fig. 3) attempts to replicate the above diagnostic, yet provide improved resolution of thermal effects through removal of variability induced by heterogeneous dose absorption in the environment, using a precise lab dose to simulate natural dose. The ratio between the applied dose and recovered D_e value should be statistically concordant with unity. For this diagnostic, a further 6 aliquots were each assigned a 10 s preheat between 180°C and 280°C.

That preheat treatment fulfilling the criterion of accuracy for both diagnostics was selected to refine the final D_e value from a further 9 aliquots. Further thermal treatments, prescribed by Murray and Wintle (2000; 2003), were applied to optimise accuracy and precision. Optical stimulation occurred at 125°C in order to minimise effects associated with photo-transferred thermoluminescence and maximise signal to noise ratios. Inter-cycle optical stimulation was conducted at 280°C to minimise recuperation.

4.1.3 Irradiation

For all samples having D_e values in excess of 100 Gy, matters of signal saturation and laboratory irradiation effects are of concern. With regards the former, the rate of signal accumulation generally adheres to a saturating exponential form and it is this that limits the precision and accuracy of D_e values for samples having absorbed large doses. For such samples, the functional range of D_e interpolation by SAR has been verified up to 600 Gy by Pawley *et al.* (2010). Age estimates based on D_e values exceeding this value should be accepted tentatively.

4.1.4 Internal consistency

Quasi-radial plots (*cf* Galbraith, 1990) are used to illustrate inter-aliquot D_e variability for natural, repeat regenerative-dose and OSL to post-IR OSL signals (Figs. 4 to 6, respectively). D_e values are standardised relative to the central D_e value for natural signals and applied dose for regenerated signals. D_e values are described as overdispersed when >5% lie beyond $\pm 2\sigma$ of the standardising value; resulting from a heterogeneous absorption of burial dose and/or response to the SAR protocol. For multi-grain aliquots, overdispersion of natural signals does not necessarily imply inaccuracy. However where

overdispersion is observed for regenerated signals, the age estimate from that sample should be accepted tentatively.

4.2 Environmental factors

4.2.1 Incomplete zeroing

Post-burial OSL signals residual of pre-burial dose absorption can result where pre-burial sunlight exposure is limited in spectrum, intensity and/or period, leading to age overestimation. This effect is particularly acute for material eroded and redeposited sub-aqueously (Olley *et al.*, 1998, 1999; Wallinga, 2002) and exposed to a burial dose of less than c. 20 Gy (e.g. Olley *et al.*, 2004), has some influence in sub-aerial contexts but is rarely of consequence where aerial transport has occurred.

Within single-aliquot regenerative-dose optical dating there are two diagnostics of partial resetting (or bleaching); signal analysis (Agersnap-Larsen *et al.*, 2000; Bailey *et al.*, 2003) and inter-aliquot D_e distribution studies (Murray *et al.*, 1995).

Within this study, signal analysis was used to quantify the change in D_e value with respect to optical stimulation time for multi-grain aliquots. This exploits the existence of traps within minerogenic dosimeters that bleach with different efficiency for a given wavelength of light to verify partial bleaching. $D_e(t)$ plots (Fig. 7; Bailey *et al.*, 2003) are constructed from separate integrals of signal decay as laboratory optical stimulation progresses. A statistically significant increase in natural $D_e(t)$ is indicative of partial bleaching assuming three conditions are fulfilled. Firstly, that a statistically significant increase in $D_e(t)$ is observed when partial bleaching is simulated within the laboratory. Secondly, that there is no significant rise in $D_e(t)$ when full bleaching is simulated. Finally, there should be no significant augmentation in $D_e(t)$ when zero dose is simulated. Where partial bleaching is detected, the age derived from the sample should be considered a maximum estimate only. However, the utility of signal analysis is strongly dependent upon a samples pre-burial experience of sunlight's spectrum and its residual to post-burial signal ratio. Given in the majority of cases, the spectral exposure history of a deposit is uncertain, the absence of an increase in natural $D_e(t)$ does not necessarily testify to the absence of partial bleaching.

4.2.2 Pedoturbation

The accuracy of sedimentation ages can further be controlled by post-burial trans-strata grain movements forced by pedo- or cryoturbation. Berger (2003) contends pedogenesis prompts a reduction in the apparent sedimentation age of parent material through bioturbation and illuviation of younger material from above and/or by biological recycling and resetting of the datable signal of surface material. Berger (2003) proposes that the chronological products of this remobilisation are A-horizon age estimates reflecting the cessation of pedogenic activity, Bc/C-horizon ages delimiting the maximum age for the initiation of pedogenesis with estimates obtained from Bt-horizons providing an intermediate age 'close to the age of cessation of soil development'. Singhvi *et al.* (2001), in contrast, suggest that B and C-horizons closely approximate the age of the parent material, the A-horizon, that of the 'soil forming episode'. At present there is no post-sampling mechanism for the direct detection of and correction for post-burial sediment remobilisation. However, intervals of palaeosol evolution can be delimited by a maximum age derived from parent material and a minimum age obtained from a unit overlying the palaeosol. Inaccuracy forced by cryoturbation may be bidirectional, heaving older material upwards or drawing younger material downwards into the level to be dated. Cryogenic deformation of matrix-

supported material is, typically, visible; sampling of such cryogenically-disturbed sediments can be avoided. Though pedo- and cryoturbated sediments were observed during this study, none of the sediment samples were located close to such deposits.

5.0 Acquisition and accuracy of D_r value

Lithogenic D_r values were defined through measurement of U, Th and K radionuclide concentration and conversion of these quantities into α , β and γ D_r values (Table 1). α and β contributions were estimated from sub-samples by laboratory-based γ spectrometry using an Ortec GEM-S high purity Ge coaxial detector system, calibrated using certified reference materials supplied by CANMET. γ dose rates were estimated from *in situ* NaI gamma spectrometry. *In situ* measurements were conducted using an EG&G μ Nomad portable NaI gamma spectrometer (calibrated using the block standards at RLAHA, University of Oxford); these reduce uncertainty relating to potential heterogeneity in the γ dose field surrounding each sample. The level of U disequilibrium was estimated by laboratory-based Ge γ spectrometry. Estimates of radionuclide concentration were converted into D_r values (Adamiec and Aitken, 1998), accounting for D_r modulation forced by grain size (Mejdahl, 1979), present moisture content (Zimmerman, 1971) and, where D_e values were generated from 5-15 μ m quartz, reduced signal sensitivity to α radiation (a -value 0.050 ± 0.002 ; Toms, unpub. data). Cosmogenic D_r values were calculated on the basis of sample depth, geographical position and matrix density (Prescott and Hutton, 1994).

The spatiotemporal validity of D_r values can be considered a function of five variables. Firstly, age estimates devoid of *in situ* γ spectrometry data should be accepted tentatively if the sampled unit is heterogeneous in texture or if the sample is located within 300 mm of strata consisting of differing texture and/or mineralogy. However, where samples are obtained throughout a vertical profile, consistent values of γ D_r based solely on laboratory measurements may evidence the homogeneity of the γ field and hence accuracy of γ D_r values. Secondly, disequilibrium can force temporal instability in U and Th emissions. The impact of this infrequent phenomenon (Olley et al., 1996) upon age estimates is usually insignificant given their associated margins of error. However, for samples where this effect is pronounced (>50% disequilibrium between ^{238}U and ^{226}Ra ; Fig. 8), the resulting age estimates should be accepted tentatively. Thirdly, pedogenically-induced variations in matrix composition of B and C-horizons, such as radionuclide and/or mineral remobilisation, may alter the rate of energy emission and/or absorption. If D_r is invariant through a dated profile and samples encompass primary parent material, then element mobility is likely limited in effect. Fourthly, spatiotemporal detractions from present moisture content are difficult to assess directly, requiring knowledge of the magnitude and timing of differing contents. However, the maximum influence of moisture content variations can be delimited by recalculating D_r for minimum (zero) and maximum (saturation) content. Finally, temporal alteration in the thickness of overburden alters cosmic D_r values. Cosmic D_r often forms a negligible portion of total D_r . It is possible to quantify the maximum influence of overburden flux by recalculating D_r for minimum (zero) and maximum (surface sample) cosmic D_r .

6.0 Estimation of Age

Age estimates reported in Table 1 provide an estimate of sediment burial period based on mean D_e and D_r values and their associated analytical uncertainties. Uncertainty in age estimates is reported as a product of systematic and experimental errors, with the magnitude of experimental errors alone shown in parenthesis (Table 1). Probability distributions approximate the inter-aliquot variability in age (Fig. 9). The

maximum influence of temporal variations in D_r forced by minima-maxima in moisture content and overburden thickness is illustrated in Fig. 9. Where uncertainty in these parameters exists this age range may prove instructive, however the combined extremes represented should not be construed as preferred age estimates.

7.0 Analytical uncertainty

All errors are based upon analytical uncertainty and quoted at 1σ confidence. Error calculations account for the propagation of systematic and/or experimental (random) errors associated with D_e and D_r values.

For D_e values, systematic errors are confined to laboratory β source calibration. Uncertainty in this respect is that combined from the delivery of the calibrating γ dose (1.2%; NPL, pers. comm.), the conversion of this dose for SiO_2 using the respective mass energy-absorption coefficient (2%; Hubbell, 1982) and experimental error, totalling 3.5%. Mass attenuation and bremsstrahlung losses during γ dose delivery are considered negligible. Experimental errors relate to D_e interpolation using sensitisation corrected dose responses. Natural and regenerated sensitisation corrected dose points (S_i) were quantified by,

$$S_i = (D_i - x.L_i) / (d_i - x.L_i)$$

Eq.1

where D_i = Natural or regenerated OSL, initial 0.2 s
 L_i = Background natural or regenerated OSL, final 5 s
 d_i = Test dose OSL, initial 0.2 s
 x = Scaling factor, 0.08

The error on each signal parameter is based on counting statistics, reflected by the square-root of measured values. The propagation of these errors within Eq. 1 generating σS_i follows the general formula given in Eq. 2. σS_i were then used to define fitting and interpolation errors within exponential plus linear regressions.

For D_r values, systematic errors accommodate uncertainty in radionuclide conversion factors (5%), β attenuation coefficients (5%), a -value (4%; derived from a systematic α source uncertainty of 3.5% and experimental error), matrix density (0.20 g.cm^{-3}), vertical thickness of sampled section (specific to sample collection device), saturation moisture content (3%), moisture content attenuation (2%), burial moisture content (25% relative, unless direct evidence exists of the magnitude and period of differing content) and NaI gamma spectrometer calibration (3%). Experimental errors are associated with radionuclide quantification for each sample by NaI and Ge gamma spectrometry.

The propagation of these errors through to age calculation was quantified using the expression,

$$\sigma y (\delta y / \delta x) = (\sum ((\delta y / \delta x_n) \cdot \sigma x_n)^2)^{1/2}$$

Eq. 2

where y is a value equivalent to that function comprising terms x_n and where σ_y and σ_{x_n} are associated uncertainties.

Errors on age estimates are presented as combined systematic and experimental errors and experimental errors alone. The former (combined) error should be considered when comparing luminescence ages herein with independent chronometric controls. The latter assumes systematic errors are common to luminescence age estimates generated by means identical to those detailed herein and enable direct comparison with those estimates.

8.0 Intrinsic assessment of reliability

Intrinsic measures of reliability in Luminescence dating are based on analytical acceptability and inference. Table 2 details the analytical acceptability of age estimates evolved in this study, drawn principally from diagnostics illustrated in Figs. 1 to 8 and detailed in sections 4.0 to 5.0. Inference of reliability comes from the level of intra-site stratigraphic consistency and the convergence of age estimates from stratigraphically equivalent units of divergent dosimetry. Hierarchically, comparable ages derived from stratigraphically equivalent units of differing D_r supersede analytical acceptability even where the latter is questionable.

At Frampton two samples were taken from the same unit, owing to the limited exposure of sediments at this site. The age of GL10017 is significantly older than GL10018. Figure 7 for the former sample indicates the occurrence of partial bleaching and thus an overestimation of age. All age estimates from Clifton are consistent with their relative stratigraphic position. Three of the five samples (GL08057, GL08059, GL10021) exhibit traits of partial bleaching. Two samples (GL10021 and GL10022) were taken from an equivalent stratigraphic unit at this site with the intention of targeting areas of differing D_r . These samples produced coeval age estimates despite having differing analytical caveats. However the dosimetry for each sample proved indistinguishable, precluding the assessment of reliability based on divergent dosimetry. The age estimates generated from Ball Mill are, statistically, consistent with their relative stratigraphic positions. Two samples (GL10025 and GL10026) exhibited moderate U disequilibrium, but the consistency of their age estimates with those devoid of this effect suggests a negligible impact on accuracy.

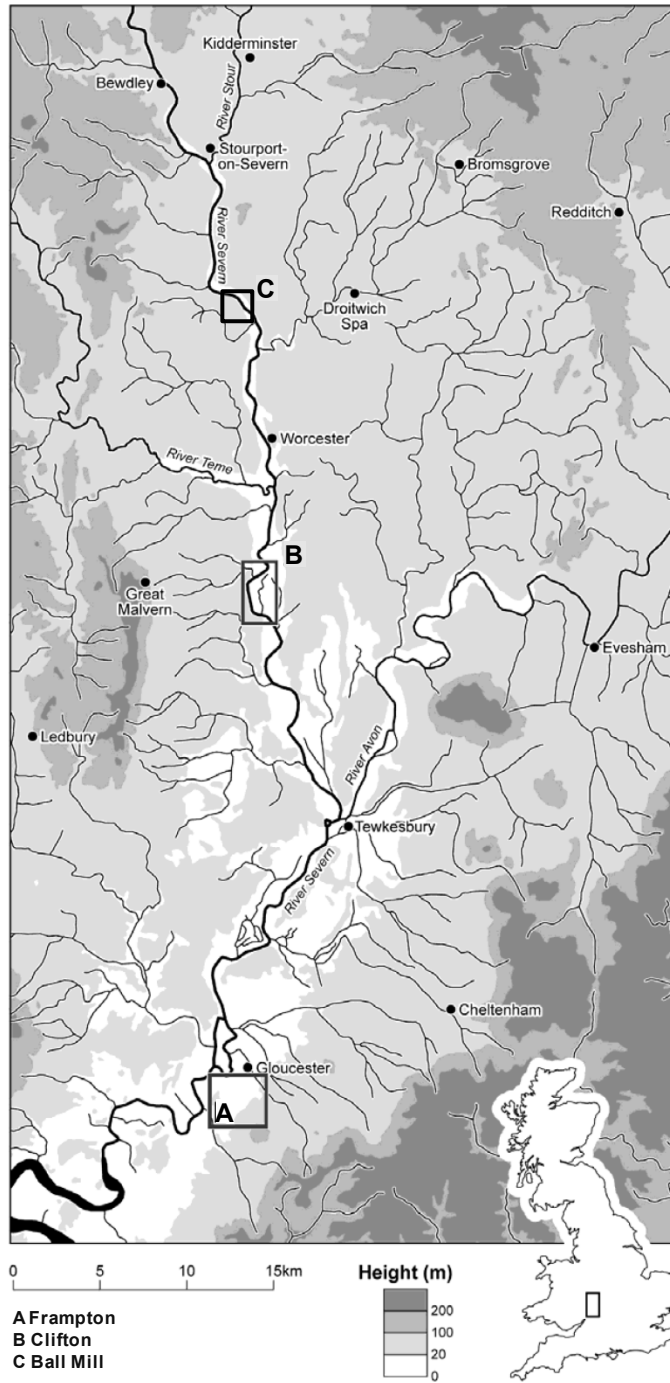
9.0 Summary and recommendations

From this pilot study, sediments associated with terraces in the Lower Severn Valley have sufficient datable mass and signal to produce Optical age estimates. The probable age of the terrace sediments at Frampton is 9.7 ± 1.2 ka (late MIS 2 to early MIS 1). The terrace deposits at Clifton formed between 18 and 5.5 ka (late MIS 2 to mid MIS 1), with subsequent alluviation recorded between 2.8 and 0.7 ka. At Ball Mill, sedimentation of terrace material occurred between 122 and 71 ka (MIS 5e to early MIS 4).

All samples, with the exception of GL08060, are accompanied by analytical caveats. These alone do not warrant rejection of the associated age estimates. However, the occurrence of partially bleached sediments at Frampton and Clifton is consistent with previous studies of sub-aqueous sediments exposed to less than c. 20 Gy during burial (Olley *et al.*, 1998, 1999, 2004; Wallinga, 2002). Correction of the resulting age overestimation may be possible through inter-aliquot D_e distribution studies. Such

analyses use aliquots of single sand grains to quantify inter-grain D_e distribution. At present, it is contended that asymmetric inter-grain D_e distributions are symptomatic of partial bleaching and/or pedoturbation (Murray *et al.*, 1995; Olley *et al.*, 1999; Olley *et al.*, 2004; Bateman *et al.*, 2003). For partial bleaching at least, it is further contended that the D_e acquired during burial is located in the minimum region of such ranges reflecting fully or well-bleached grains. Therefore, a single grain approach to further Optical dating of Terraces 1 and 2 in the Lower Severn Valley is advocated.

As a pilot study, the opportunity to pursue multiple samples of divergent dosimetry from equivalent stratigraphic units is limited. In the instances where two samples were obtained from the same unit (Frampton and Clifton), the D_r values proved to be indistinguishable. It is recommended that any further Optical dating should attempt to either profile dosimetry within a unit prior to sampling or take multiple samples from the same unit, prioritising for analysis those with significantly different D_r values.



Map 1 Location of study sites

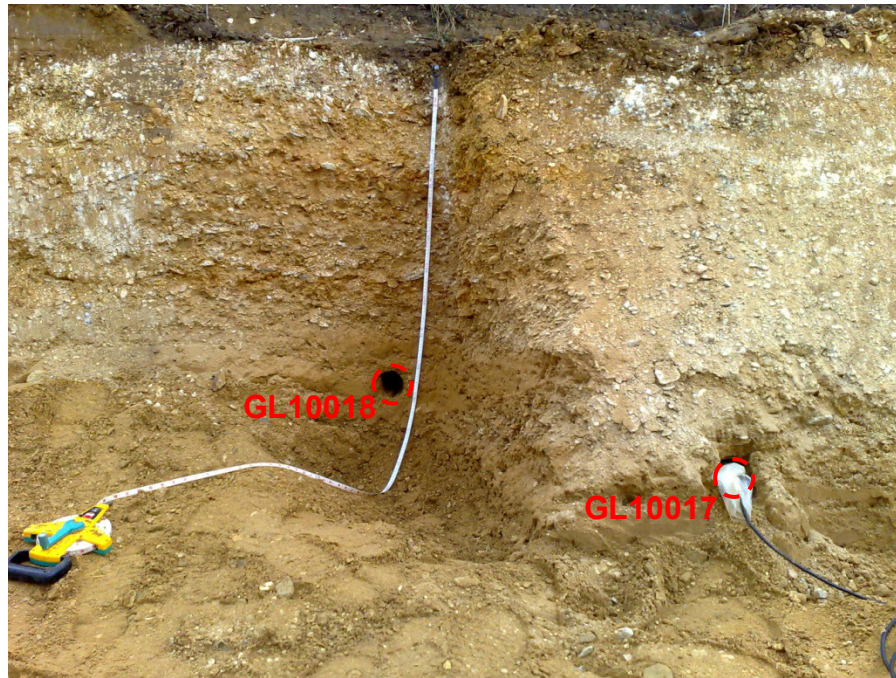


Image 1 Optical dating samples from Frampton, Gloucestershire (51°45'28.58"N, 2°20'26.60"W)

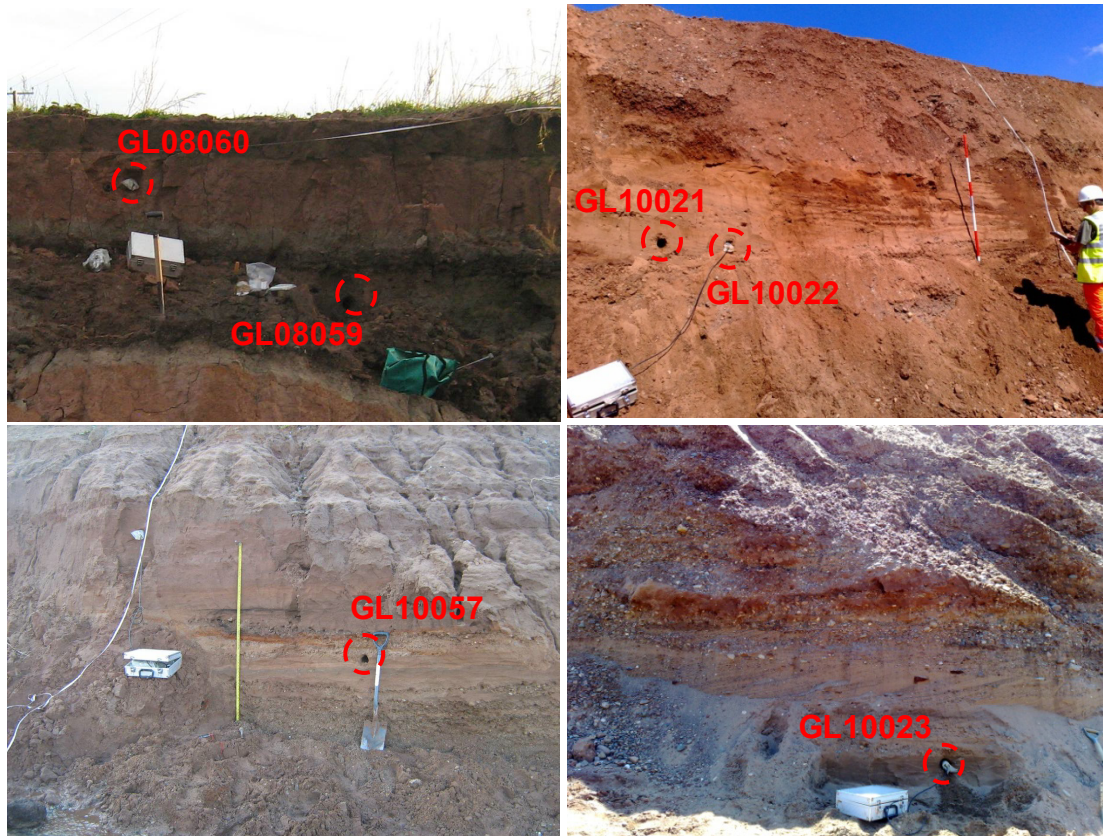


Image 2 Optical dating samples from Clifton, Worcestershire (GL08 057, 059 and 060 52°45'28.58"N, 2°13'43.40"W; GL10 021 and 022 52°07'10.01"N, 2°13'28.53"W; GL10023 52°07'11.19"N, 2°13'31.19"W)



Image 3 Optical dating samples from Ball Mill, Worcestershire (52°15'02.39"N, 2°15'09.15"W)

Field Code	Lab Code	Location	Overburden (m)	Grain size (µm)	Moisture content (%)	NaI γ-spectrometry (in situ)			γ D _r (Gy.ka ⁻¹)	I. based)	Ge γ-spectrometry (lab)			α D _r		β D _r		Cosmic D _r (Gy.ka ⁻¹)	Total D _r (Gy.ka ⁻¹)	1.1.2.1.1.1.1 Preheat	1.1.2.1.1.1.3 D _e	1.1.2.1.1.1.5	Age
						K (%)	Th (ppm)	U (ppm)			K (%)	Th (ppm)	U (ppm)	1.1.1.1 (Gy.ka ⁻¹)	1.1.2 (Gy.ka ⁻¹)	1.1.2.1.1.1.2 (°C for 10s)	1.1.2.1.1.1.4 (Gy)			1.1.2.1.1.1.6	(ka)		
CLIF04	GL08060	52°N, 2°W, 10m	0.5	5-15	18 ± 5	1.48 ± 0.03	8.26 ± 0.26	3.49 ± 0.17	1.15 ± 0.04	2.32 ± 0.10	11.69 ± 0.70	2.35 ± 0.13	0.44 ± 0.05	1.88 ± 0.19	0.19 ± 0.02	3.66 ± 0.20	200	2.9 ± 0.1		0.78 ± 0.06 (0.05)			
CLIF03	GL08059	52°N, 2°W, 10m	1.7	125-180	16 ± 4	0.84 ± 0.02	3.89 ± 0.19	1.90 ± 0.13	0.60 ± 0.03	1.41 ± 0.07	5.44 ± 0.41	1.24 ± 0.08	-	1.03 ± 0.11	0.16 ± 0.01	1.79 ± 0.11	240	4.4 ± 0.5		2.5 ± 0.3 (0.3)			
CLIF01	GL08057	52°N, 2°W, 10m	5.0	125-180	8 ± 2	0.98 ± 0.02	3.43 ± 0.18	1.57 ± 0.12	0.58 ± 0.02	1.22 ± 0.06	3.89 ± 0.36	0.89 ± 0.07	-	1.00 ± 0.08	0.09 ± 0.01	1.67 ± 0.08	220	11.0 ± 1.6		6.6 ± 1.0 (0.9)			
CLIF05	GL10021	52°N, 2°W, 10m	3.5	125-180	5 ± 1	0.88 ± 0.02	2.48 ± 0.15	0.98 ± 0.09	0.44 ± 0.02	1.16 ± 0.06	2.54 ± 0.30	0.60 ± 0.06	-	0.93 ± 0.07	0.12 ± 0.01	1.49 ± 0.08	240	24.6 ± 2.4		16 ± 2 (2)			
CLIF06	GL10022	52°N, 2°W, 10m	3.5	180-250	4 ± 1	0.86 ± 0.02	2.13 ± 0.12	1.25 ± 0.09	0.45 ± 0.02	1.18 ± 0.06	2.42 ± 0.31	0.66 ± 0.06	-	0.94 ± 0.07	0.12 ± 0.01	1.51 ± 0.08	240	22.9 ± 2.1		15 ± 2 (1)			
CLIF07	GL10023	52°N, 2°W, 10m	3.0	125-180	8 ± 2	1.17 ± 0.02	4.02 ± 0.15	2.35 ± 0.10	0.74 ± 0.03	1.30 ± 0.06	4.12 ± 0.39	0.87 ± 0.07	-	1.05 ± 0.08	0.13 ± 0.01	1.92 ± 0.09	260	22.8 ± 3.7		12 ± 2 (2)			
FRAM01	GL10017	52°N, 2°W, 20m	0.9	125-180	11 ± 3	0.17 ± 0.01	1.49 ± 0.11	1.41 ± 0.09	0.27 ± 0.01	0.54 ± 0.03	2.02 ± 0.26	0.72 ± 0.06	-	0.46 ± 0.04	0.18 ± 0.02	0.91 ± 0.05	240	16.4 ± 6.1		18 ± 7 (7)			
FRAM02	GL10018	52°N, 2°W, 20m	0.9	125-180	11 ± 3	0.19 ± 0.01	1.23 ± 0.10	1.30 ± 0.08	0.25 ± 0.01	0.53 ± 0.03	1.69 ± 0.30	0.64 ± 0.06	-	0.44 ± 0.04	0.18 ± 0.02	0.87 ± 0.05	240	8.5 ± 0.9		9.7 ± 1.2 (1.1)			
BMIL01	GL10024	52°N, 2°W, 30m	0.7	125-180	16 ± 4	1.00 ± 0.02	3.73 ± 0.16	1.85 ± 0.11	0.63 ± 0.02	1.48 ± 0.07	7.10 ± 0.48	1.45 ± 0.09	-	1.17 ± 0.11	0.18 ± 0.02	1.98 ± 0.11	260	181.3 ± 25.9		92 ± 14 (13)			
BMIL02	GL10025	52°N, 2°W, 30m	1.0	125-180	8 ± 2	0.93 ± 0.02	2.42 ± 0.14	1.42 ± 0.10	0.50 ± 0.02	1.34 ± 0.06	2.79 ± 0.27	0.70 ± 0.06	-	1.04 ± 0.08	0.18 ± 0.01	1.71 ± 0.09	280	161.6 ± 22.1		94 ± 14 (13)			
BMIL04	GL10027	52°N, 2°W, 30m	4.5	125-180	5 ± 1	0.94 ± 0.02	1.93 ± 0.12	0.95 ± 0.08	0.43 ± 0.02	1.11 ± 0.05	2.68 ± 0.31	0.62 ± 0.06	-	0.90 ± 0.07	0.10 ± 0.01	1.43 ± 0.07	280	118.8 ± 16.7		83 ± 12 (12)			
BMIL03	GL10026	52°N, 2°W, 30m	2.0	180-250	14 ± 4	0.91 ± 0.02	2.61 ± 0.13	1.49 ± 0.09	0.51 ± 0.02	1.05 ± 0.05	2.48 ± 0.33	0.59 ± 0.06	-	0.73 ± 0.07	0.15 ± 0.01	1.40 ± 0.08	280	151.3 ± 18.2		108 ± 14 (13)			

Table 1 D_r, D_e and Age data of submitted samples, listed in stratigraphic order at each site. Uncertainties in age are quoted at 1σ confidence, are based on analytical errors and reflect combined systematic and experimental variability and (in parenthesis) experimental variability alone (see 6.0). Blue indicates samples with accepted age estimates, red, age estimates with caveats (see Table 2).

Generic considerations	Field Code	Lab Code	Sample specific considerations
None	CLIF04	GL08060	Accept
	CLIF03	GL08059	Partially bleached (see 4.2.1; Fig. 7) Accept as maximum age
	CLIF01	GL08057	Partially bleached (see 4.2.1; Fig. 7) Accept as maximum age
	CLIF05	GL10021	Overdispersion of regenerative-dose data (see 4.1.4; Fig. 5) Partially bleached (see 4.2.1; Fig. 7) Accept tentatively as maximum age
	CLIF06	GL10022	Overdispersion of regenerative-dose data (see 4.1.4; Fig. 5) Minor U disequilibrium (see 5.0; Fig. 8) Accept tentatively
	CLIF07	GL10023	Overdispersion of regenerative-dose data (see 4.1.4; Fig. 5) Accept tentatively
	FRAM01	GL10017	Partially bleached (see 4.2.1; Fig. 7) Accept as maximum age
	FRAM02	GL10018	Overdispersion of regenerative-dose data (see 4.1.4; Fig. 5) Accept tentatively
	BMIL01	GL10024	Overdispersion of regenerative-dose data (see 4.1.4; Fig. 5) Accept tentatively
	BMIL02	GL10025	Overdispersion of regenerative-dose data (see 4.1.4; Fig. 5) Moderate U disequilibrium (see 5.0; Fig. 8) Accept tentatively
	BMIL04	GL10027	Overdispersion of regenerative-dose data (see 4.1.4; Fig. 5) Accept tentatively
	BMIL03	GL10026	Overdispersion of regenerative-dose data (see 4.1.4; Fig. 5) Moderate U disequilibrium (see 5.0; Fig. 8) Accept tentatively

Table 2 Analytical validity of sample suite age estimates and caveats for consideration

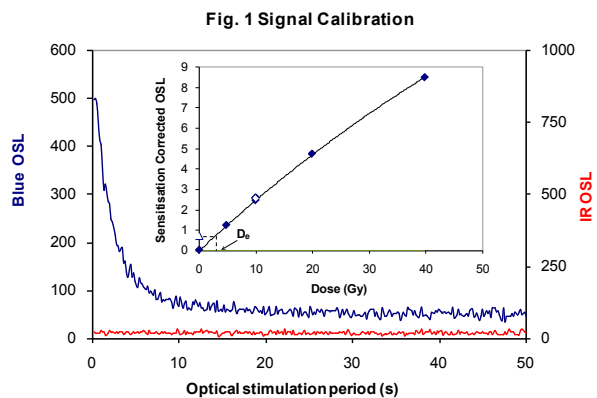


Fig. 1 Signal Calibration Natural blue and laboratory-induced infrared (IR) OSL signals. Detectable IR signal decays are diagnostic of feldspar contamination. Inset, the natural blue OSL signal (open triangle) of each aliquot is calibrated against known laboratory doses to yield equivalent dose (D_0) values. Repeats of low and high doses (open diamonds) illustrate the success of sensitivity correction.

Fig. 2 D_0 Preheat Dependence The acquisition of D_0 values is necessarily predicated upon thermal treatment of aliquots succeeding environmental and laboratory irradiation. The D_0 preheat dependence test quantifies the combined effects of thermal transfer and sensitisation on the natural signal. Insignificant adjustment in D_0 may reflect limited influence of these effects.

Fig. 3 Dose Recovery Attempts to replicate the above diagnostic, yet provide improved resolution of thermal effects through removal of variability induced by heterogeneous dose absorption in the environment and using a precise lab dose to simulate natural dose. Based on this and D_0 preheat dependence data an appropriate thermal treatment is selected to refine the final D_0 value.

Fig. 4 Inter-aliquot D_0 distribution Provides a measure of inter-aliquot concordance in D_0 values derived from natural irradiation. Discordant data (those points lying beyond ± 2 standardised $\ln D_0$) reflects heterogeneous dose absorption and/or inaccuracies in calibration.

Fig. 5 Low and High Repeat Regenerative-dose Ratio Measures the statistical concordance of signals from repeated low and high regenerative-doses. Discordant data (those points lying beyond ± 2 standardised $\ln D_0$) indicate inaccurate sensitivity correction.

Fig. 6 OSL to Post-IR OSL Ratio Measures the statistical concordance of OSL and post-IR OSL responses to the same regenerative-dose. Discordant, underestimating data (those points lying below -2 standardised $\ln D_0$) highlight the presence of significant feldspar contamination.

Fig. 7 Signal Analysis Statistically significant increase in natural D_0 value with signal stimulation period is indicative of a partially-bleached signal, provided a significant increase in D_0 results from simulated partial bleaching followed by insignificant adjustment in D_0 for simulated zero and full bleach conditions. Ages from such samples are considered maximum estimates. In the absence of a significant rise in D_0 with stimulation time, simulated partial bleaching and zero/full bleach tests are not assessed.

Fig. 8 U Activity Statistical concordance (equilibrium) in the activities of the daughter radionuclide ^{226}Ra with its parent ^{238}U may signify the temporal stability of D_0 emissions from these chains. Significant differences (disequilibrium; $>50\%$) in activity indicate addition or removal of isotopes creating a time-dependent shift in D_0 values and increased uncertainty in the accuracy of age estimates. A 20% disequilibrium marker is also shown.

Fig. 9 Age Range The mean age range provides an estimate of sediment burial period based on mean D_0 and D_1 values with associated analytical uncertainties. The probability distribution indicates the inter-aliquot variability in age. The maximum influence of temporal variations in D_0 forced by minima-maxima variation in moisture content and overburden thickness may prove instructive where there is uncertainty in these parameters, however the combined extremes represented should not be construed as preferred age estimates.

Fig. 2 D_0 Preheat Dependence

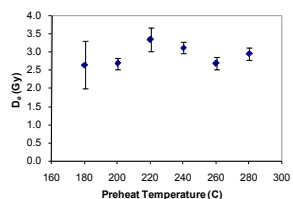


Fig. 3 Dose Recovery

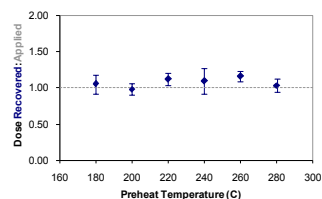


Fig. 4 Inter-aliquot D_0 distribution

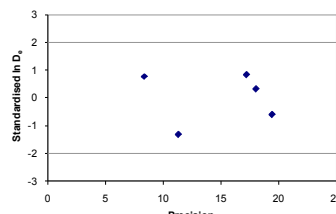


Fig. 5 Low and High Repeat Regenerative-dose Ratio

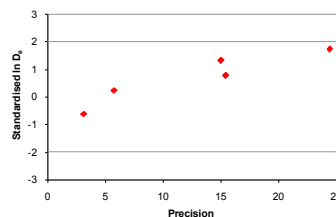


Fig. 6 OSL to Post-IR OSL Ratio

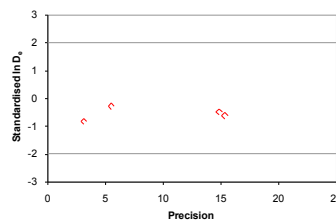


Fig. 7 Signal Analysis

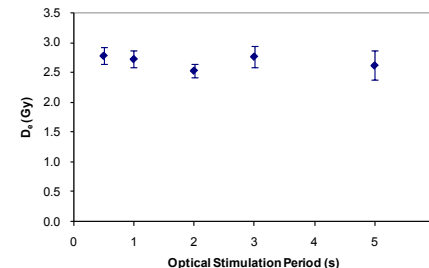


Fig. 8 U Decay Activity

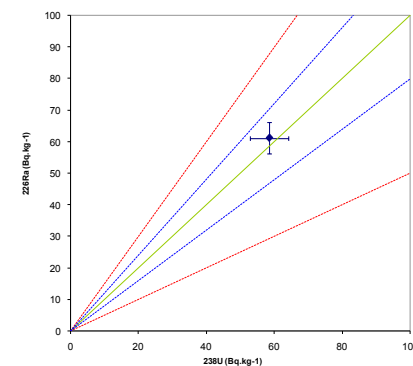
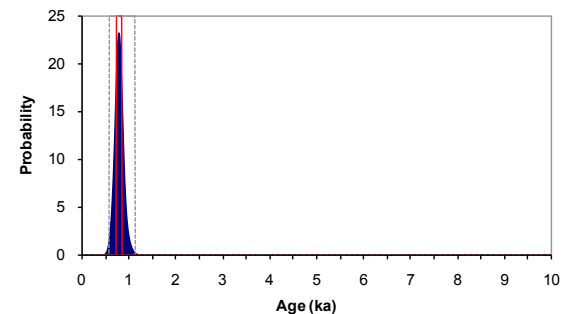


Fig. 9 Age Range



Sample: GL08060

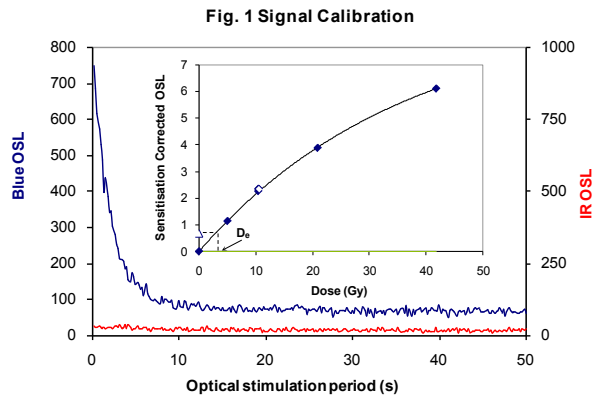


Fig. 1 Signal Calibration Natural blue and laboratory-induced infrared (IR) OSL signals. Detectable IR signal decays are diagnostic of feldspar contamination. Inset, the natural blue OSL signal (open triangle) of each aliquot is calibrated against known laboratory doses to yield equivalent dose (D_e) values. Repeats of low and high doses (open diamonds) illustrate the success of sensitivity correction.

Fig. 2 D_e Preheat Dependence The acquisition of D_e values is necessarily predicated upon thermal treatment of aliquots succeeding environmental and laboratory irradiation. The D_e preheat dependence test quantifies the combined effects of thermal transfer and sensitisation on the natural signal. Insignificant adjustment in D_e may reflect limited influence of these effects.

Fig. 3 Dose Recovery Attempts to replicate the above diagnostic, yet provide improved resolution of thermal effects through removal of variability induced by heterogeneous dose absorption in the environment and using a precise lab dose to simulate natural dose. Based on this and D_e preheat dependence data an appropriate thermal treatment is selected to refine the final D_e value.

Fig. 4 Inter-aliquot D_e distribution Provides a measure of inter-aliquot statistical concordance in D_e values derived from natural irradiation. Discordant data (those points lying beyond ± 2 standardised $\ln D_e$) reflects heterogeneous dose absorption and/or inaccuracies in calibration.

Fig. 5 Low and High Repeat Regenerative-dose Ratio Measures the statistical concordance of signals from repeated low and high regenerative-doses. Discordant data (those points lying beyond ± 2 standardised $\ln D_e$) indicate inaccurate sensitivity correction.

Fig. 6 OSL to Post-IR OSL Ratio Measures the statistical concordance of OSL and post-IR OSL responses to the same regenerative-dose. Discordant, underestimating data (those points lying below -2 standardised $\ln D_e$) highlight the presence of significant feldspar contamination.

Fig. 7 Signal Analysis Statistically significant increase in natural D_e value with signal stimulation period is indicative of a partially-bleached signal, provided a significant increase in D_e results from simulated partial bleaching followed by insignificant adjustment in D_e for simulated zero and full bleach conditions. Ages from such samples are considered maximum estimates. In the absence of a significant rise in D_e with stimulation time, simulated partial bleaching and zero/full bleach tests are not assessed.

Fig. 8 U Activity Statistical concordance (equilibrium) in the activities of the daughter radionuclide ^{226}Ra with its parent ^{238}U may signify the temporal stability of D_e emissions from these chains. Significant differences (disequilibrium; $>50\%$) in activity indicate addition or removal of isotopes creating a time-dependent shift in D_e values and increased uncertainty in the accuracy of age estimates. A 20% disequilibrium marker is also shown.

Fig. 9 Age Range The mean age range provides an estimate of sediment burial period based on mean D_e and D_e values with associated analytical uncertainties. The probability distribution indicates the inter-aliquot variability in age. The maximum influence of temporal variations in D_e forced by minima-maxima variation in moisture content and overburden thickness may prove instructive where there is uncertainty in these parameters, however the combined extremes represented should not be construed as preferred age estimates.

Fig. 2 D_e Preheat Dependence

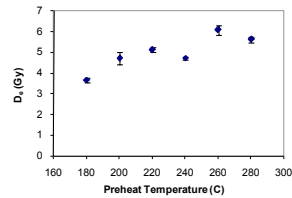


Fig. 3 Dose Recovery

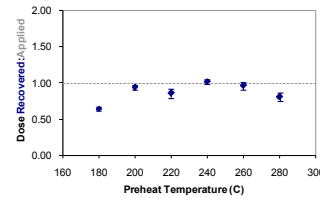


Fig. 4 Inter-aliquot D_e distribution

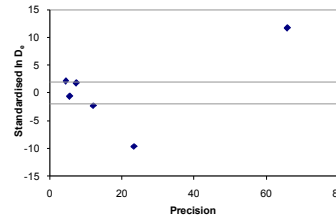


Fig. 5 Low and High Repeat Regenerative-dose Ratio

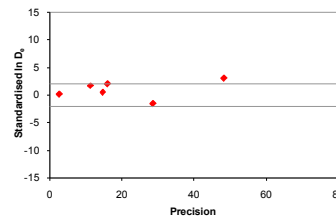


Fig. 6 OSL to Post-IR OSL Ratio

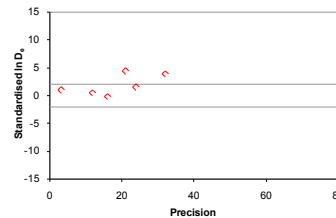


Fig. 7 Signal Analysis

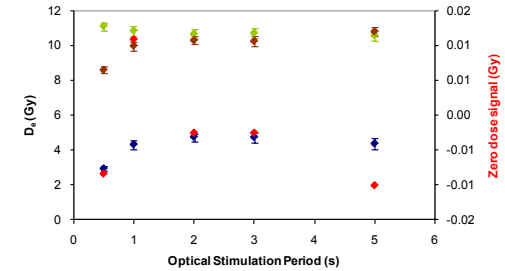


Fig. 8 U Decay Activity

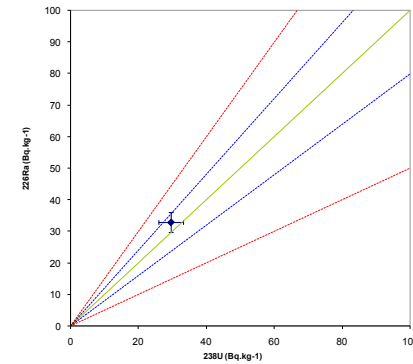
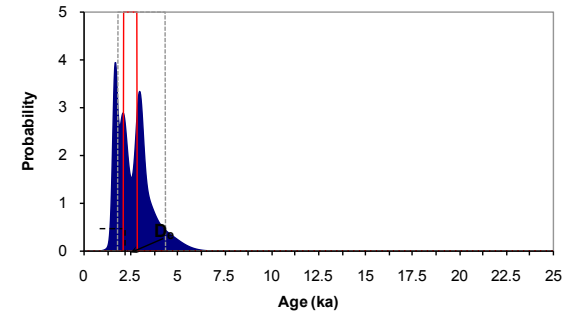


Fig. 9 Age Range



Sample: GL08059

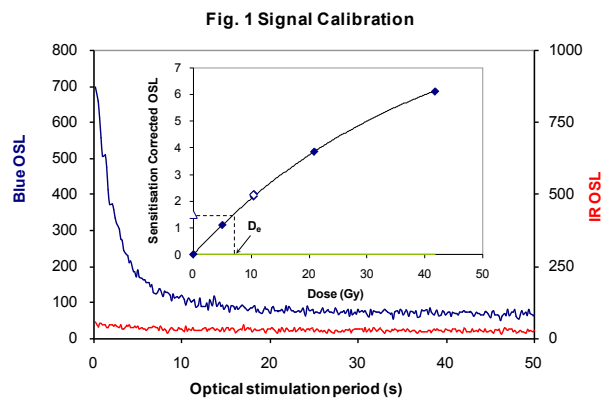


Fig. 1 Signal Calibration Natural blue and laboratory-induced infrared (IR) OSL signals. Detectable IR signal decays are diagnostic of feldspar contamination. Inset, the natural blue OSL signal (open triangle) of each aliquot is calibrated against known laboratory doses to yield equivalent dose (D_e) values. Repeats of low and high doses (open diamonds) illustrate the success of sensitivity correction.

Fig. 2 D_e Preheat Dependence The acquisition of D_e values is necessarily predicated upon thermal treatment of aliquots succeeding environmental and laboratory irradiation. The D_e preheat dependence test quantifies the combined effects of thermal transfer and sensitisation on the natural signal. Insignificant adjustment in D_e may reflect limited influence of these effects.

Fig. 3 Dose Recovery Attempts to replicate the above diagnostic, yet provide improved resolution of thermal effects through removal of variability induced by heterogeneous dose absorption in the environment and using a precise lab dose to simulate natural dose. Based on this and D_e preheat dependence data an appropriate thermal treatment is selected to refine the final D_e value.

Fig. 4 Inter-aliquot D_e distribution Provides a measure of inter-aliquot statistical concordance in D_e values derived from natural irradiation. Discordant data (those points lying beyond ± 2 standardised $\ln D_e$) reflects heterogeneous dose absorption and/or inaccuracies in calibration.

Fig. 5 Low and High Repeat Regenerative-dose Ratio Measures the statistical concordance of signals from repeated low and high regenerative-doses. Discordant data (those points lying beyond ± 2 standardised $\ln D_e$) indicate inaccurate sensitivity correction.

Fig. 6 OSL to Post-IR OSL Ratio Measures the statistical concordance of OSL and post-IR OSL responses to the same regenerative-dose. Discordant, underestimating data (those points lying below -2 standardised $\ln D_e$) highlight the presence of significant feldspar contamination.

Fig. 7 Signal Analysis Statistically significant increase in natural D_e value with signal stimulation period is indicative of a partially-bleached signal, provided a significant increase in D_e results from simulated partial bleaching followed by insignificant adjustment in D_e for simulated zero and full bleach conditions. Ages from such samples are considered maximum estimates. In the absence of a significant rise in D_e with stimulation time, simulated partial bleaching and zero/full bleach tests are not assessed.

Fig. 8 U Activity Statistical concordance (equilibrium) in the activities of the daughter radionuclide ^{226}Ra with its parent ^{238}U may signify the temporal stability of D_e emissions from these chains. Significant differences (disequilibrium; $>50\%$) in activity indicate addition or removal of isotopes creating a time-dependent shift in D_e values and increased uncertainty in the accuracy of age estimates. A 20% disequilibrium marker is also shown.

Fig. 9 Age Range The mean age range provides an estimate of sediment burial period based on mean D_e and D_e values with associated analytical uncertainties. The probability distribution indicates the inter-aliquot variability in age. The maximum influence of temporal variations in D_e , forced by minima-maxima variation in moisture content and overburden thickness may prove instructive where there is uncertainty in these parameters, however the combined extremes represented should not be construed as preferred age estimates.

Fig. 2 D_e Preheat Dependence

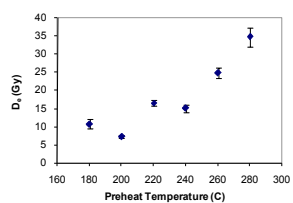


Fig. 3 Dose Recovery

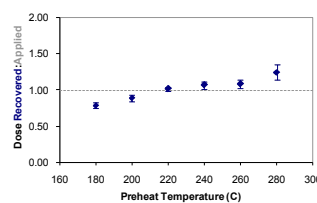


Fig. 4 Inter-aliquot D_e distribution

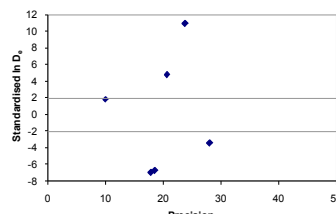


Fig. 5 Low and High Repeat Regenerative-dose Ratio

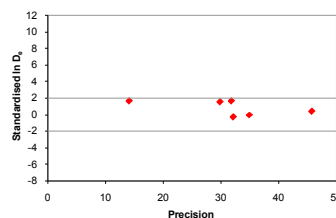


Fig. 6 OSL to Post-IR OSL Ratio

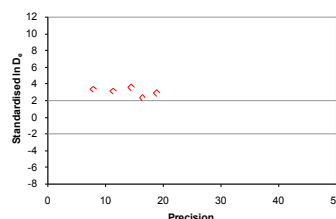


Fig. 7 Signal Analysis

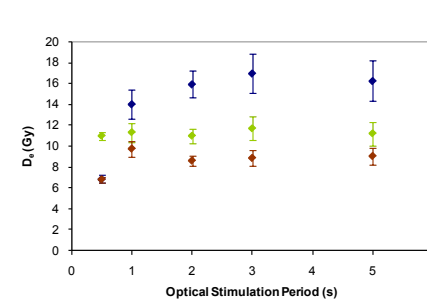


Fig. 8 U Decay Activity

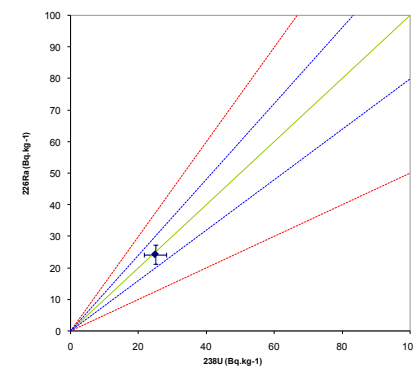
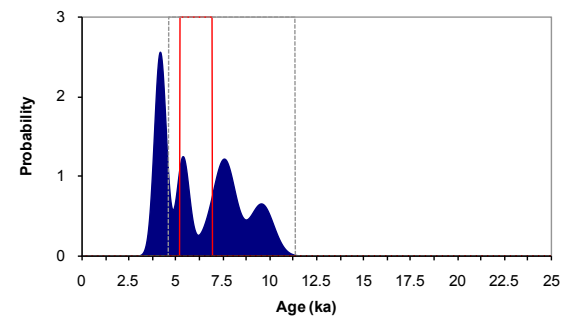


Fig. 9 Age Range



Sample: GL08057

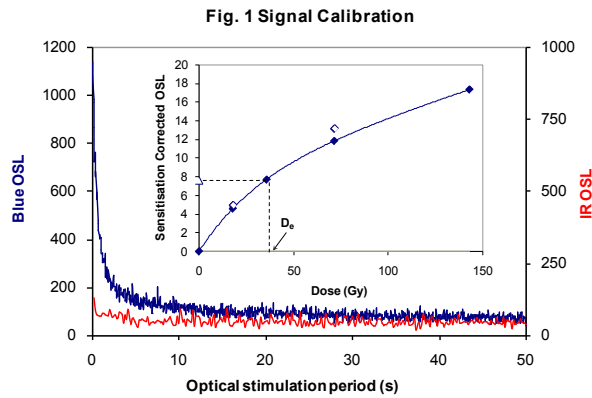


Fig. 1 Signal Calibration Natural blue and laboratory-induced infrared (IR) OSL signals. Detectable IR signal decays are diagnostic of feldspar contamination. Inset, the natural blue OSL signal (open triangle) of each aliquot is calibrated against known laboratory doses to yield equivalent dose (D_e) values. Repeats of low and high doses (open diamonds) illustrate the success of sensitivity correction.

Fig. 2 D_e Preheat Dependence The acquisition of D_e values is necessarily predicated upon thermal treatment of aliquots succeeding environmental and laboratory irradiation. The D_e preheat dependence test quantifies the combined effects of thermal transfer and sensitisation on the natural signal. Insignificant adjustment in D_e may reflect limited influence of these effects.

Fig. 3 Dose Recovery Attempts to replicate the above diagnostic, yet provide improved resolution of thermal effects through removal of variability induced by heterogeneous dose absorption in the environment and using a precise lab dose to simulate natural dose. Based on this and D_e preheat dependence data an appropriate thermal treatment is selected to refine the final D_e value.

Fig. 4 Inter-aliquot D_e distribution Provides a measure of inter-aliquot statistical concordance in D_e values derived from natural irradiation. Discordant data (those points lying beyond ± 2 standardised $\ln D_e$) reflects heterogeneous dose absorption and/or inaccuracies in calibration.

Fig. 5 Low and High Repeat Regenerative-dose Ratio Measures the statistical concordance of signals from repeated low and high regenerative-doses. Discordant data (those points lying beyond ± 2 standardised $\ln D_e$) indicate inaccurate sensitivity correction.

Fig. 6 OSL to Post-IR OSL Ratio Measures the statistical concordance of OSL and post-IR OSL responses to the same regenerative-dose. Discordant, underestimating data (those points lying below -2 standardised $\ln D_e$) highlight the presence of significant feldspar contamination.

Fig. 7 Signal Analysis Statistically significant increase in natural D_e value with signal stimulation period is indicative of a partially-bleached signal. Provided a significant increase in D_e results from simulated partial bleaching followed by insignificant adjustment in D_e for simulated zero and full bleach conditions. Ages from such samples are considered maximum estimates. In the absence of a significant rise in D_e with stimulation time, simulated partial bleaching and zero/full bleach tests are not assessed.

Fig. 8 U Activity Statistical concordance (equilibrium) in the activities of the daughter radionuclide ^{226}Ra with its parent ^{238}U may signify the temporal stability of D_e emissions from these chains. Significant differences (disequilibrium; $>50\%$) in activity indicate addition or removal of isotopes creating a time-dependent shift in D_e values and increased uncertainty in the accuracy of age estimates. A 20% disequilibrium marker is also shown.

Fig. 9 Age Range The mean age range provides an estimate of sediment burial period based on mean D_e and D_e values with associated analytical uncertainties. The probability distribution indicates the inter-aliquot variability in age. The maximum influence of temporal variations in D_e , forced by minima-maxima variation in moisture content and overburden thickness may prove instructive where there is uncertainty in these parameters, however the combined extremes represented should not be construed as preferred age estimates.

Fig. 2 D_e Preheat Dependence

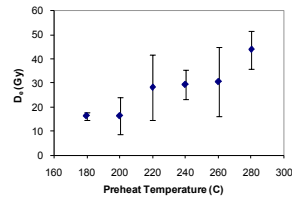


Fig. 3 Dose Recovery

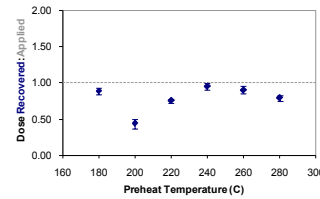


Fig. 4 Inter-aliquot D_e distribution

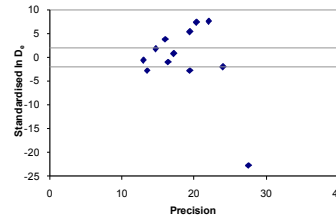


Fig. 5 Low and High Repeat Regenerative-dose Ratio

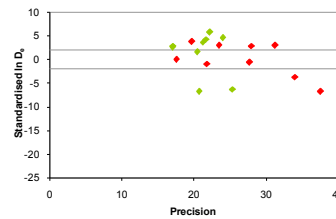


Fig. 6 OSL to Post-IR OSL Ratio

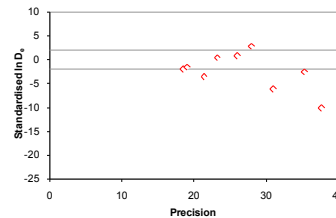


Fig. 7 Signal Analysis

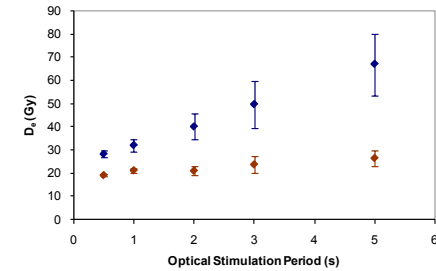


Fig. 8 U Decay Activity

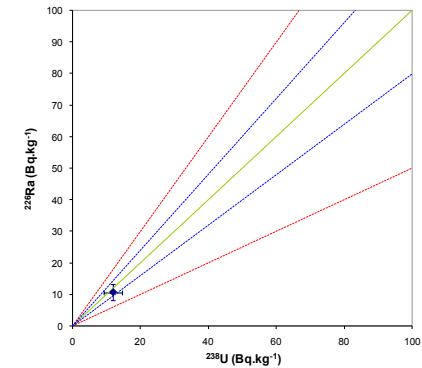
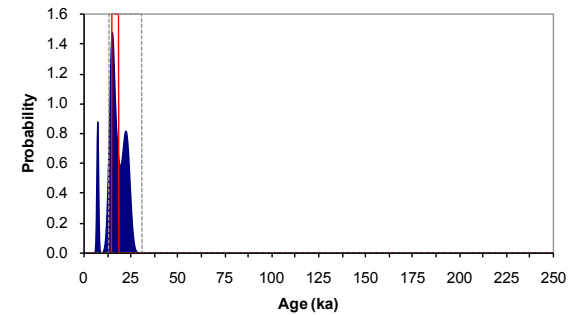


Fig. 9 Age Range



Sample: GL10021

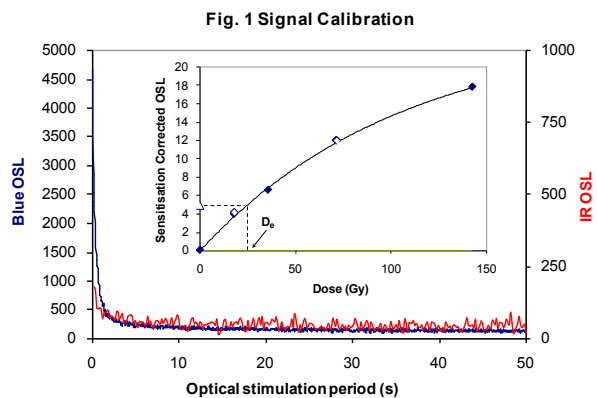


Fig. 1 Signal Calibration

Fig. 1 Signal Calibration Natural blue and laboratory-induced infrared (IR) OSL signals. Detectable IR signal decays are diagnostic of feldspar contamination. Inset, the natural blue OSL signal (open triangle) of each aliquot is calibrated against known laboratory doses to yield equivalent dose (D_e) values. Repeats of low and high doses (open diamonds) illustrate the success of sensitivity correction.

Fig. 2 D_e Preheat Dependence The acquisition of D_e values is necessarily predicated upon thermal treatment of aliquots succeeding environmental and laboratory irradiation. The D_e preheat dependence test quantifies the combined effects of thermal transfer and sensitisation on the natural signal. Insignificant adjustment in D_e may reflect limited influence of these effects.

Fig. 3 Dose Recovery Attempts to replicate the above diagnostic, yet provide improved resolution of thermal effects through removal of variability induced by heterogeneous dose absorption in the environment and using a precise lab dose to simulate natural dose. Based on this and D_e preheat dependence data an appropriate thermal treatment is selected to refine the final D_e value.

Fig. 4 Inter-aliquot D_e distribution Provides a measure of inter-aliquot statistical concordance in D_e values derived from natural irradiation. Discordant data (those points lying beyond ± 2 standardised in D_e) reflects heterogeneous dose absorption and/or inaccuracies in calibration.

Fig. 5 Low and High Repeat Regenerative-dose Ratio Measures the statistical concordance of signals from repeated low and high regenerative-doses. Discordant data (those points lying beyond ± 2 standardised in D_e) indicate inaccurate sensitivity correction.

Fig. 6 OSL to Post-IR OSL Ratio Measures the statistical concordance of OSL and post-IR OSL responses to the same regenerative-dose. Discordant, underestimating data (those points lying below ± 2 standardised in D_e) highlight the presence of significant feldspar contamination.

Fig. 7 Signal Analysis Statistically significant increase in natural D_e value with signal stimulation period is indicative of a partially-bleached signal, provided a significant increase in D_e results from simulated partial bleaching followed by insignificant adjustment in D_e for simulated zero and full bleach conditions. Ages from such samples are considered maximum estimates. In the absence of a significant rise in D_e with stimulation time, simulated partial bleaching and zero/full bleach tests are not assessed.

Fig. 8 U Activity Statistical concordance (equilibrium) in the activities of the daughter radionuclide ^{226}Ra with its parent ^{238}U may signify the temporal stability of D_e emissions from these chains. Significant differences (disequilibrium; $>50\%$) in activity indicate addition or removal of isotopes creating a time-dependent shift in D_e values and increased uncertainty in the accuracy of age estimates. A 20% disequilibrium marker is also shown.

Fig. 9 Age Range The mean age range provides an estimate of sediment burial period based on mean D_e and D_e values with associated analytical uncertainties. The probability distribution indicates the inter-aliquot variability in age. The maximum influence of temporal variations in D_e , forced by minima-maxima variation in moisture content and overburden thickness may prove instructive where there is uncertainty in these parameters, however the combined extremes represented should not be construed as preferred age estimates.

Fig. 2 D_e Preheat Dependence

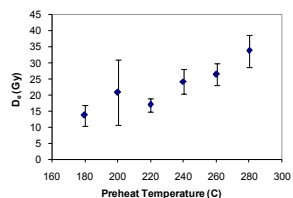


Fig. 3 Dose Recovery

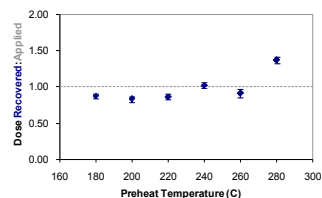


Fig. 4 Inter-aliquot D_e distribution

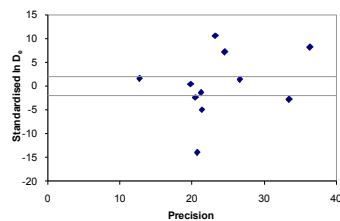


Fig. 5 Low and High Repeat Regenerative-dose Ratio

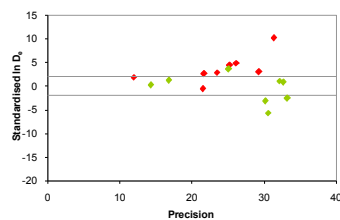


Fig. 6 OSL to Post-IR OSL Ratio

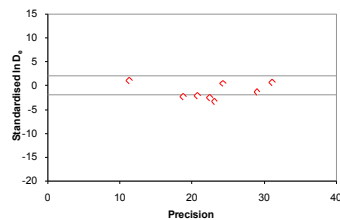


Fig. 7 Signal Analysis

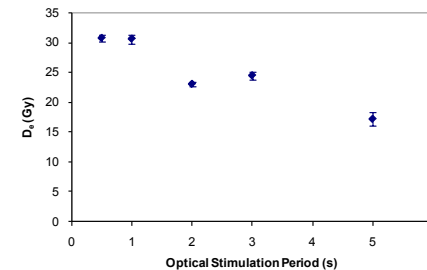


Fig. 8 U Decay Activity

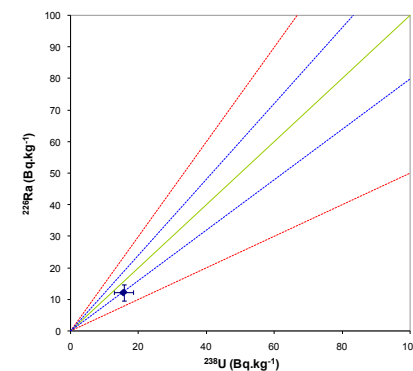
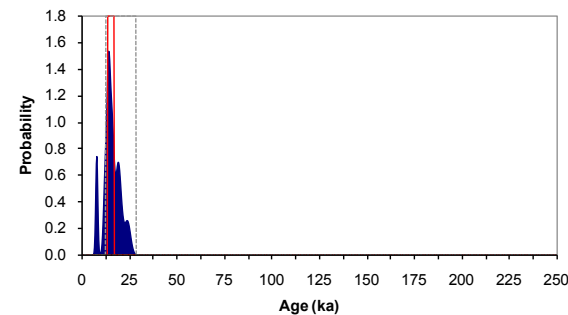


Fig. 9 Age Range



Sample: GL10022

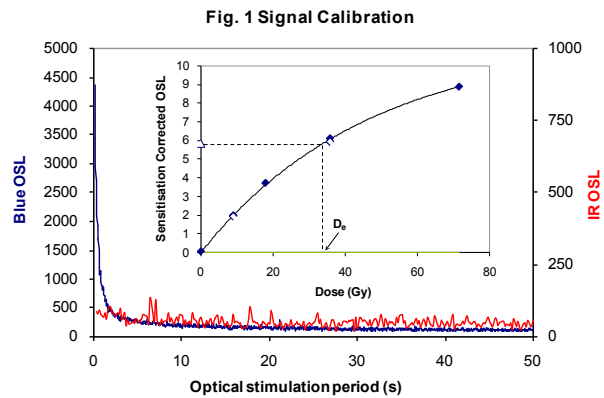


Fig. 1 Signal Calibration Natural blue and laboratory-induced infrared (IR) OSL signals. Detectable IR signal decays are diagnostic of feldspar contamination. Inset, the natural blue OSL signal (open triangle) of each aliquot is calibrated against known laboratory doses to yield equivalent dose (D_e) values. Repeats of low and high doses (open diamonds) illustrate the success of sensitivity correction.

Fig. 2 D_e Preheat Dependence The acquisition of D_e values is necessarily predicated upon thermal treatment of aliquots succeeding environmental and laboratory irradiation. The D_e preheat dependence test quantifies the combined effects of thermal transfer and sensitisation on the natural signal. Insignificant adjustment in D_e may reflect limited influence of these effects.

Fig. 3 Dose Recovery Attempts to replicate the above diagnostic, yet provide improved resolution of thermal effects through removal of variability induced by heterogeneous dose absorption in the environment and using a precise lab dose to simulate natural dose. Based on this and D_e preheat dependence data an appropriate thermal treatment is selected to refine the final D_e value.

Fig. 4 Inter-aliquot D_e distribution Provides a measure of inter-aliquot statistical concordance in D_e values derived from natural irradiation. Discordant data (those points lying beyond ± 2 standardised $\ln D_e$) reflects heterogeneous dose absorption and/or inaccuracies in calibration.

Fig. 5 Low and High Repeat Regenerative-dose Ratio Measures the statistical concordance of signals from repeated low and high regenerative-doses. Discordant data (those points lying beyond ± 2 standardised $\ln D_e$) indicate inaccurate sensitivity correction.

Fig. 6 OSL to Post-IR OSL Ratio Measures the statistical concordance of OSL and post-IR OSL responses to the same regenerative-dose. Discordant, underestimating data (those points lying below -2 standardised $\ln D_e$) highlight the presence of significant feldspar contamination.

Fig. 7 Signal Analysis Statistically significant increase in natural D_e value with signal stimulation period is indicative of a partially-bleached signal, provided a significant increase in D_e results from simulated partial bleaching followed by insignificant adjustment in D_e for simulated zero and full bleach conditions. Ages from such samples are considered maximum estimates. In the absence of a significant rise in D_e with stimulation time, simulated partial bleaching and zero/full bleach tests are not assessed.

Fig. 8 U Activity Statistical concordance (equilibrium) in the activities of the daughter radionuclide ^{226}Ra with its parent ^{238}U may signify the temporal stability of D_e emissions from these chains. Significant differences (disequilibrium; $>50\%$) in activity indicate addition or removal of isotopes creating a time-dependent shift in D_e values and increased uncertainty in the accuracy of age estimates. A 20% disequilibrium marker is also shown.

Fig. 9 Age Range The mean age range provides an estimate of sediment burial period based on mean D_e and D_e values with associated analytical uncertainties. The probability distribution indicates the inter-aliquot variability in age. The maximum influence of temporal variations in D_e , forced by minima-maxima variation in moisture content and overburden thickness may prove instructive where there is uncertainty in these parameters, however the combined extremes represented should not be construed as preferred age estimates.

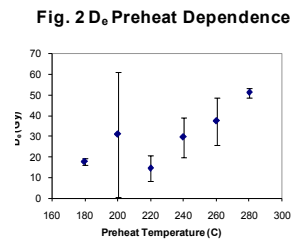


Fig. 2 D_e Preheat Dependence

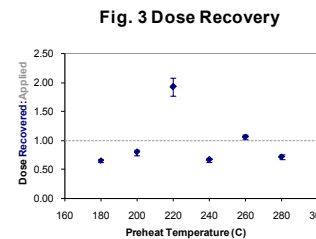


Fig. 3 Dose Recovery

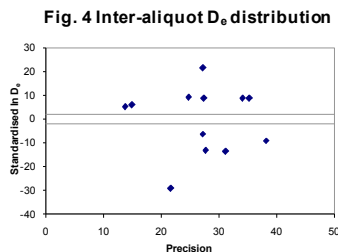


Fig. 4 Inter-aliquot D_e distribution

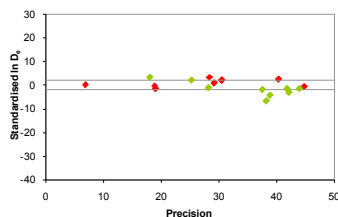


Fig. 5 Low and High Repeat Regenerative-dose Ratio

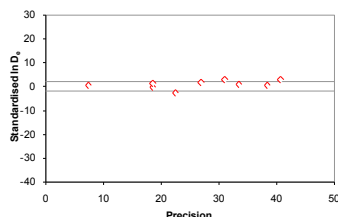


Fig. 6 OSL to Post-IR OSL Ratio

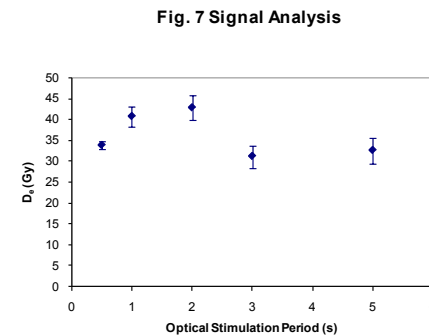


Fig. 7 Signal Analysis

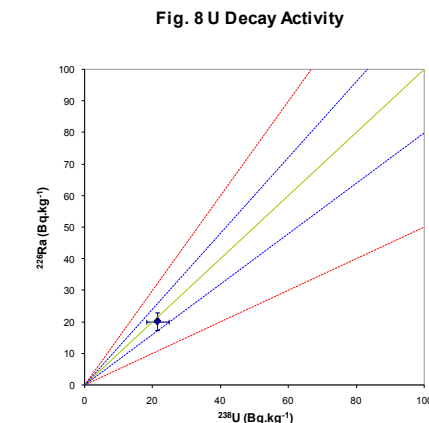


Fig. 8 U Decay Activity

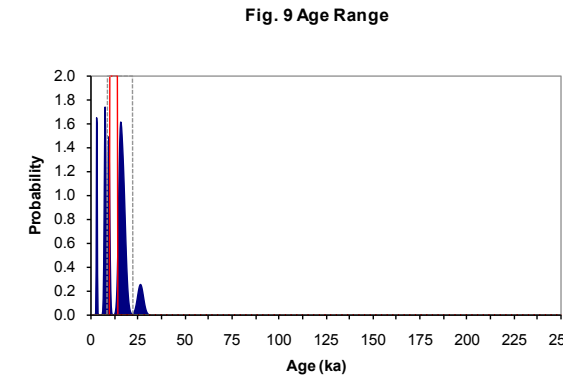


Fig. 9 Age Range

Sample: GL10023

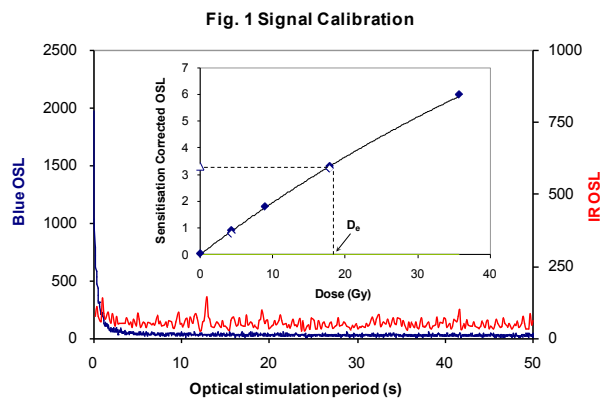


Fig. 1 Signal Calibration Natural blue and laboratory-induced infrared (IR) OSL signals. Detectable IR signal decays are diagnostic of feldspar contamination. Inset, the natural blue OSL signal (open triangle) of each aliquot is calibrated against known laboratory doses to yield equivalent dose (D_0) values. Repeats of low and high doses (open diamonds) illustrate the success of sensitivity correction.

Fig. 2 D_0 Preheat Dependence The acquisition of D_0 values is necessarily predicated upon thermal treatment of aliquots succeeding environmental and laboratory irradiation. The D_0 preheat dependence test quantifies the combined effects of thermal transfer and sensitisation on the natural signal. Insignificant adjustment in D_0 may reflect limited influence of these effects.

Fig. 3 Dose Recovery Attempts to replicate the above diagnostic, yet provide improved resolution of thermal effects through removal of variability induced by heterogeneous dose absorption in the environment and using a precise lab dose to simulate natural dose. Based on this and D_0 preheat dependence data an appropriate thermal treatment is selected to refine the final D_0 value.

Fig. 4 Inter-aliquot D_0 distribution Provides a measure of inter-aliquot statistical concordance in D_0 values derived from natural irradiation. Discordant data (those points lying beyond ± 2 standardised $\ln D_0$) reflects heterogeneous dose absorption and/or inaccuracies in calibration.

Fig. 5 Low and High Repeat Regenerative-dose Ratio Measures the statistical concordance of signals from repeated low and high regenerative-doses. Discordant data (those points lying beyond ± 2 standardised $\ln D_0$) indicate inaccurate sensitivity correction.

Fig. 6 OSL to Post-IR OSL Ratio Measures the statistical concordance of OSL and post-IR OSL responses to the same regenerative-dose. Discordant, underestimating data (those points lying below -2 standardised $\ln D_0$) highlight the presence of significant feldspar contamination.

Fig. 7 Signal Analysis Statistically significant increase in natural D_0 value with signal stimulation period is indicative of a partially-bleached signal, provided a significant increase in D_0 results from simulated partial bleaching followed by insignificant adjustment in D_0 for simulated zero and full bleach conditions. Ages from such samples are considered maximum estimates. In the absence of a significant rise in D_0 with stimulation time, simulated partial bleaching and zero/full bleach tests are not assessed.

Fig. 8 U Activity Statistical concordance (equilibrium) in the activities of the daughter radionuclide ^{226}Ra with its parent ^{238}U may signify the temporal stability of D_0 emissions from these chains. Significant differences (disequilibrium; $>50\%$) in activity indicate addition or removal of isotopes creating a time-dependent shift in D_0 values and increased uncertainty in the accuracy of age estimates. A 20% disequilibrium marker is also shown.

Fig. 9 Age Range The mean age range provides an estimate of sediment burial period based on mean D_0 and D_0 values with associated analytical uncertainties. The probability distribution indicates the inter-aliquot variability in age. The maximum influence of temporal variations in D_0 , forced by minima-maxima variation in moisture content and overburden thickness may prove instructive where there is uncertainty in these parameters, however the combined extremes represented should not be construed as preferred age estimates.

Fig. 2 D_0 Preheat Dependence

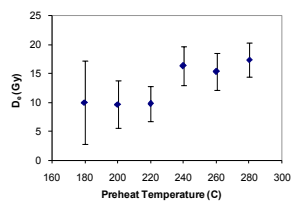


Fig. 3 Dose Recovery

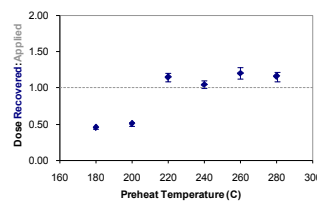


Fig. 4 Inter-aliquot D_0 distribution

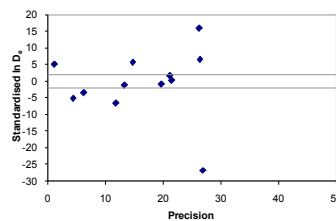


Fig. 5 Low and High Repeat Regenerative-dose Ratio

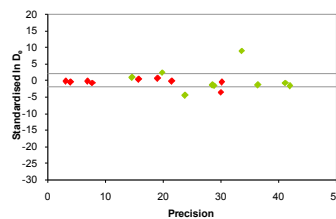


Fig. 6 OSL to Post-IR OSL Ratio

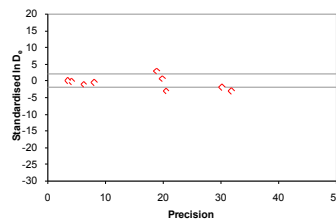


Fig. 7 Signal Analysis

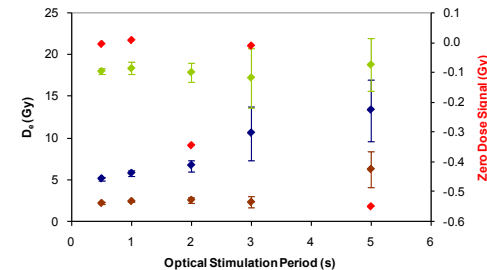


Fig. 8 U Decay Activity

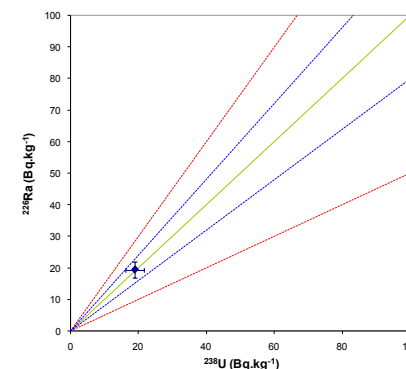
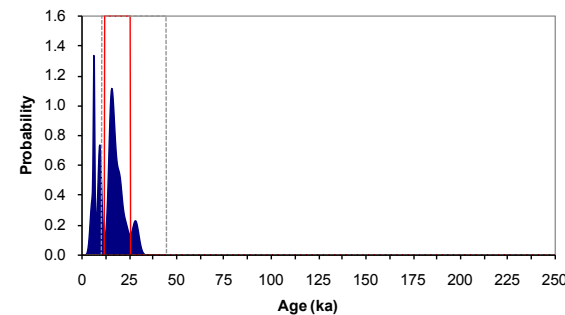


Fig. 9 Age Range



Sample: GL10017

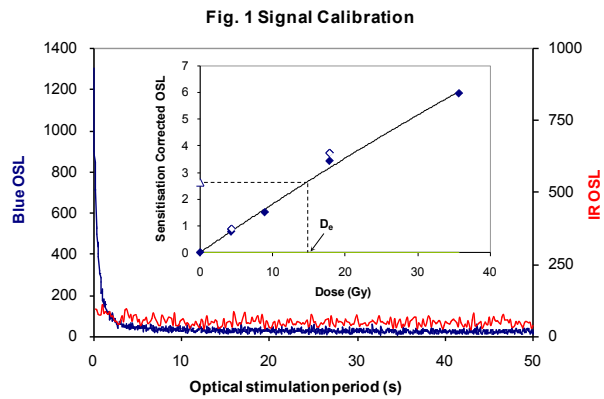


Fig. 1 Signal Calibration Natural blue and laboratory-induced infrared (IR) OSL signals. Detectable IR signal decays are diagnostic of feldspar contamination. Inset, the natural blue OSL signal (open triangle) of each aliquot is calibrated against known laboratory doses to yield equivalent dose (D_e) values. Repeats of low and high doses (open diamonds) illustrate the success of sensitivity correction.

Fig. 2 D_e Preheat Dependence The acquisition of D_e values is necessarily predicated upon thermal treatment of aliquots succeeding environmental and laboratory irradiation. The D_e preheat dependence test quantifies the combined effects of thermal transfer and sensitisation on the natural signal. Insignificant adjustment in D_e may reflect limited influence of these effects.

Fig. 3 Dose Recovery Attempts to replicate the above diagnostic, yet provide improved resolution of thermal effects through removal of variability induced by heterogeneous dose absorption in the environment and using a precise lab dose to simulate natural dose. Based on this and D_e preheat dependence data an appropriate thermal treatment is selected to refine the final D_e value.

Fig. 4 Inter-aliquot D_e distribution Provides a measure of inter-aliquot statistical concordance in D_e values derived from natural irradiation. Discordant data (those points lying beyond ± 2 standardised $\ln D_e$) reflects heterogeneous dose absorption and/or inaccuracies in calibration.

Fig. 5 Low and High Repeat Regenerative-dose Ratio Measures the statistical concordance of signals from repeated low and high regenerative-doses. Discordant data (those points lying beyond ± 2 standardised $\ln D_e$) indicate inaccurate sensitivity correction.

Fig. 6 OSL to Post-IR OSL Ratio Measures the statistical concordance of OSL and post-IR OSL responses to the same regenerative-dose. Discordant, underestimating data (those points lying below -2 standardised $\ln D_e$) highlight the presence of significant feldspar contamination.

Fig. 7 Signal Analysis Statistically significant increase in natural D_e value with signal stimulation period is indicative of a partially-bleached signal, provided a significant increase in D_e results from simulated partial bleaching followed by insignificant adjustment in D_e for simulated zero and full bleach conditions. Ages from such samples are considered maximum estimates. In the absence of a significant rise in D_e with stimulation time, simulated partial bleaching and zero/full bleach tests are not assessed.

Fig. 8 U Activity Statistical concordance (equilibrium) in the activities of the daughter radionuclide ^{226}Ra with its parent ^{238}U may signify the temporal stability of D_e emissions from these chains. Significant differences (disequilibrium; $>50\%$) in activity indicate addition or removal of isotopes creating a time-dependent shift in D_e values and increased uncertainty in the accuracy of age estimates. A 20% disequilibrium marker is also shown.

Fig. 9 Age Range The mean age range provides an estimate of sediment burial period based on mean D_e and D_e values with associated analytical uncertainties. The probability distribution indicates the inter-aliquot variability in age. The maximum influence of temporal variations in D_e , forced by minima-maxima variation in moisture content and overburden thickness may prove instructive where there is uncertainty in these parameters, however the combined extremes represented should not be construed as preferred age estimates.

Fig. 2 D_e Preheat Dependence

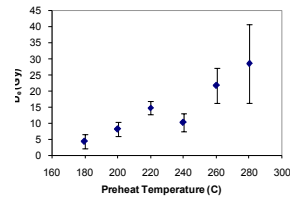


Fig. 3 Dose Recovery

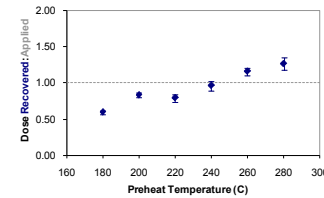


Fig. 4 Inter-aliquot D_e distribution

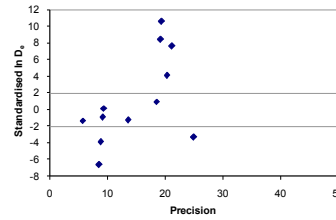


Fig. 5 Low and High Repeat Regenerative-dose Ratio

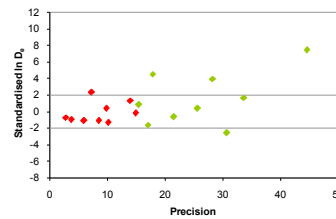


Fig. 6 OSL to Post-IR OSL Ratio

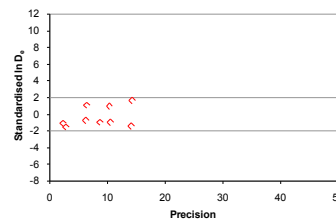


Fig. 7 Signal Analysis

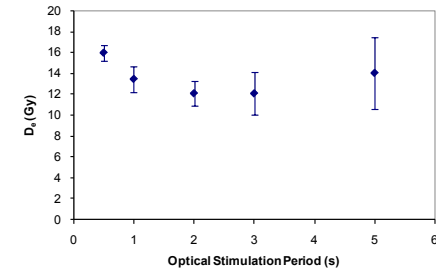


Fig. 8 U Decay Activity

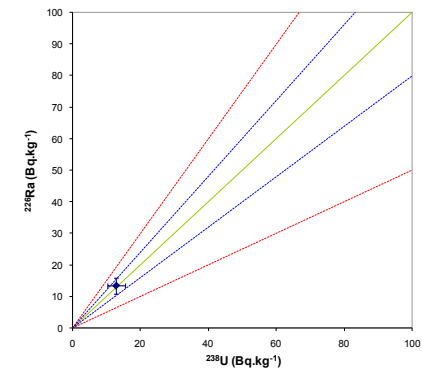
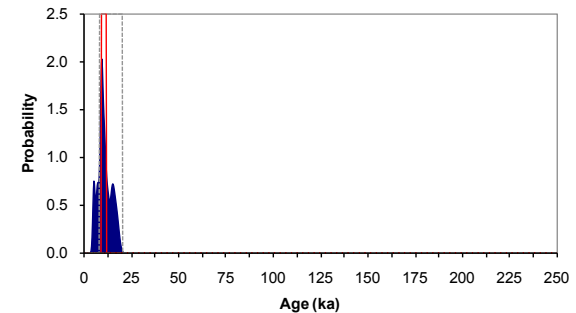


Fig. 9 Age Range



Sample: GL10018

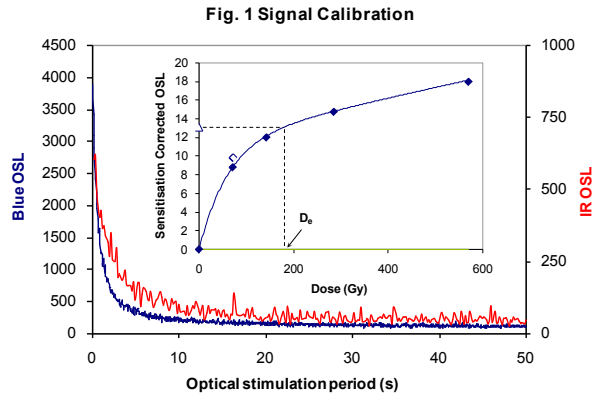


Fig. 1 Signal Calibration Natural blue and laboratory-induced infrared (IR) OSL signals. Detectable IR signal decays are diagnostic of feldspar contamination. Inset, the natural blue OSL signal (open triangle) of each aliquot is calibrated against known laboratory doses to yield equivalent dose (D_0) values. Repeats of low and high doses (open diamonds) illustrate the success of sensitivity correction.

Fig. 2 D_0 Preheat Dependence The acquisition of D_0 values is necessarily predicated upon thermal treatment of aliquots succeeding environmental and laboratory irradiation. The D_0 preheat dependence test quantifies the combined effects of thermal transfer and sensitisation on the natural signal. Insignificant adjustment in D_0 may reflect limited influence of these effects.

Fig. 3 Dose Recovery Attempts to replicate the above diagnostic, yet provide improved resolution of thermal effects through removal of variability induced by heterogeneous dose absorption in the environment and using a precise lab dose to simulate natural dose. Based on this and D_0 preheat dependence data an appropriate thermal treatment is selected to refine the final D_0 value.

Fig. 4 Inter-aliquot D_0 distribution Provides a measure of inter-aliquot statistical concordance in D_0 values derived from natural irradiation. Discordant data (those points lying beyond ± 2 standardised $\ln D_0$) reflects heterogeneous dose absorption and/or inaccuracies in calibration.

Fig. 5 Low and High Repeat Regenerative-dose Ratio Measures the statistical concordance of signals from repeated low and high regenerative-doses. Discordant data (those points lying beyond ± 2 standardised $\ln D_0$) indicate inaccurate sensitivity correction.

Fig. 6 OSL to Post-IR OSL Ratio Measures the statistical concordance of OSL and post-IR OSL responses to the same regenerative-dose. Discordant, underestimating data (those points lying below -2 standardised $\ln D_0$) highlight the presence of significant feldspar contamination.

Fig. 7 Signal Analysis Statistically significant increase in natural D_0 value with signal stimulation period is indicative of a partially-bleached signal, provided a significant increase in D_0 results from simulated partial bleaching followed by insignificant adjustment in D_0 for simulated zero and full bleach conditions. Ages from such samples are considered maximum estimates. In the absence of a significant rise in D_0 with stimulation time, simulated partial bleaching and zero/full bleach tests are not assessed.

Fig. 8 U Activity Statistical concordance (equilibrium) in the activities of the daughter radionuclide ^{226}Ra with its parent ^{238}U may signify the temporal stability of D_0 emissions from these chains. Significant differences (disequilibrium; $>50\%$) in activity indicate addition or removal of isotopes creating a time-dependent shift in D_0 values and increased uncertainty in the accuracy of age estimates. A 20% disequilibrium marker is also shown.

Fig. 9 Age Range The mean age range provides an estimate of sediment burial period based on mean D_0 and D_0 values with associated analytical uncertainties. The probability distribution indicates the inter-aliquot variability in age. The maximum influence of temporal variations in D_0 forced by minima-maxima variation in moisture content and overburden thickness may prove instructive where there is uncertainty in these parameters, however the combined extremes represented should not be construed as preferred age estimates.

Fig. 2 D_0 Preheat Dependence

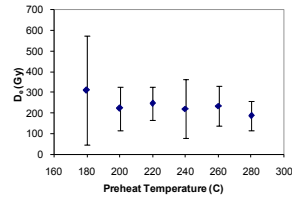


Fig. 3 Dose Recovery

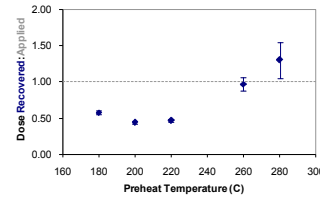


Fig. 4 Inter-aliquot D_0 distribution

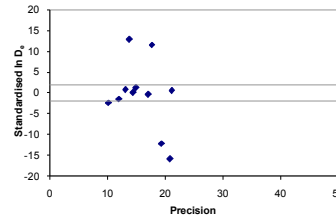


Fig. 5 Low and High Repeat Regenerative-dose Ratio

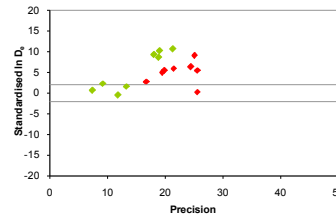


Fig. 6 OSL to Post-IR OSL Ratio

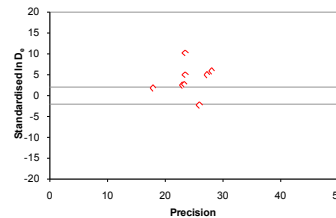


Fig. 7 Signal Analysis

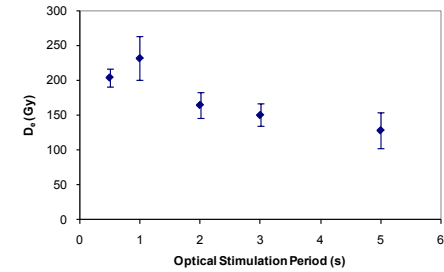


Fig. 8 U Decay Activity

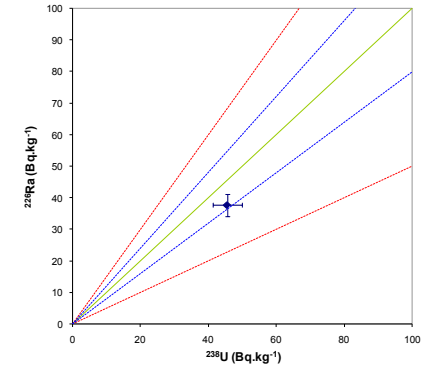
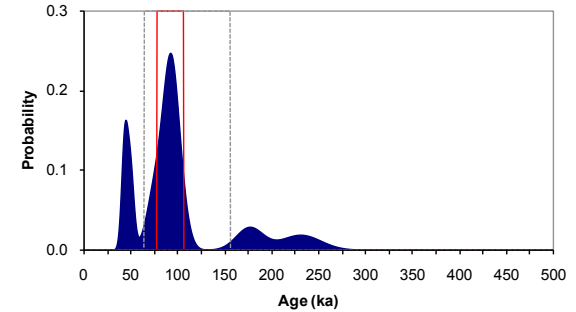


Fig. 9 Age Range



Sample: GL10024

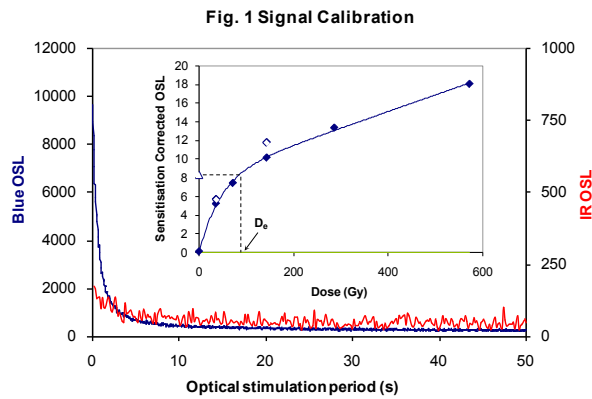


Fig. 1 Signal Calibration Natural blue and laboratory-induced infrared (IR) OSL signals. Detectable IR signal decays are diagnostic of feldspar contamination. Inset, the natural blue OSL signal (open triangle) of each aliquot is calibrated against known laboratory doses to yield equivalent dose (D_0) values. Repeats of low and high doses (open diamonds) illustrate the success of sensitivity correction.

Fig. 2 D_0 Preheat Dependence The acquisition of D_0 values is necessarily predicated upon thermal treatment of aliquots succeeding environmental and laboratory irradiation. The D_0 preheat dependence test quantifies the combined effects of thermal transfer and sensitisation on the natural signal. Insignificant adjustment in D_0 may reflect limited influence of these effects.

Fig. 3 Dose Recovery Attempts to replicate the above diagnostic, yet provide improved resolution of thermal effects through removal of variability induced by heterogeneous dose absorption in the environment and using a precise lab dose to simulate natural dose. Based on this and D_0 preheat dependence data an appropriate thermal treatment is selected to refine the final D_0 value.

Fig. 4 Inter-aliquot D_0 distribution Provides a measure of inter-aliquot statistical concordance in D_0 values derived from natural irradiation. Discordant data (those points lying beyond ± 2 standardised in D_0) reflects heterogeneous dose absorption and/or inaccuracies in calibration.

Fig. 5 Low and High Repeat Regenerative-dose Ratio Measures the statistical concordance of signals from repeated low and high regenerative-doses. Discordant data (those points lying beyond ± 2 standardised in D_0) indicate inaccurate sensitivity correction.

Fig. 6 OSL to Post-IR OSL Ratio Measures the statistical concordance of OSL and post-IR OSL responses to the same regenerative-dose. Discordant, underestimating data (those points lying below -2 standardised in D_0) highlight the presence of significant feldspar contamination.

Fig. 7 Signal Analysis Statistically significant increase in natural D_0 value with signal stimulation period is indicative of a partially-bleached signal. Provided a significant increase in D_0 results from simulated partial bleaching followed by insignificant adjustment in D_0 for simulated zero and full bleach conditions. Ages from such samples are considered maximum estimates. In the absence of a significant rise in D_0 with stimulation time, simulated partial bleaching and zero/full bleach tests are not assessed.

Fig. 8 U Activity Statistical concordance (equilibrium) in the activities of the daughter radionuclide ^{226}Ra with its parent ^{238}U may signify the temporal stability of D_0 emissions from these chains. Significant differences (disequilibrium; $>50\%$) in activity indicate addition or removal of isotopes creating a time-dependent shift in D_0 values and increased uncertainty in the accuracy of age estimates. A 20% disequilibrium marker is also shown.

Fig. 9 Age Range The mean age range provides an estimate of sediment burial period based on mean D_0 and D_0 values with associated analytical uncertainties. The probability distribution indicates the inter-aliquot variability in age. The maximum influence of temporal variations in D_0 , forced by minima-maxima variation in moisture content and overburden thickness may prove instructive where there is uncertainty in these parameters, however the combined extremes represented should not be construed as preferred age estimates.

Fig. 2 D_0 Preheat Dependence

Insufficient sample mass

Fig. 3 Dose Recovery

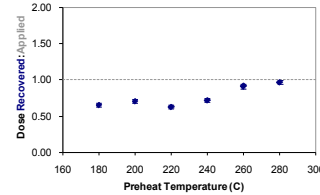


Fig. 7 Signal Analysis

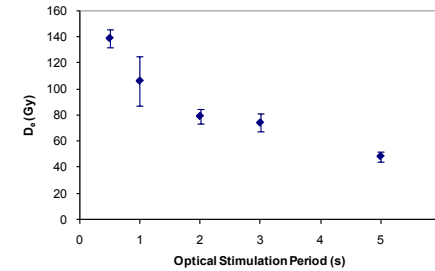


Fig. 4 Inter-aliquot D_0 distribution

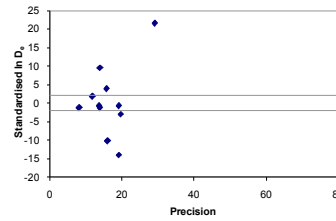


Fig. 5 Low and High Repeat Regenerative-dose Ratio

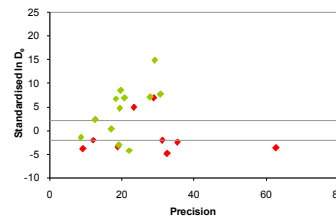


Fig. 8 U Decay Activity

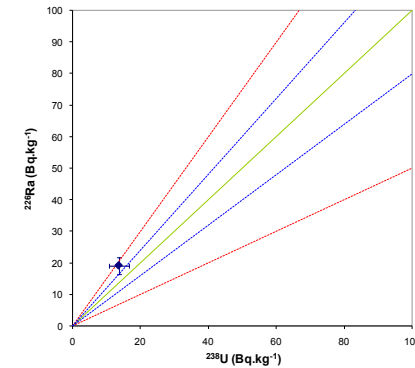


Fig. 6 OSL to Post-IR OSL Ratio

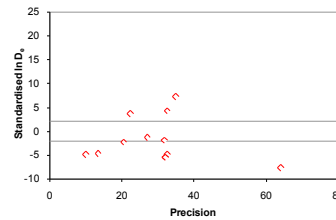
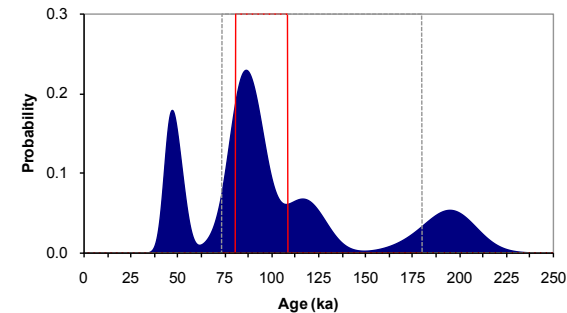


Fig. 9 Age Range



Sample: GL10025

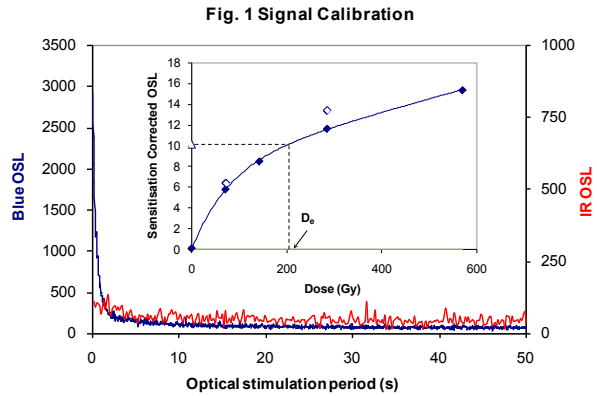


Fig. 1 Signal Calibration Natural blue and laboratory-induced infrared (IR) OSL signals. Detectable IR signal decays are diagnostic of feldspar contamination. Inset, the natural blue OSL signal (open triangle) of each aliquot is calibrated against known laboratory doses to yield equivalent dose (D_e) values. Repeats of low and high doses (open diamonds) illustrate the success of sensitivity correction.

Fig. 2 D_e Preheat Dependence The acquisition of D_e values is necessarily predicated upon thermal treatment of aliquots succeeding environmental and laboratory irradiation. The D_e preheat dependence test quantifies the combined effects of thermal transfer and sensitisation on the natural signal. Insignificant adjustment in D_e may reflect limited influence of these effects.

Fig. 3 Dose Recovery Attempts to replicate the above diagnostic, yet provide improved resolution of thermal effects through removal of variability induced by heterogeneous dose absorption in the environment and using a precise lab dose to simulate natural dose. Based on this and D_e preheat dependence data an appropriate thermal treatment is selected to refine the final D_e value.

Fig. 4 Inter-aliquot D_e distribution Provides a measure of inter-aliquot statistical concordance in D_e values derived from natural irradiation. Discordant data (those points lying beyond ± 2 standardised $\ln D_e$) reflects heterogeneous dose absorption and/or inaccuracies in calibration.

Fig. 5 Low and High Repeat Regenerative-dose Ratio Measures the statistical concordance of signals from repeated low and high regenerative-doses. Discordant data (those points lying beyond ± 2 standardised $\ln D_e$) indicate inaccurate sensitivity correction.

Fig. 6 OSL to Post-IR OSL Ratio Measures the statistical concordance of OSL and post-IR OSL responses to the same regenerative-dose. Discordant, underestimating data (those points lying below -2 standardised $\ln D_e$) highlight the presence of significant feldspar contamination.

Fig. 7 Signal Analysis Statistically significant increase in natural D_e value with signal stimulation period is indicative of a partially-bleached signal, provided a significant increase in D_e results from simulated partial bleaching followed by insignificant adjustment in D_e for simulated zero and full bleach conditions. Ages from such samples are considered maximum estimates. In the absence of a significant rise in D_e with stimulation time, simulated partial bleaching and zero/full bleach tests are not assessed.

Fig. 8 U Activity Statistical concordance (equilibrium) in the activities of the daughter radionuclide ^{226}Ra with its parent ^{238}U may signify the temporal stability of D_e emissions from these chains. Significant differences (disequilibrium; $>50\%$) in activity indicate addition or removal of isotopes creating a time-dependent shift in D_e values and increased uncertainty in the accuracy of age estimates. A 20% disequilibrium marker is also shown.

Fig. 9 Age Range The mean age range provides an estimate of sediment burial period based on mean D_e and D_e values with associated analytical uncertainties. The probability distribution indicates the inter-aliquot variability in age. The maximum influence of temporal variations in D_e forced by minima-maxima variation in moisture content and overburden thickness may prove instructive where there is uncertainty in these parameters, however the combined extremes represented should not be construed as preferred age estimates.

Fig. 2 D_e Preheat Dependence

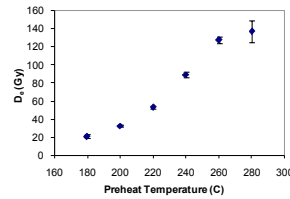


Fig. 3 Dose Recovery

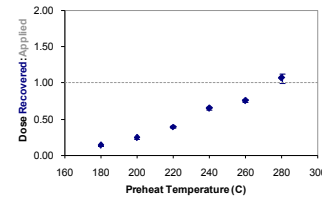


Fig. 4 Inter-aliquot D_e distribution

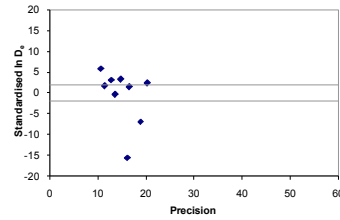


Fig. 5 Low and High Repeat Regenerative-dose Ratio

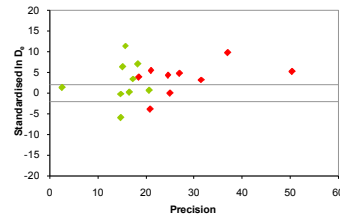


Fig. 6 OSL to Post-IR OSL Ratio

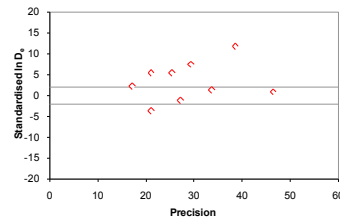


Fig. 7 Signal Analysis

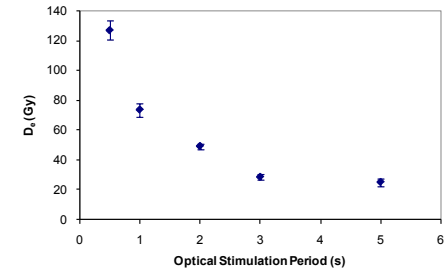


Fig. 8 U Decay Activity

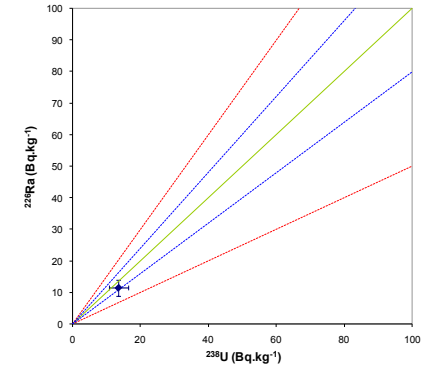
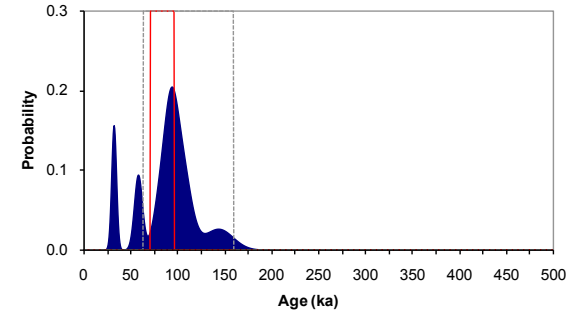


Fig. 9 Age Range



Sample: GL10027

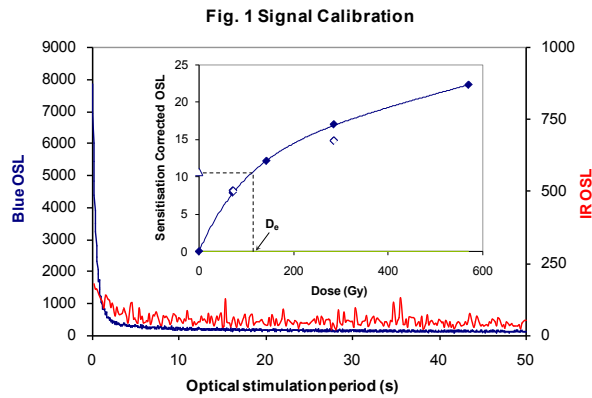


Fig. 1 Signal Calibration Natural blue and laboratory-induced infrared (IR) OSL signals. Detectable IR signal decays are diagnostic of feldspar contamination. Inset, the natural blue OSL signal (open triangle) of each aliquot is calibrated against known laboratory doses to yield equivalent dose (D_e) values. Repeats of low and high doses (open diamonds) illustrate the success of sensitivity correction.

Fig. 2 D_e Preheat Dependence The acquisition of D_e values is necessarily predicated upon thermal treatment of aliquots succeeding environmental and laboratory irradiation. The D_e preheat dependence test quantifies the combined effects of thermal transfer and sensitisation on the natural signal. Insignificant adjustment in D_e may reflect limited influence of these effects.

Fig. 3 Dose Recovery Attempts to replicate the above diagnostic, yet provide improved resolution of thermal effects through removal of variability induced by heterogeneous dose absorption in the environment and using a precise lab dose to simulate natural dose. Based on this and D_e preheat dependence data an appropriate thermal treatment is selected to refine the final D_e value.

Fig. 4 Inter-aliquot D_e distribution Provides a measure of inter-aliquot statistical concordance in D_e values derived from natural irradiation. Discordant data (those points lying beyond ± 2 standardised $\ln D_e$) reflects heterogeneous dose absorption and/or inaccuracies in calibration.

Fig. 5 Low and High Repeat Regenerative-dose Ratio Measures the statistical concordance of signals from repeated low and high regenerative-doses. Discordant data (those points lying beyond ± 2 standardised $\ln D_e$) indicate inaccurate sensitivity correction.

Fig. 6 OSL to Post-IR OSL Ratio Measures the statistical concordance of OSL and post-IR OSL responses to the same regenerative-dose. Discordant, underestimating data (those points lying below -2 standardised $\ln D_e$) highlight the presence of significant feldspar contamination.

Fig. 7 Signal Analysis Statistically significant increase in natural D_e value with signal stimulation period is indicative of a partially-bleached signal, provided a significant increase in D_e results from simulated partial bleaching followed by insignificant adjustment in D_e for simulated zero and full bleach conditions. Ages from such samples are considered maximum estimates. In the absence of a significant rise in D_e with stimulation time, simulated partial bleaching and zero/full bleach tests are not assessed.

Fig. 8 U Activity Statistical concordance (equilibrium) in the activities of the daughter radionuclide ^{226}Ra with its parent ^{238}U may signify the temporal stability of D_e emissions from these chains. Significant differences (disequilibrium; $>50\%$) in activity indicate addition or removal of isotopes creating a time-dependent shift in D_e values and increased uncertainty in the accuracy of age estimates. A 20% disequilibrium marker is also shown.

Fig. 9 Age Range The mean age range provides an estimate of sediment burial period based on mean D_e and D_e values with associated analytical uncertainties. The probability distribution indicates the inter-aliquot variability in age. The maximum influence of temporal variations in D_e forced by minima-maxima variation in moisture content and overburden thickness may prove instructive where there is uncertainty in these parameters, however the combined extremes represented should not be construed as preferred age estimates.

Fig. 2 D_e Preheat Dependence

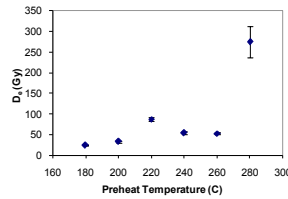


Fig. 3 Dose Recovery

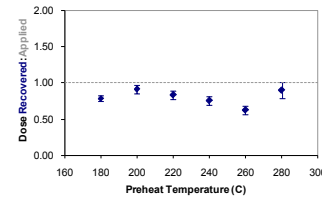


Fig. 7 Signal Analysis

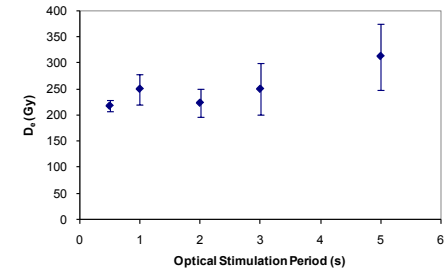


Fig. 4 Inter-aliquot D_e distribution

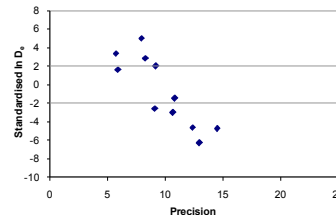


Fig. 8 U Decay Activity

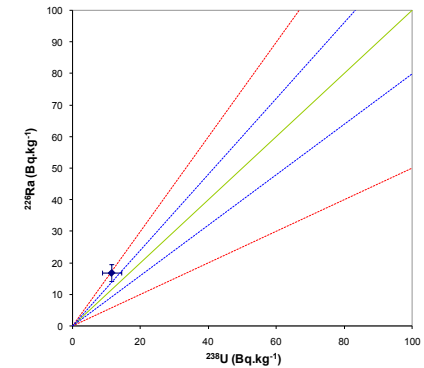


Fig. 5 Low and High Repeat Regenerative-dose Ratio

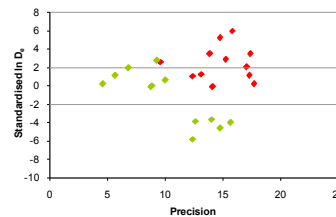


Fig. 6 OSL to Post-IR OSL Ratio

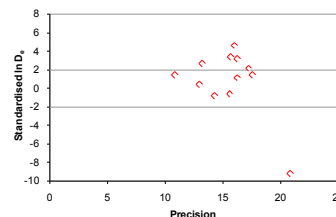
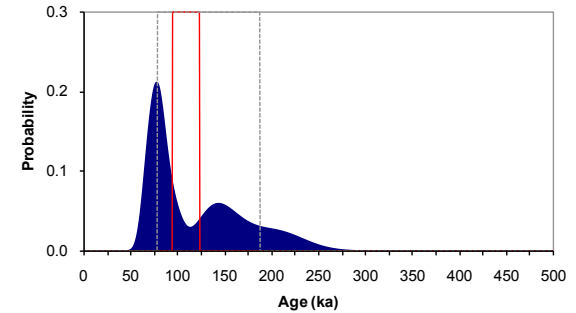


Fig. 9 Age Range



Sample: GL10026

Appendix 4

Mapping and assessment of palaeochannels and other features with potential organic survival using historic and OS mapping

1. Mapping

The potential for mapping of geomorphological features with palaeoenvironmental potential from OS, other historic maps and aerial photographs has been recognised elsewhere (Baker 2006). This was undertaken for the two pilot study areas.

Methodology was based upon map-based approaches developed within the Trent Valley (Baker 2006; Baker 2007) and also by the WHEAS environmental team on three study areas within Worcestershire.

The focus of the work lay in identifying features visible on 1st edition (1880s) OS maps which may contain organic deposits and have potential for palaeoenvironmental studies. Other GIS layers were also consulted including the 2nd Edition OS map, modern OS maps, aerial photographs and the Historic Environment Record (HER).

The following features of both natural and artificial origin were identified and digitally mapped as a separate layer within the project GIS (ArcGIS 9, ARCMAP: Version 9.3):

- Peat bog, reed swamp;
- Osier beds;
- Natural ponds;
- Areas where a watercourse follows along a parish or County boundary, then diverts (usually a meander separates away from the boundary line). Peat deposits may have formed inside the meander, and as most boundaries have their origins in the early medieval period, any peaty areas located in such areas may be of some antiquity. Marked as 'meander movement'. Pronounced meander loops were also included;
- Visible former channel alignments (on aerial photographs);
- Fishponds and moats; and
- Mill ponds, leats and races

Polygons were traced over each feature type and relevant information on each feature added in an 'attribute' table.

The resultant mapping was compared with the paleochannel mapping derived from the LiDAR analysis to provide a cross-checking mechanism and thus more comprehensive and reliable information on palaeochannels.

2. Scoring of features according to potential

An assessment was made of the potential for analysis for each feature based upon estimated size on the 1st Edition OS map/AP transcription and any apparent change in the waterlogged state of the feature on modern OS maps, such as drying out or silting up.

Secondly, accessibility was scored based upon the extent to which the feature is presently covered by development such as buildings, tarmac or trees. Features were 'flagged' where there was archaeological or historical information available through the HER which is of direct relevance. This did not, however, affect the scoring as high scores are biased towards features of known archaeological or historical relevance but many natural features of unknown date could also be of high potential.

This is a basic level of scoring intended to be used as a first stage of assessment for all projects using this mapping data. Table 1 shows the questions that were applied to each feature to facilitate the scoring of potential. Under each question is a direction to which source was referred to. The scores are weighted to take account of how important these aspects are in assessing the potential. For questions 2 and 3 a level of personal interpretation is needed.

Questions	Aspect of potential represented	Potential		
		LOW	HIGH	
What is the surface area of the feature? (Refer to 1 st Ed OS map)	Potential for organic remains to survive	Small (<500m ²) 1	Medium (501-1999m ²) 3	Large (2000> m ²) 5
Has there been any change in the apparent level of waterlogging? (Compare between 1 st Ed OS and modern map)	Potential for organic remains to survive	Major Change (No longer mapped) 1	Minor Change (A decrease but still there) 2	No Change or a 'Positive' Change 3
To what level is the feature accessible/covered today? (Refer to modern map)	Accessibility	Fully Covered 1	Semi/Partially Covered 3	Open 5

Table 1: Scoring system for assessing potential

The size of the feature is particularly important as the larger the feature the greater the potential for organic deposits to survive. Larger volumes of organic material are less prone to wetting and drying and consequently decay. The potential for recovering a sequence which represents a long time span and several phases of environmental change is also greater. For this work only surface area can be recorded as volume (the ideal measurement) is unknown.

The extent to which there have been changes in waterlogging of the features has also been used to assess the potential for organic deposits to survive. This was estimated by comparing the extent of waterlogging indicated on both first Edition OS and the modern OS maps (also by referring to any aerial photographs available). Any major drying out may have caused decay of organic deposits.

The accessibility of the mapped features was determined by categorising these as 'open', 'semi-open' or 'covered' according to the modern OS map and any aerial photographs available. The extent to which cover will have damaged the deposits and the likelihood of this cover being removed may vary with the type of cover (trees, buildings or hard surfaces for example). This variability was not considered but should be considered for any more detailed scoring potential.

In addition, where information on the history or archaeology of a feature was available on the HER it was added to the 'attribute' table and was flagged on the GIS map. This information was not used in scoring potential as, for instance, availability of documentary evidence on a medieval moat may improve the potential of this feature for projects focussing on medieval landscape but not for those focussing on prehistoric landscape: potential needs to be considered in a more general form.

The overall potential of the features was then categorised as high, medium and low based on the scores detailed in Table 2.

Scale of feature (m ²)	Total Sum	Priority Level	Priority Score
Large (2000>)	13	High – Green	1
	8-12	Medium – Amber	2
	7	Low – Red	3
Medium (501- 999)	11	High – Green	1
	6-10	Medium – Amber	2
	5	Low – Red	3
Small (<500)	9	High – Green	1
	4-8	Medium – Amber	2
	3	Low – Red	3

Table 2: Scoring

Note: Although no 'ground truthing' of these deposits through augering was undertaken, the importance of undertaking such work is recognised and is included as a suggested future task for any extension project which may be developed.

Appendix 5: Model Report Form

THE GEOARCHAEOLOGICAL RESOURCE OF THE LOWER SEVERN VALLEY				
LANDFORM UNIT GEOMORPHOLOGICAL CHARACTER				
POLYGON NO		COUNTY		CENTROID
HER REFERENCE		INTERPRETATION		
ASSOCIATED LANDFORM UNITS	POLYGON NUMBERS			
	DESCRIPTION			
UNIT DESCRIPTION				
HLC TYPE				
CULTURAL ASSOCIATIONS	NEW MONUMENTS			
	DESCRIPTION			
POTENTIAL				

Appendix 6: Worcestershire Report Forms

THE GEOARCHAEOLOGICAL RESOURCE OF THE LOWER SEVERN VALLEY					
LANDFORM UNIT GEOMORPHOLOGICAL CHARACTER					
POLYGON NO	4000	COUNTY	Worcestershire	CENTROID	384399/24 6227
HER REFERENCE	N/A	INTERPRETATION	Floodplain		
ASSOCIATED LANDFORM UNITS	POLYGON NUMBERS	Palaeochannels 4047, 4046, 4049, 4048, 4066, 4043, 4071, 4042 Levees: 4069, 4070, 4073			
	DESCRIPTION	The modern river has deposited overbank material over the floodplain in 3 discrete levees along the length of the study. Although there are 8 palaeochannels visible within the floodplain, 6 of these are small in comparison to polygons 4071 and 4074 that are between 90-110m wide. Although not confirmed, it is thought that these two channels are segments of a larger channel that has been truncated by the present river. Polygon 4071 has previously been examined and has provided both plant macrofossil and palynological remains recording the valley's environmental history between 4690-4450 cal BC to 1040-830 cal BC.			
UNIT DESCRIPTION	<p>Current flood plain of the River Severn is approximately 8km long and 1km wide and covers an area of 4.13km². This contains is deep alluvial deposits, the upper surface of which are at a height of between 10.89-12.22m OD.</p> <p>The cut of the current floodplain appears to have eroded former terrace units more on the western side of the Severn as Terraces 4 and 5 appear better preserved/wider on the east side of the river.</p>				
HLC TYPE	Watermeadow and Field Amalgamation polygons dominate the current floodplain but the floodplain also includes areas of Ornamental, Parkland and Recreational, Modern Subdivision, Parliamentary Enclosure, Recent Woodland, Woodland Plantation.				
CULTURAL ASSOCIATIONS	NEW MONUMENTS	3002: Enclosure/field boundary.			
	DESCRIPTION	<p>Only one prehistoric (Iron Age) and one Roman settlement have been identified on the floodplain, although there are three undated enclosures and 1 undated cluster of cropmarks that may also be of prehistoric/Roman origin. Two Bronze Age spears have been found as find spots in the banks of the river.</p> <p>As would be expected monuments on the floodplain are dominated by remains associated with the river. These include medieval quays and fish weirs, a post-medieval ferry/landing stage and a sunken barge. Landscape components of the floodplain include medieval and post-medieval ridge and furrow and water-meadow systems.</p> <p>Modern archaeological remains are dominated by Second World War defences intended to stop planes landing on the flood plain.</p>			
POTENTIAL	The current floodplain has the potential to preserve archaeological remains from prehistoric to modern in date. Pre-medieval remains are likely to be buried below deep alluvial deposits and this material may account for the lack of cropmarks on the floodplain. Only 1 possible enclosure was identified within the floodplain on the LiDAR images, again highlighting how the alluvial material is likely to be masking archaeological remains. The preservation of Iron Age/Roman settlement remains below these deposits would suggest that there is considerable archaeological potential within the floodplain. At present no palaeoenvironmental remains have been discovered within the floodplain; however, as alluvial material has sealed such deposits on Terrace 5, it is possible they also exist here.				

THE GEOARCHAEOLOGICAL RESOURCE OF THE LOWER SEVERN VALLEY				
LANDFORM UNIT GEOMORPHOLOGICAL CHARACTER				
POLYGON NO	4001	COUNTY	Worcestershire	CENTROID 383435/249553
HER REFERENCE	N/A	INTERPRETATION	Fourth Terrace (Holt Heath Member)	
ASSOCIATED LANDFORM UNITS	POLYGON NUMBERS	Terrace 4: 4003 and 4075		
	DESCRIPTION	This terrace unit is mirrored on the western bank of the River Severn by the larger Terrace 4 Unit 4003 and to the south by 4075.		
UNIT DESCRIPTION	Fourth terrace of the River Severn on the western bank aligned approximately N-S. 1.12km long and 0.39km wide, covering an area of 0.38km ² , at between 23.11-26.40m OD.			
HLC TYPE	The HLC type within this unit is dominated by religious sites and a nucleated cluster (Callow End).			
CULTURAL ASSOCIATIONS	NEW MONUMENTS	N/A		
	DESCRIPTION	The only known archaeological monument on this unit is a Medieval moated house.		
POTENTIAL	The lack of new and known archaeological remains on this unit probably results from its small size and the limited numbers of archaeological investigations. The good potential for archaeological preservation upon this unit is therefore inferred from the remains located on Unit 4003, although the small size of this terrace unit on the western side of the river does limit this potential.			

THE GEOARCHAEOLOGICAL RESOURCE OF THE LOWER SEVERN VALLEY					
LANDFORM UNIT GEOMORPHOLOGICAL CHARACTER					
POLYGON NO	4003	COUNTY	Worcestershire	CENTROID	385761/247504
HER REFERENCE	N/A	INTERPRETATION	Fourth Terrace (Holt Heath Member)		
ASSOCIATED LANDFORM UNITS	POLYGON NUMBERS	Terrace 4: 4001 and 4075			
	DESCRIPTION	This terrace unit is mirrored on the eastern bank of the River Severn by the smaller Terrace 4 units 4001 and 4075. As with Terrace 5, the units of Terrace 4 on the west bank of the river appear more degraded/eroded. This may also relate to larger and higher solid geological outcrops leading up to the Malvern Hills limiting the area available for terrace deposition?			
UNIT DESCRIPTION	Fourth terrace of the River Severn on the east bank aligned approximately N-S. 5.75km long and 0.86km wide, covering an area of 3.09km ² , at between 20.20-24.62m OD. This unit runs for most of the study area.				
HLC TYPE	The HLC type within this unit is dominated by Piecemeal Enclosure and Field Amalgamation with areas of Modern Expansion, Isolated Farmstead, Nucleated Cluster and Sports Ground.				
CULTURAL ASSOCIATIONS	NEW MONUMENTS	3015: Enclosure (Roman?) 4058: Palaeochannel			
	DESCRIPTION	Only one probable Iron Age or Roman enclosure was identified on the LiDAR images although there are a further five undated enclosures on this terrace unit that have been identified through cropmark evidence. Further prehistoric remains on this terrace include the cropmarks of a ring-ditch and a possible Neolithic henge? A ruined medieval chapel is also recorded on the HER.			
POTENTIAL	This terrace unit contains a significant number of cropmark enclosures of probable prehistoric and Roman date. As only one new enclosure was discovered on the LiDAR images it implies that alluviation and heavy ploughing may have limited any surface topography. Only one small palaeochannel was identified on this terrace that is likely to be of low palaeoenvironmental potential. A larger channel was however identified on the first edition OS map, although most of this channel lay outside of the study area, although its size and alignment is similar to the channels on Terrace 5, Unit 4011. This is therefore likely to have the potential to preserve good palaeoenvironmental remains.				

THE GEOARCHAEOLOGICAL RESOURCE OF THE LOWER SEVERN VALLEY					
LANDFORM UNIT GEOMORPHOLOGICAL CHARACTER					
POLYGON NO	4004	COUNTY	Worcestershire	CENTROID	382879/246086
HER REFERENCE	N/A	INTERPRETATION	Third Terrace (Kidderminster Member)		
ASSOCIATED LANDFORM UNITS	POLYGON NUMBERS	Terrace 3: 4009 (possibly 4023, 4026 and 4030)			
	DESCRIPTION	Based on the height of this deposit this unit is thought to be part of Terrace 3. This is of comparable height to Unit 4009, which may also be part of Terrace 3. This has not been confirmed and both units may be solid geology. Other confirmed Terrace 3 units on the western bank include 4023, 4026 and 4030.			
UNIT DESCRIPTION	This is thought to be the Third terrace of the River Severn on the western bank although it is possible it is solid geology not drift. It is possibly the largest of the Terrace 3 units measuring 2.4km long and 1.43km wide, covering an area of 2.14km ² , between 23.19-36.63m OD.				
HLC TYPE	The HLC type within this unit is dominated by Field Amalgamation and Modern Subdivision with areas of Parliamentary Enclosure, Small Irregular or Rectilinear Fields, Clustered Settlement and Isolated Farmstead.				
CULTURAL ASSOCIATIONS	NEW MONUMENTS	3040:8 Quarry pits 3001: Building platform/Barrow/mound 3007: Boundary ditch/field system 3004: Quarry pit/pond 3005: Earthwork ditch?			
	DESCRIPTION	There are no dated archaeological remains within this unit however it does contain a possible Roman/medieval drove road, and ridge and furrow remains. Although not initially identified on the Lidar images there is also a probable palaeochannel running approximately east west on the southern side of this unit.			
POTENTIAL	The unit has a reasonable potential to produce prehistoric to post-medieval remains, and palaeoenvironmental remains from the palaeochannel on the southern side of this unit.				

THE GEOARCHAEOLOGICAL RESOURCE OF THE LOWER SEVERN VALLEY					
LANDFORM UNIT GEOMORPHOLOGICAL CHARACTER					
POLYGON NO	4009	COUNTY	Worcestershire	CENTROID	382457/247570
HER REFERENCE	N/A	INTERPRETATION	Third Terrace (Kidderminster Member) ?		
ASSOCIATED LANDFORM UNITS	POLYGON NUMBERS	Terrace 3: 4004, possibly (4023, 4026 and 4030) Palaeochannel: 4052			
	DESCRIPTION	It is unclear as to whether this unit is drift or solid geology and is mirrored on the western bank of the River Severn by possibly four other units? Those on the western bank are not confirmed as there has been a lot of erosion and much of the mapped units on the western bank of the River may be solid geology.			
UNIT DESCRIPTION	This is thought to be the Third terrace of the River Severn on the western bank although it is possible it is solid geology not drift. 1.28km long and 1.150km wide, covering an area of 0.96km ² , between 28.41-39.65m OD.				
HLC TYPE	The HLC type within this unit is dominated by Parliamentary Enclosure and Parkland with areas of Parliamentary Enclosure				
CULTURAL ASSOCIATIONS	NEW MONUMENTS	3040:9 Quarry pits 3006: Curvilinear Enclosure 3030: Trackway			
	DESCRIPTION	The archaeological remains on this unit include two enclosures of probable prehistoric and Roman date, an undated trackway/drove road running east west to the river, a medieval moat house and 10 elongated quarry pits.			
POTENTIAL	The unit has a reasonable potential to produce prehistoric to post-medieval remains, and palaeoenvironmental remains from channel 4052.				

THE GEOARCHAEOLOGICAL RESOURCE OF THE LOWER SEVERN VALLEY

LANDFORM UNIT GEOMORPHOLOGICAL CHARACTER

POLYGON NO	4011	COUNTY	Worcestershire	CENTROID	385037/246617
HER REFERENCE	N/A	INTERPRETATION	Fifth Terrace (Worcester Member)		
ASSOCIATED LANDFORM UNITS	POLYGON NUMBERS	Terrace 5: 4007, 4076 Palaeochannels: 4039, 4040, 4041, 4045, 4050, 4067, 4068, 4071, 4072, 4074,			
	DESCRIPTION	This terrace unit mirrored on the western bank of the River Severn by two smaller units 4007, 4076. The size of the opposing units suggests that the river has eroded the terrace units on the western bank more. This unit also contains 10 palaeochannels of varying sizes, including three large N-S aligned channels 4039, 4040 and 4071 between 95-157m wide. Both channels 4040 (3980 BC base) and 4071 (4690-4450 cal BC to 1040-830 cal BC) have previously been examined and have provided both plant macro-fossil and palynological remains recording the valley's environmental history.			
UNIT DESCRIPTION	Fifth terrace of the River Severn on the eastern bank aligned approximately N-S. 6.4km long and 1.5km wide, covering an area of 5.57km ² , at a height of between 15.38-18.94m OD. The current gravel extraction within the pilot study area is targeting the sands and gravels of this unit.				
HLC TYPE	The HLC type within this unit is dominated by Fields and Enclosed Land/Field Amalgamation, although the following types are also present Watermeadow, Piecemeal Enclosure, Nucleated Cluster, Modern Expansion, Modern Subdivision, Piecemeal Enclosure, Recent Woodland (Secondary), Sand and Gravel Extraction Site, Other Common/Green and Interrupted Row.				
CULTURAL ASSOCIATIONS	NEW MONUMENTS	3022: Possible enclosure 3039: Ridge and furrow 3021: Earthwork? 3041: Building platform 3012: Building platform 3029: Watermeadow 3025: Watermeadow 3024: Watermeadow 3023: Watermeadow			
	DESCRIPTION	The earliest archaeological remains are Neolithic in date, and represent temporary settlement within the valley. Bronze Age activity is confined by the cropmark evidence of 8 ring ditches/round barrows, five of which form a small cemetery. Iron Age activity is represented by a promontory enclosure at Kempsey and a settlement within Clifton Quarry. There are numerous undated cropmark enclosures, field boundaries, pit alignments and earthworks that are also likely to be of prehistoric or Roman date. Medieval remains include two deserted medieval settlements, the medieval settlements of Kempsey and a possible earthwork castle. The small amount of ridge and furrow is also likely to be of medieval origin. Again there are also water meadows. As with the lower floodplain there is also evidence for second world war defences including a battery searchlight.			

POTENTIAL	<p>This terrace unit contains the largest number of cropmarks and investigated archaeological remains than any other unit within the study area. This may result from there being less alluvium masking the archaeological remains, specifically on the higher ground and due to a greater number of archaeological investigations having taking place on this unit, largely as a result of quarrying. These results show that there is a high potential for this terrace to produce archaeological remains from the early prehistoric periods to the 1940's, although pre-medieval remains are likely to be buried below alluvial deposits on the lower half of the terrace unit, closer to the river. The presence of the three large N-S aligned channels 4039, 4040 and 4071 also illustrates the terraces potential to preserve palaeoenvironmental remains.</p>
------------------	---

THE GEOARCHAEOLOGICAL RESOURCE OF THE LOWER SEVERN VALLEY				
LANDFORM UNIT GEOMORPHOLOGICAL CHARACTER				
POLYGON NO	4012	COUNTY	Worcestershire	CENTROID 382921/382921
HER REFERENCE	N/A	INTERPRETATION	Valley floor/floodplain	
ASSOCIATED LANDFORM UNITS	POLYGON NUMBERS	Palaeochannels; 4053, 4054, 4055		
	DESCRIPTION	There are only three small palaeochannels visible on this unit.		
UNIT DESCRIPTION	This is thought to be an active valley base/floodplain running in an approximate E-W direction, possibly formed from run off from the Malvern hills. To the west there are two independent valleys that become combined to form single wider valley to the east. It is 4.39km long and 0.053-0.13km wide, covering an area of 0.25km ² .			
HLC TYPE	The HLC type within this unit is dominated by Piecemeal Enclosure, Parkland and Field Amalgamation			
CULTURAL ASSOCIATIONS	NEW MONUMENTS	N/A		
	DESCRIPTION	Prehistoric/Roman enclosure		
POTENTIAL	It is difficult to assess the potential of this unit as few records exist on the HER. However these results from there having been no interventions upon this unit, therefore all periods may be represented upon it However the apparent erosion caused by the runoff the higher terraces may also have eroded earlier archaeological remains.			

THE GEOARCHAEOLOGICAL RESOURCE OF THE LOWER SEVERN VALLEY				
LANDFORM UNIT GEOMORPHOLOGICAL CHARACTER				
POLYGON NO	4016	COUNTY	Worcestershire	CENTROID 385111/249079
HER REFERENCE	N/A	INTERPRETATION	Valley floor/floodplain	
ASSOCIATED LANDFORM UNITS	POLYGON NUMBERS	Palaeochannels; 4059, 4060		
	DESCRIPTION	There are only two small palaeochannels visible on this unit.		
UNIT DESCRIPTION	This is thought to be an active valley base/floodplain running in an approximate E-W direction, possibly formed from run off from Terraces 1 and 2. It is 0.98km long and 0.019km wide, covering an area of 0.023km ² .			
HLC TYPE	The HLC type within this unit is dominated by Nucleated Cluster, Field Amalgamation and Recent Woodland (Secondary).			
CULTURAL ASSOCIATIONS	NEW MONUMENTS	N/A		
	DESCRIPTION	N/A		
POTENTIAL	It is difficult to assess the potential of this unit as few records exist on the HER. However these results from there having been no interventions upon this unit, therefore all periods may be represented upon it. However the apparent erosion caused by the runoff the higher terraces may also have eroded earlier archaeological remains. There is also the potential for palaeoenvironmental remains within 2 small palaeochannels.			

THE GEOARCHAEOLOGICAL RESOURCE OF THE LOWER SEVERN VALLEY				
LANDFORM UNIT GEOMORPHOLOGICAL CHARACTER				
POLYGON NO	4018	COUNTY	Worcestershire	CENTROID 384446/242912
HER REFERENCE	N/A	INTERPRETATION	Fifth Terrace (Worcester Member)	
ASSOCIATED LANDFORM UNITS	POLYGON NUMBERS	Terrace 1: 4011 and 4076		
	DESCRIPTION	This terrace unit is mirrored on the eastern bank of the River Severn by the larger Terrace 5 unit 4011 and by 4076 to the north.		
UNIT DESCRIPTION	Fifth terrace of the River Severn on the western bank aligned approximately N-S. 1.75km long and 0.21km wide, covering an area of 0.25km ² , at a height of between 13.80-17.06m OD. Although there is no quarrying on this unit, large scale extraction is proceeding on Terrace 5, unit 4011 on the eastern bank of the river. This unit is very narrow in comparison to 4011 and 4076 and is likely to have been eroded by the river.			
HLC TYPE	The HLC type within this unit is Parliamentary Enclosure.			
CULTURAL ASSOCIATIONS	NEW MONUMENTS	N/A		
	DESCRIPTION	N/A		
POTENTIAL	The lack of new and known monuments on this unit probably results from its small size and due to the lack of archaeological investigations. The good potential for archaeological preservation upon this unit is therefore inferred from the remains located on unit 4011, although the small size of this terrace unit does limit this potential.			

THE GEOARCHAEOLOGICAL RESOURCE OF THE LOWER SEVERN VALLEY

LANDFORM UNIT GEOMORPHOLOGICAL CHARACTER

POLYGON NO	4019	COUNTY	Worcestershire	CENTROID	385859/248872
HER REFERENCE	N/A	INTERPRETATION	First Terrace (Spring Hill Member)		
ASSOCIATED LANDFORM UNITS	POLYGON NUMBERS	Terrace 1: 4025			
	DESCRIPTION	This terrace unit is mirrored on the western bank of the River Severn by two small areas of surviving terrace (4025) although these may be thin.			
UNIT DESCRIPTION	This is thought to be the fifth terrace of the River Severn based upon BGS mapping, only one small area survive on the eastern side of the Severn 0.50km long and 0.31km wide, covering an area of 0.11km ² , between 46.72-50.0m OD.				
HLC TYPE	The HLC type within this unit is dominated by Field Amalgamation with a small area of Clustered Settlement.				
CULTURAL ASSOCIATIONS	NEW MONUMENTS	N/A			
	DESCRIPTION	Two pairs of parallel ditch aligned roughly NE-SW are the only known archaeological features on this unit.			
POTENTIAL	No significant archaeological remains are known to exist on this unit and the small size of this terrace limits the potential of their being many.				

THE GEOARCHAEOLOGICAL RESOURCE OF THE LOWER SEVERN VALLEY				
LANDFORM UNIT GEOMORPHOLOGICAL CHARACTER				
POLYGON NO	4020	COUNTY	Worcestershire	CENTROID 385680/242827
HER REFERENCE	N/A	INTERPRETATION	Third Terrace (Kidderminster Member)	
ASSOCIATED LANDFORM UNITS	POLYGON NUMBERS	Terrace 3: 4023, 4026 and 4030 (possibly 4009, 4004)		
	DESCRIPTION	This terrace unit is mirrored on the western bank of the River Severn by the possibly five other units? These are not confirmed as there has been a lot of erosion and much of the mapped units on the western bank of the River may be solid geology.		
UNIT DESCRIPTION	Third terrace of the River Severn on the western bank aligned approximately N-S. 2.11km long and 0.37km wide, covering an area of 0.77km ² , between 27.94-32.37m OD.			
HLC TYPE	The HLC type within this unit is dominated by Parliamentary Enclosure and Piecemeal Enclosure with areas of Ancient-Semi-Natural Woodland and Country House.			
CULTURAL ASSOCIATIONS	NEW MONUMENTS	3026:Ridge and Furrow 3027: Ridge and Furrow		
	DESCRIPTION	Other than ridge and furrow only a second world war searchlight battery and a weapons on the SMR. The ridge and furrow is mostly surrounding a single farmstead at Day House Cottages.		
POTENTIAL	The lack of new and known monuments on this unit probably results from its small size and due to the lack of archaeological investigations.			

THE GEOARCHAEOLOGICAL RESOURCE OF THE LOWER SEVERN VALLEY				
LANDFORM UNIT GEOMORPHOLOGICAL CHARACTER				
POLYGON NO	4023	COUNTY	Worcestershire	CENTROID 383853/244418
HER REFERENCE	N/A	INTERPRETATION	Third Terrace (Kidderminster Member)	
ASSOCIATED LANDFORM UNITS	POLYGON NUMBERS	Terrace 3: 4020, 4026 and 4030 (possibly 4004, 4009)		
	DESCRIPTION	This terrace unit is mirrored on the western bank of the River Severn by the possibly four other units? and one on the eastern bank. Those on the western bank are not confirmed as there has been a lot of erosion and much of the mapped units on the western bank of the River may be solid geology.		
UNIT DESCRIPTION	This is thought to be the Third terrace of the River Severn on the western bank. 0.88km long and 0.19km wide, covering an area of 0.21km ² , between 23.19-36.63m OD.			
HLC TYPE	The HLC type within this unit is dominated by Ancient-Semi-Natural Woodland with areas of Parliamentary Enclosure, Interrupted Row and Field Amalgamation.			
CULTURAL ASSOCIATIONS	NEW MONUMENTS	N/A		
	DESCRIPTION	There are no recorded sites on this unit within the HER.		
POTENTIAL	The small size and the lack of identified archaeological remains limits the potential of the unit to preserve archaeological remains, however the lack of identified archaeological remains may result from the lack of activities and woodland coverage.			

THE GEOARCHAEOLOGICAL RESOURCE OF THE LOWER SEVERN VALLEY				
LANDFORM UNIT GEOMORPHOLOGICAL CHARACTER				
POLYGON NO	4024	COUNTY	Worcestershire	CENTROID 383006/248470
HER REFERENCE	N/A	INTERPRETATION	Second Terrace (Bushley Green Member)	
ASSOCIATED LANDFORM UNITS	POLYGON NUMBERS	N/A		
	DESCRIPTION	N/A		
UNIT DESCRIPTION	This is thought to be the Second terrace of the River Severn as mapped by the BGS. Running in an approximate NE-SW direction. 1.78km long and 0.14km wide, covering an area of 0.34km ² , between 46.21-62.94m OD			
HLC TYPE	The HLC type within this unit is dominated by Common Grazed Woodland, Assarted Enclosure and Field Reorganisation with areas of Other Common/ Green and Waste/Common/Green-edge Sett.			
CULTURAL ASSOCIATIONS	NEW MONUMENTS	3000: Earthwork enclosure 3040: 5 Quarry pits 3011: Building platform? 3010: Earthwork/barrow?		
	DESCRIPTION	No records exist on the HER		
POTENTIAL	Although no records exist on the HER, this is likely to be as a result of the lack of activities and the density of woodland. The most important monument discovered on this unit is earthwork 3000, which is possibly a prehistoric promontory enclosure, similar to the one at Kempsey. It is therefore concluded that this unit has the potential to contain important prehistoric remains.			

THE GEOARCHAEOLOGICAL RESOURCE OF THE LOWER SEVERN VALLEY				
LANDFORM UNIT GEOMORPHOLOGICAL CHARACTER				
POLYGON NO	4025	COUNTY	Worcestershire	CENTROID 382968/249377
HER REFERENCE	N/A	INTERPRETATION	First Terrace (Spring Hill Member)	
ASSOCIATED LANDFORM UNITS	POLYGON NUMBERS	Terrace 1: 4019		
	DESCRIPTION	This terrace unit is mirrored on the eastern bank of the River Severn by one small area of surviving Terrace 1 (4019) although this may be thin.		
UNIT DESCRIPTION	This is thought to be the fifth terrace of the River Severn based upon BGS mapping, only two small areas survive on the western side of the Severn 0.45km long and 0.12km wide, covering an area of 0.08km ² , between 50.01-54.22m OD.			
HLC TYPE	The HLC type within this unit is dominated by Field Amalgamation with a small area of Clustered Settlement.			
CULTURAL ASSOCIATIONS	NEW MONUMENTS	N/A		
	DESCRIPTION	N/A		
POTENTIAL	No archaeological remains are known to exist on this unit and the small size of these terrace remains limits their potential.			

THE GEOARCHAEOLOGICAL RESOURCE OF THE LOWER SEVERN VALLEY

LANDFORM UNIT GEOMORPHOLOGICAL CHARACTER

POLYGON NO	4026	COUNTY	Worcestershire	CENTROID	383545/248377
HER REFERENCE	N/A	INTERPRETATION	Third Terrace (Kidderminster Member)		
ASSOCIATED LANDFORM UNITS	POLYGON NUMBERS	Terrace 3: 4020, 4023 and 4030 (possibly 4004, 4009) Palaeochannels: 4064, 4065			
	DESCRIPTION	This terrace unit is mirrored on the western bank of the River Severn by the possibly four other units? and one on the eastern bank. Those on the western bank are not confirmed as there has been a lot of erosion and much of the mapped units on the western bank of the River may be solid geology.			
UNIT DESCRIPTION	Third terrace of the River Severn on the western bank aligned approximately N-S. 1.11km long and 0.35km wide, covering an area of 0.26km ² , between 28.64-36.40m OD.				
HLC TYPE	The HLC type within this unit is dominated by Field Reorganisation, Piecemeal Enclosure and Assarted Enclosure with areas of Isolated Farmstead, Replanted Ancient Woodland and Ancient-Semi-Natural Woodland.				
CULTURAL ASSOCIATIONS	NEW MONUMENTS	3040: Quarry pit			
	DESCRIPTION	Only one quarry pit and a small area of ridge and furrow have been identified on this unit. The lack of new and known monuments on this unit probably results from its small size and due to the lack of archaeological investigations.			
POTENTIAL	The lack of new and known monuments on this unit probably results from its small size and due to the lack of archaeological investigations.				

THE GEOARCHAEOLOGICAL RESOURCE OF THE LOWER SEVERN VALLEY				
LANDFORM UNIT GEOMORPHOLOGICAL CHARACTER				
POLYGON NO	4027	COUNTY	Worcestershire	CENTROID 382842/245842
HER REFERENCE	N/A	INTERPRETATION	Indeterminate	
ASSOCIATED LANDFORM UNITS	POLYGON NUMBERS	N/A		
	DESCRIPTION	N/A		
UNIT DESCRIPTION	It is unclear what this unit is, although it appears to be an area solid geology that has not been eroded although the BGS mapping has recorded it as sand and gravel deposit. It is 0.33km long and 0.11km wide, covering an area of 0.035km ² at between 61.99-69.53m asl.			
HLC TYPE	The HLC type within this unit is dominated by Ancient-Semi-Natural Woodland.			
CULTURAL ASSOCIATIONS	NEW MONUMENTS	N/A		
	DESCRIPTION	An Iron Age Hill fort is situated on top of this outcrop, the ramparts of which can be seen on the LiDAR images.		
POTENTIAL	As there is thought to be an Iron Age hill fort on top of this mound, it has potential to contain significant prehistoric remains.			

THE GEOARCHAEOLOGICAL RESOURCE OF THE LOWER SEVERN VALLEY				
LANDFORM UNIT GEOMORPHOLOGICAL CHARACTER				
POLYGON NO	4029	COUNTY	Worcestershire	CENTROID 38347/248826
HER REFERENCE	N/A	INTERPRETATION	Valley floor/floodplain	
ASSOCIATED LANDFORM UNITS	POLYGON NUMBERS	N/A		
	DESCRIPTION	N/A		
UNIT DESCRIPTION	This is thought to be an active valley base/floodplain running in an approximate E-W direction, possibly formed from run off from Terraces 3 and 4 and runs onto Terrace 1. It is 0.76km long and 0.14km wide, covering an area of 0.05km ² .			
HLC TYPE	The HLC type within this unit is dominated by Parkland and Field Amalgamation.			
CULTURAL ASSOCIATIONS	NEW MONUMENTS	N/A		
	DESCRIPTION	Ridge and furrow		
POTENTIAL	It is difficult to assess the potential of this unit as no records exist on the HER. However this results from there having been no interventions upon this unit, therefore all periods may be represented upon it. However the apparent erosion caused by the runoff the higher terraces may also have eroded earlier archaeological remains.			

THE GEOARCHAEOLOGICAL RESOURCE OF THE LOWER SEVERN VALLEY				
LANDFORM UNIT GEOMORPHOLOGICAL CHARACTER				
POLYGON NO	4030	COUNTY	Worcestershire	CENTROID 383545/248377
HER REFERENCE	N/A	INTERPRETATION	Third Terrace (Kidderminster Member)	
ASSOCIATED LANDFORM UNITS	POLYGON NUMBERS	Terrace 3: 4020, 4023 and 4026 (possibly 4009, 4004)		
	DESCRIPTION	This terrace unit is mirrored on the western bank of the River Severn by the possibly four other units? and one on the eastern bank. Those on the western bank are not confirmed as there has been a lot of erosion and much of the mapped units on the western bank of the River may be solid geology.		
UNIT DESCRIPTION	Third terrace of the River Severn on the western bank aligned approximately N-S. 0.23km long and 0.20km wide, covering an area of 0.03km ² , between 26.75-32.90m OD.			
HLC TYPE	The HLC type within this unit is dominated by Parkland.			
CULTURAL ASSOCIATIONS	NEW MONUMENTS	N/A		
	DESCRIPTION	Only a small area of ridge and furrow record on the HER		
POTENTIAL	The small size and the lack of identified archaeological remains limits the potential of the unit to preserve archaeological remains, however the lack of identified archaeological remains may result from the lack of activities and woodland coverage.			

THE GEOARCHAEOLOGICAL RESOURCE OF THE LOWER SEVERN VALLEY

LANDFORM UNIT GEOMORPHOLOGICAL CHARACTER

POLYGON NO	4031	COUNTY	Worcestershire	CENTROID	382412/249218
HER REFERENCE	N/A	INTERPRETATION	Indeterminate		
ASSOCIATED LANDFORM UNITS	POLYGON NUMBERS	Palaeochannel: 4056			
	DESCRIPTION	Only one new palaeochannel was identified within the north-west corner of the unit.			
UNIT DESCRIPTION	It is unclear what this unit is, although it appears to be an area of erosion it is not thought to be drift geology and is solid in nature (mudstone). It is 1.64km long and 1.38km wide, covering an area of 1.0km ² , between 33.72-39.57m asl.				
HLC TYPE	The HLC type within this unit is dominated by Ancient-Semi-Natural Woodland and Replanted Ancient Woodland with areas of Ornamental, Parkland & Recreational, Settlement and Fields & Enclosed Land.				
CULTURAL ASSOCIATIONS	NEW MONUMENTS	3040: 3 Quarry pits			
	DESCRIPTION	No records exist on the HER			
POTENTIAL	It is difficult to assess the potential of this unit as no records exist on the HER. However this results from there having been no interventions upon this unit, therefore all periods may be represented upon it.				

THE GEOARCHAEOLOGICAL RESOURCE OF THE LOWER SEVERN VALLEY					
LANDFORM UNIT GEOMORPHOLOGICAL CHARACTER					
POLYGON NO	4032	COUNTY	Worcestershire	CENTROID	382759/244102
HER REFERENCE	N/A	INTERPRETATION	Indeterminate		
ASSOCIATED LANDFORM UNITS	POLYGON NUMBERS	N/A			
	DESCRIPTION	N/A			
UNIT DESCRIPTION	It is unclear what this unit is, although it appears to be an area solid geology that has not been eroded it may be a terrace drift deposit associated with the floodplain/channel 4035. It is 0.84km long and 0.21km wide, covering an area of 0.16km ² , between 21.63-26.35m asl.				
HLC TYPE	The HLC type within this unit is dominated by Ancient-Semi-Natural Woodland.				
CULTURAL ASSOCIATIONS	NEW MONUMENTS	3040: 2 Quarry pits 3035: Ridge and furrow			
	DESCRIPTION	Only one small area of ridge and furrow is recorded on the HER, of medieval or post-medieval date.			
POTENTIAL	It is difficult to assess the potential of this unit as few records exist on the HER, except for an area of ridge and furrow. However this results from there having been no interventions upon this unit, therefore all periods may be represented upon it.				

THE GEOARCHAEOLOGICAL RESOURCE OF THE LOWER SEVERN VALLEY				
LANDFORM UNIT GEOMORPHOLOGICAL CHARACTER				
POLYGON NO	4033	COUNTY	Worcestershire	CENTROID 382359/244519
HER REFERENCE	N/A	INTERPRETATION	Indeterminate	
ASSOCIATED LANDFORM UNITS	POLYGON NUMBERS	N/A		
	DESCRIPTION	N/A		
UNIT DESCRIPTION	It is unclear what this unit is, although it appears to be an area solid geology that has not been eroded it may be a terrace drift deposit associated with the floodplain/channel 4035. It is 0.84km long and 0.21km wide, covering an area of 0.16km ² , between 21.63-26.35m asl.			
HLC TYPE	The HLC type within this unit is dominated by Ancient-Semi-Natural Woodland.			
CULTURAL ASSOCIATIONS	NEW MONUMENTS	3040: 2 Quarry pits 3036: Ridge and furrow		
	DESCRIPTION	No archaeological remains are recorded on the HER, however two large fields of ridge and furrow were identified on the Lidar images.		
POTENTIAL	It is difficult to assess the potential of this unit as no records exist on the HER. However this results from there having been no interventions upon this unit, therefore all periods may be represented upon it.			

THE GEOARCHAEOLOGICAL RESOURCE OF THE LOWER SEVERN VALLEY					
LANDFORM UNIT GEOMORPHOLOGICAL CHARACTER					
POLYGON NO	4035	COUNTY	Worcestershire	CENTROID	3382948/2446658
HER REFERENCE	N/A	INTERPRETATION	Valley floor/floodplain		
ASSOCIATED LANDFORM UNITS	POLYGON NUMBERS	Levees: 4061, 4062 Palaeochannels: 4063, 4051 Terraces?: 4032, 4033			
	DESCRIPTION	There are only two small palaeochannels visible on this unit, and the levee is associated with a current watercourse. Polygons 4032 and 4033 may be terrace units associated with this valley?			
UNIT DESCRIPTION	This is thought to be the valley base/floodplain of a former channel running in an approximate E-W direction, possibly formed from run off from the Malvern hills. To the west the valley appears to be two separate palaeochannels that form one wide valley to the east. It is 1.90km long and 0.86km wide, covering an area of 1.05km ² , between 21.08-27.32m asl.				
HLC TYPE	The HLC type within this unit is dominated by Small Irregular or Rectilinear Fields, Parliamentary Enclosure and Field Amalgamation with areas of Interrupted Row, Modern Subdivision.				
CULTURAL ASSOCIATIONS	NEW MONUMENTS	3033, 3034, 3037: Ridge and Furrow			
	DESCRIPTION	Although no recorded archaeological sites exist on the HER although three ridge and furrow blocks were identified on the Lidar Images. A possible large E-W aligned palaeochannel and a mill pond/race complex were also identified on the first edition OS mapping.			
POTENTIAL	It is difficult to assess the potential of this unit as no records exist on the HER. However this results from there having been no interventions upon this unit, therefore all periods may be represented upon it. The large E-W aligned palaeochannel and the mill ponds/race also have the potential to preserve palaeoenvironmental remains.				

THE GEOARCHAEOLOGICAL RESOURCE OF THE LOWER SEVERN VALLEY				
LANDFORM UNIT GEOMORPHOLOGICAL CHARACTER				
POLYGON NO	4075	COUNTY	Worcestershire	CENTROID 384166/243286
HER REFERENCE	N/A	INTERPRETATION	Fourth Terrace (Holt Heath Member)	
ASSOCIATED LANDFORM UNITS	POLYGON NUMBERS	Terrace 4: 4001 and 4003		
	DESCRIPTION	This terrace unit is mirrored on the eastern bank of the River Severn by the larger Terrace 4 unit 4003 and to the north by 4001.		
UNIT DESCRIPTION	Second terrace of the River Severn on the western bank aligned approximately N-S. 2.80km long and 0.26km wide, covering an area of 0.77km ² , at between 20.62-28.9m OD. The northern end of this unit has been eroded by 3 small valleys aligned approximately E-W.			
HLC TYPE	The HLC type within this unit is dominated by Parliamentary Enclosure and Piecemeal Enclosure with areas of Replanted Ancient Woodland and Isolated Farmstead.			
CULTURAL ASSOCIATIONS	NEW MONUMENTS	3014: Earthwork/barrow? 3040: 4 quarry pits		
	DESCRIPTION	There are no known archaeological sites on this terrace and only a possible small barrow and 4 elongated (post-medieval?) were discovered on the Lidar images.		
POTENTIAL	The lack of new and known monuments on this unit probably results from its small size and due to the lack of archaeological investigations. The good potential for archaeological preservation upon this unit is therefore inferred from the remains located on unit 4003, although the small size of this terrace unit does limit this potential.			

THE GEOARCHAEOLOGICAL RESOURCE OF THE LOWER SEVERN VALLEY					
LANDFORM UNIT GEOMORPHOLOGICAL CHARACTER					
POLYGON NO	4076	COUNTY	Worcestershire	CENTROID	384010/249329
HER REFERENCE		INTERPRETATION	Fifth Terrace (Worcester Member)		
ASSOCIATED LANDFORM UNITS	POLYGON NUMBERS	Terrace 5: 4011 and 4018 Palaeochannel:4044			
	DESCRIPTION	This terrace unit is mirrored on the eastern bank of the River Severn by the larger Terrace 5 unit 4011 and by 4018 to the south. The latter has been eroded by the river and is much smaller than 4076 and 4011. The only palaeochannel is small and is the remnant of a watercourse's original location prior to canalisation.			
UNIT DESCRIPTION	Fifth terrace of the River Severn on the western bank aligned approximately N-S. 2.09km long and 0.8km wide, covering an area of 0.87km ² , at a height of between 12.53-16.88m OD. Although there is no quarrying on this unit, large scale extraction is proceeding on Terrace 4, unit 4011 on the eastern bank of the river.				
HLC TYPE	The HLC type within this unit is dominated by Piecemeal Enclosure, Field Amalgamation and Parliamentary Enclosure, although the following types are also present Nucleated Row, Isolated Farmstead and Minor Dispersed Settlement.				
CULTURAL ASSOCIATIONS	NEW MONUMENTS	3028: Watermeadow 3003: Building platform			
	DESCRIPTION	There are few associations on the HER for this terrace. The earliest is of two small Roman enclosures/occupation areas to the east of Callow End and an area of medieval ridge and furrow.			
POTENTIAL	Although there are few known archaeological sites on this terrace unit, as there are numerous sites visible on Terrace 5, unit 4011, it is also likely this unit has a similar potential. The lack of known archaeological sites is therefore a lack of archaeological investigations rather than a true reflection of past activities upon it.				

Appendix 7: Gloucestershire Report Forms

THE GEOARCHAEOLOGICAL RESOURCE OF THE LOWER SEVERN VALLEY					
LANDFORM UNIT GEOMORPHOLOGICAL CHARACTER					
POLYGON NO	2004	COUNTY	Gloucestershire	CENTROID	377432/207426
HER REFERENCE		INTERPRETATION	Terrace 2		
ASSOCIATED LANDFORM UNITS	POLYGON NUMBERS	Terrace 2 units: 2014, 2020			
	DESCRIPTION	<p>2014 - A ribbon of Terrace 2 on the eastern bank of the River Frome aligned northwest to southeast and measuring 1.6 km x 0.230 km at its widest point. It has a maximum height of approximately 14m amsl and an area of 0.501km².</p> <p>2020 - A terrace unit of the River Severn located on the eastern bank of the River Severn and flanked further to the east by the River Frome. With an area of 6.12 km² it measures approximately 2.4km x 2.9km.</p>			
UNIT DESCRIPTION	A ribbon of terrace on the eastern bank of the River Frome aligned northwest to southeast and measuring 0.891km x 0.280km for the element that is contained in the survey area. It continues to the southeast outside of the survey area. The portion of the terrace within the survey area has an area of 0.18km ² . It gently slopes upward to the east. Bounded to the east by the terrace edge (2009) and to the west by the terrace edge (2002). It has a gentle slope upward from west to east rising from an average of 12m amsl to 18m amsl.				
HLC TYPE	A2 Less regular enclosure partly reflecting former unenclosed cultivation patterns				
CULTURAL ASSOCIATIONS	NEW MONUMENTS	None			
	DESCRIPTION	<p>Ancient Ridge and Furrow cultivation lies over this area. The western edges of the cultivation respect the western edge of the terrace, however, the eastern edge runs up the slight rise of the terrace edge terrace edge 2009</p> <p>The only known cultural feature is a wharf on the disused Stroudwater canal that follows the terrace edge to the west.</p>			
POTENTIAL	The relatively small area of the unit makes meaningful interpretation difficult. Given the presence of prehistoric monuments on the larger remnant of Terrace 1 there may equally be such cultural remains on this terrace unit.				

THE GEOARCHAEOLOGICAL RESOURCE OF THE LOWER SEVERN VALLEY					
LANDFORM UNIT GEOMORPHOLOGICAL CHARACTER					
POLYGON NO	2006	COUNTY	Gloucestershire	CENTROID	376484/208166
HER REFERENCE		INTERPRETATION	Flood Plain – River Frome		
ASSOCIATED LANDFORM UNITS	POLYGON NUMBERS	2007, 2008, 2011, 2012, 2024			
	DESCRIPTION	All of these units form the same feature. They have been digitised separately either side of the river but form one continuous landform unit.			
UNIT DESCRIPTION	The valley floor of the River Frome aligned north west to south east. The River Frome (2001) meanders through this feature discharging towards the north. The channels within this area have been heavily canalised over time. Running for a length of 3,15km within the study area, it has a maximum width of approximately 0.28 km. The total area coverage is 1.32 km ² . The terrace edges are more prominent to the eastern side of the valley floor than to the west. The unit sits at about 7-8m asl.				
HLC TYPE	A1D Irregular enclosure reflecting former unenclosed cultivation patterns D1r Riverine Pasture, probably meadows now enclosed				
CULTURAL ASSOCIATIONS	NEW MONUMENTS	1013 Water meadow 1018 Water meadow 1021 Water meadow 1022 Water meadow 1043 Water meadow			
	DESCRIPTION	The majority of the recorded monuments in this unit are post-medieval dating from the construction of the Stroudwater canal (GSMR 11154, 30711) or later. An odd Roman coin find (GSMR 7017) hints at Roman presence in the area. Disused railways (GSMR 11104), Mills (GSMR 7508, 7005), WWII relics (GSMR 21835,20803,13907,29211)mix with post-medieval mooring sites (GSMR 33477) and elements of old field boundaries (GSMR 13181,13180) to form a landscape shaped by later human activity. A DMV site touches the site and the odd element of Ridge and Furrow cultivation is extant. Obvious from the LIDAR and NMP mapping, are the extensive areas of Watermeadow that exists along the length of the valley floor.			
POTENTIAL	The evidence for prehistoric or Roman activity is fragile but this does not preclude the presence of further evidence that has not yet been identified. The presence of the post-Medieval cultural remains is consistent with the rest of the study areas and merely serves to indicate the longevity of the land use in this lower area of the Severn basin.				

THE GEOARCHAEOLOGICAL RESOURCE OF THE LOWER SEVERN VALLEY					
LANDFORM UNIT GEOMORPHOLOGICAL CHARACTER					
POLYGON NO	2014	COUNTY	Gloucestershire	CENTROID	376306/209090
HER REFERENCE		INTERPRETATION	Terrace 2		
ASSOCIATED LANDFORM UNITS	POLYGON NUMBERS	Terrace 2 units: 2020, 2004			
	DESCRIPTION	<p>2004 - A ribbon of terrace on the eastern bank of the River Frome aligned northwest to southeast and measuring 0.891km x 0.280km for the element that is contained in the survey area. It gently slopes upward to the east.</p> <p>2020 - A terrace unit of the River Severn located on the eastern bank of the River Severn and flanked further to the east by the River Frome. With an area of 6.12 km² it measures approximately 2.4km x 2.9km.</p>			
UNIT DESCRIPTION	A ribbon of terrace on the eastern bank of the River Frome aligned northwest to southeast and measuring 1.6 km x 0.230 km at its widest point. It has a maximum height of approximately 14m asl and an area of 0.501km ² . The unit sits at the northern end of the small valley cut by the River Frome truncated to the north by landform unit 2017.				
HLC TYPE	A2 Less regular enclosure partly reflecting former unenclosed cultivation patterns				
CULTURAL ASSOCIATIONS	NEW MONUMENTS	1014 Possible Trackway 1016 Earthwork Bank 1025 Earthwork Bank			
	DESCRIPTION	Albeit not geographically large, the area contains an early Norman chapel and earthworks associated with a possible deserted medieval village. New monuments identified during the study include a possible trackway associated with both the church and the deserted settlement. Two earthwork banks of an unknown date are likely to be remnant headland features. The area is overlain with numerous traces of Ridge and Furrow, the edges of the unit blocks coinciding neatly with the boundaries of the terrace.			
POTENTIAL	The relatively small area of the unit makes meaningful interpretation difficult. The presence of the settlement above the floodplain of the River Frome is probably due to the fertile and dry location. Consequently, more evidence of habitation associated with the existing deserted village or earlier. The presence of the earthwork banks may indicate undetected cultural remains dating to before the medieval period. Given the presence of prehistoric monuments on the larger remnant of Terrace 1 there may equally be such cultural remains on this terrace unit.				

THE GEOARCHAEOLOGICAL RESOURCE OF THE LOWER SEVERN VALLEY					
LANDFORM UNIT GEOMORPHOLOGICAL CHARACTER					
POLYGON NO	2016	COUNTY	Gloucestershire	CENTROID	377445/208768
HER REFERENCE		INTERPRETATION	Terrace 1		
ASSOCIATED LANDFORM UNITS	POLYGON NUMBERS	None			
	DESCRIPTION	None			
UNIT DESCRIPTION	A terrace unit located to the east of the study area. On its western edge lies the terrace edge (2009) which falls away to the two remnant pieces of Terrace 2. It has a general north-south alignment. Measuring approximately 1km x 2.36 km it covers an area of approximately 2.069 km ² . Gently undulating over its entirety it has been eroded by subsequent minor streams creating small valleys draining to the north. It appears to have a maximum height of 32m asl in the southwest portion gently sloping down to the east and cut by subsequent features.				
HLC TYPE	A1 Irregular enclosure reflecting former unenclosed cultivation patterns A2 Less irregular enclosure partly reflecting former unenclosed cultivation patterns A4 Less regular organised enclosure partly reflecting former unenclosed cultivation patterns G3 Existing settlement – extent by mid 19 th century G4 Existing settlement – present extent				
CULTURAL ASSOCIATIONS	NEW MONUMENTS	None			
	DESCRIPTION	Ancient Ridge and Furrow cultivation lies over this area. The western edges of the cultivation respect the western edge of the terrace, however, the eastern edge runs up to the bottom of the terrace edge 2009, although the geomorphological character is more confusing in that area. Finds of flints in an evaluation (GSMR 17251) hint at the possibility of prehistoric activity and small fragments of Roman pottery (GSMR 17251) and a Roman coin find (7509) indicate Roman activity dispersed across the area. Sherds of Medieval pottery and structural remains have appeared in evaluations (GSMR 17264, 9382, 19917) including evidence of metalworking. This is supported by 'Oldbury' fieldnames (GSMR 17264). A toll house (GSMR 5232) and Grade II listed building (GSMR 22154) typify later post-medieval use of the landscape and a WWII searchlight battery (GSMR 27071) brings us up to date.			
POTENTIAL	The relatively small area of the unit makes meaningful interpretation difficult. Given the presence of a few flints there may be prehistoric activity elsewhere on this unit. Equally Roman cultural material may be found anywhere. Given the intensive land use since the medieval period any cultural remains from this period or later will be well represented.				

THE GEOARCHAEOLOGICAL RESOURCE OF THE LOWER SEVERN VALLEY					
LANDFORM UNIT GEOMORPHOLOGICAL CHARACTER					
POLYGON NO	2017	COUNTY	Gloucestershire	CENTROID	374478/2094213
HER REFERENCE		INTERPRETATION	Paleochannel?		
ASSOCIATED LANDFORM UNITS	POLYGON NUMBERS	2018			
	DESCRIPTION	A small section of possible paleochannel located in the north eastern extremity of the study area. It appears to be the same feature as 2017. The area is 0.37 km ² although this is only the portion contained within the study area.			
UNIT DESCRIPTION	A possible wide paleochannel oriented east to west across the survey area. It is difficult to identify as a definite paleochannel as the extremities of the feature are not within the survey area, however, the land is much lower lying than that surrounding. Mapped in 2 segments, it has a total length of approximately 4.5 km and is approximately 1.2 km wide at its widest point. The total area measures approximately 2.81km ² . It is possible cut by the drainage channels of the River Frome although modern canalisation on this area makes distinction difficult. Old gravel extraction areas exist within the boundaries of this unit. The average height of this unit is approximately 7.5m asl.				
HLC TYPE	A2 Less irregular enclosure partly reflecting former unenclosed cultivation patterns A3 Regular organised enclosure partly reflecting former unenclosed cultivation patterns G2 Existing settlement of medieval or earlier origin G4 Existing settlement - present extent				
CULTURAL ASSOCIATIONS	NEW MONUMENTS	1027 Earthwork Bank 1028 Earthwork Bank 1029 Earthwork Bank 1044 Earthwork Bank 1046 Earthwork Bank 1047 Earthwork Bank 1048 Earthwork Bank 1049 Earthwork Bank			
	DESCRIPTION	The village of Saul sits in the centre of the feature, itself surrounded to the south and west by former mineral extraction quarries. The evidence for early cultural deposits is thin. No prehistoric or Roman deposits are contained within the HER. The new monuments described above are all large earthwork banks that appear larger than normal however, are highly likely to be remnant headlands or field boundaries. Crop marks of a possible medieval origin (GSMR 3644) and a sherd of pottery (GSMR 20502) are the only evidence that compliment the medieval village of Saul. The remaining HER entries relate to the post-medieval buildings of Saul and a couple of negative watching briefs.			
POTENTIAL	The evidence for prehistoric or Roman activity is fragile but this does not preclude the presence of further evidence that has not yet been identified. The presence of the Medieval and post-Medieval cultural remains is consistent with the rest of the study areas and merely serves to indicate the longevity of the land use in this lower area of the Severn basin. Therefore the possibility of discovering medieval cultural evidence over this larger area remains high.				

THE GEOARCHAEOLOGICAL RESOURCE OF THE LOWER SEVERN VALLEY					
LANDFORM UNIT GEOMORPHOLOGICAL CHARACTER					
POLYGON NO	2018	COUNTY	Gloucestershire	CENTROID	377249/209846
HER REFERENCE		INTERPRETATION	Paleochannel?		
ASSOCIATED LANDFORM UNITS	POLYGON NUMBERS	2017			
	DESCRIPTION	The main section of possible paleochannel located in the centre of the study area. It appears to be the same feature as 2017. The area is 2.12 km ² .			
UNIT DESCRIPTION	A possible wide paleochannel oriented east to west across the survey area. It is difficult to identify as a definite paleochannel as the extremities of the feature are not within the survey area, however, the land is much lower lying than that surrounding. Mapped in 2 segments, it has a total length of approximately 1.5 km and is approximately 0.32 km wide at its widest point. The total area measures approximately 0.37 km ² . However, the feature is at the extreme northeast corner of the survey area and is therefore not fully represented. Both this and feature 2017 are both possibly cut by the drainage channels of the River Frome although modern canalisation on this area makes distinction difficult.				
HLC TYPE	A2 Less irregular enclosure partly reflecting former unenclosed cultivation patterns				
CULTURAL ASSOCIATIONS	NEW MONUMENTS	None			
	DESCRIPTION	There are relatively few HER entries for this relatively small area. One relates to a medieval moat (GSMR 5234); the two other to Post-medieval buildings.			
POTENTIAL	The evidence for any cultural remains in the area is very fragile. However, as it has an affinity to the main area (2017), it could be considered that similar archaeology could be located here. This unit contained predominantly medieval or later archaeology with no evidence of earlier periods being exposed this far in this potential old paleochannel.				

THE GEOARCHAEOLOGICAL RESOURCE OF THE LOWER SEVERN VALLEY					
LANDFORM UNIT GEOMORPHOLOGICAL CHARACTER					
POLYGON NO	2020	COUNTY	Gloucestershire	CENTROID	375540/207631
HER REFERENCE		INTERPRETATION	Terrace 2		
ASSOCIATED LANDFORM UNITS	POLYGON NUMBERS	Terrace 2 units: 2014, 2004			
	DESCRIPTION	<p>2004 – A ribbon of terrace on the eastern bank of the River Frome aligned northwest to southeast and measuring 0.891km x 0.280km for the element that is contained in the survey area. It gently slopes upward to the east.</p> <p>2014 – A ribbon of terrace on the eastern bank of the River Frome aligned northwest to southeast and measuring 1.6km x 0.230km at its widest point. It has a maximum height of approximately 14m amsl.</p>			
UNIT DESCRIPTION	A terrace unit of the River Severn, that dominates the study area, located on the eastern bank of the river and flanked further to the east by the Frome which appears to have cut into this feature to produce separate elements of the feature described above. Measuring 6.12 km ² , it is bounded to the north and west by the line of the modern Gloucester to Sharpness canal and is the largest landform unit in the study area. There is a gradual slope upwards to the east away from the River Severn. Mostly covered with alluvium.				
HLC TYPE	<p>The area contains a number of different HLC descriptions as follows:</p> <p>A2 Less regular enclosure partly reflecting former unenclosed cultivation patterns A3 Regular organised enclosure ignoring former unenclosed cultivation patterns A4 Less regular organised enclosure partly reflecting former unenclosed cultivation patterns F1 Surviving post-medieval designed ornamental landscape G2 Existing settlement of medieval or earlier origin G3 Existing settlement – extent by mid 19th century G4 Existing settlement – present extent H2 Active industrial site</p>				
CULTURAL ASSOCIATIONS	NEW MONUMENTS	<p>1019 Earthwork ditch associated with DMV 1024 Earthwork Bank 1026 Possible quarry 1030 Earthwork Bank 1031 Earthwork Bank 1038 Cultivation terraces 1045 Earthwork bank</p>			
	DESCRIPTION	<p>This unit has hosted occupation from across the spectrum of archaeology. Numerous archaeological sites and artefacts from all periods are present on the area. Palaeolithic (GSMR 13102), Neolithic artefacts (GSMR 32644) and Bronze Age barrows (GSMR 5243, 5245) and prehistoric settlements (GSMR 5236) have been identified from cropmarks and during excavation ahead of the many gravel extraction quarries that dominate the area. The Roman period is well represented with a Roman road (GSMR 12306) running through the centre of the unit from southeast to northwest. There are traces of Roman settlement (GSMR 5235, Roman burials (GSMR 5240, 13196) and individual finds of Roman pottery and coins. A significant level of Ridge and Furrow cultivation exists across the area much probably dating from the medieval period, indicating the depth of alluvium in the area. Medieval earthworks, buildings and stray finds of medieval pottery also testify to the intense use of the landscape during this period. Many of the buildings in the extended village of Frampton-on-Severn, that dominates the north-western edge of this unit, have medieval origins and many are listed as being constructed in the centuries that immediately follow. Railways serving the gravel extraction sites, mills and water management features on the River Frome are characteristics of the post-medieval period. WWII is represented by pillboxes.</p> <p>The new monuments identified as part of the study include earthwork banks that do appear to coincide with the boundaries on the Tithe map. Cultivation terraces and ditches may date to the medieval period.</p>			

POTENTIAL	<p>This is a large section of terrace and cultural artefacts of all periods are appearing across the area. As this unit has obviously been intensively used for many periods there is no particular pattern to the evidence of occupation but does mean that cultural artefacts for all of these periods may still be discovered in the area.</p> <p>Similar terraces in the Lower Severn Valley will probably also have witnessed habitation for a long period and therefore may contain similar layers of cultural material. The depth of alluvium, witnessed by the extensive Ridge and Furrow, and large terrace units formed by greater variations of the river system in its lower reaches, will make pinpointing potential archaeological sites more difficult.</p>
------------------	--

THE GEOARCHAEOLOGICAL RESOURCE OF THE LOWER SEVERN VALLEY				
LANDFORM UNIT GEOMORPHOLOGICAL CHARACTER				
POLYGON NO	2021	COUNTY	Gloucestershire	CENTROID 374298/208289
HER REFERENCE		INTERPRETATION	Indeterminate Lens	
ASSOCIATED LANDFORM UNITS	POLYGON NUMBERS	None		
	DESCRIPTION			
UNIT DESCRIPTION	A relatively small elongated lens oriented northwest to southeast. It lies between the lower lying area of the potential paleochannel (2017), Terrace 2 (2020) and the marshy area of the tidal area of the River Severn. A distinct feature in the landscape, it measures approximately 1.18km x 0.26km. At its highest point is about 12.7m amsl with a ridge line of about 12m amsl. It is bisected by the Gloucester-Sharpness Canal. A small area of gravel extraction is visible to the northwest of the feature but this does not appear to be on an industrial scale.			
HLC TYPE	A2 Less irregular enclosure partly reflecting former unenclosed cultivation patterns			
CULTURAL ASSOCIATIONS	NEW MONUMENTS	None		
	DESCRIPTION	Three small medieval quarries are known on the lens (GSMR 26424) reinforcing its construction as a gravel lens. The only other records are that of Saul Lodge (GSMR 17083) and DBA for a proposed marina site.		
POTENTIAL	No significant archaeology has been revealed within this unit. The potential is therefore difficult to assess as there is not a comparable unit in the study area. The presence of prehistoric material on other gravel deposits in the area does not preclude the possible presence here, particularly as this may be a drier promontory protruding into the old paleochannel (2017).			